HEAT TRANSFER ENHANCEMENT BY CARBON NANOSTRUCTURE-BASED NANOFLUIDS IN AN ANNULAR HEAT EXCHANGER

HAMED KHAJEH ARZANI

THESIS SUBMITTED IN FULFILMENT OF THE REQUIREMENTS FOR THE DEGREE OF DOCTOR Of PHILOSOPHY

FACULTY OF ENGINEERING

UNIVERSITY OF MALAYA

KUALA LUMPUR

2016

UNIVERSITI MALAYA
ORIGINAL LITERARY WORK DECLARATION

Name of Candidate: Hamed Khajeh Arzani

Registration/Matric No: KHA130111

Name of Degree: Doctor of Philosophy
Title of Project Paper/Research Report/Dissertation/Thesis ("this Work"):

Heat Transfer Enhancement by Nanofluid Flowing in an Annular Heat Exchanger
Field of Study: Heat Transfer

I do solemnly and sincerely declare that:

(1) I am the sole author of this Work;
(2) This Work is original;
(3) Any use of any work in which copyright exists was done by way of fair dealing and for permitted purposes and any excerpt or extract from, or reference to or reproduction of any copyright work has been disclosed expressly and sufficiently and the title of the Work and its authorship have been acknowledged in this Work;
(4) I do not have any actual knowledge nor do I ought reasonably to know that the making of this work constitutes an infringement of any copyright work;
(5) I hereby assign all and every rights in the copyright to this Work to the University of Malaya ("UM"), who henceforth shall be owner of the copyright in this Work and that any reproduction or use in any form or by any means whatsoever is prohibited without the written consent of UM having been first had and obtained;
(6) I am fully aware that if in the course of making this Work I have infringed any copyright whether intentionally or otherwise, I may be subject to legal action or any other action as may be determined by UM.

Candidate's Signature Date

Subscribed and solemnly declared before,

Witness's Signature Date

Name:
Designation:

ABSTRACT

Present thesis work introduces a new design of heat exchangers utilizing an annular profile which opens a new gateway for realizing optimization of higher energy transfer. To apprehend this goal, nanofluids have been studied for this application as it has got thermal conductivity higher than conventional liquids. In this study, a cooling loop apparatus was designed and built to evaluate the transition and turbulent heat transfer performance of water and ethylene glycol based nanofluids. Also numerical simulation was employed as an approximating procedure for prediction of the results in this study. Two-phase mixture model has been considered for simulation of the nanofluids flow in two and three dimensional annular heat exchanger.

Graphene Nanoplatelets (GNP) were stably dispersed in aqueous media by covalent and non-covalent functionalization. At a constant concentration, the measurement has shown that the thermal conductivity of covalent nanofluid (GNP-COOH/water) is higher than the non-covalent nanofluid (GNP-SDBS/water), which is higher than distilled water.

In the second phase of the study, multi-walled carbon nanotubes (MWCNT) has been covalently functionalized with Aspartic acid (Asp) to achieve a highly dispersed colloidal suspension of MWCNT. After investigation of stability of colloidal suspensions with Uv-vis spectroscopy, the prepared coolants have the promising properties such as high thermal conductivity as compared with water. Forced convection heat transfer coefficient and pressure drop were also investigated at three different heat fluxes and four weight concentrations. The observed high heat transfer rate, poor change in the pressure drop in the presence of different weight concentrations provided a suitable condition for this novel alternative coolant.

In the third phase of study, the improvement of colloidal stability of Graphene Nanoplatelets (GNP) in aqueous media has been implemented by functionalization with tetrahydrofurfuryl polyethylene glycol in a quick electrophonic addition reaction method. To address this issue, surface functionalization of GNP was analyzed by Raman spectroscopy, and thermogravimetric analysis. In addition, the morphology of treated samples was investigated by transmission electron microscopy (TEM). The steady-state forced convective heat transfer experiments and the simulation results confirmed the promising cooling capabilities of the TGNP/water.

The last phase is related to the thermophysical and heat transfer performance of covalently functionalized GNP-based water/ethylene glycol nanofluid in an annular channel. After experimentally measuring thermophysical properties of the prepared samples, a computational fluid dynamics study has been carried out to study the heat transfer and pressure drop of well-dispersed and stabilized nanofluids. Based on the results of this investigation, there is a significant enhancement on the heat transfer rate associated with the loading of well-dispersed GNP in basefluid.

ABSTRAK

Thesis ini memperkenalkan reka bentuk terbaru penukar haba menggunakan annular distributor yang membuka ruang baru untuk merealisasikan penggunaan tenaga yang lebih optimum. Bagi merealisasikan matlamat ini, nanofluids telah digunakan seperti dalam kerja yang diterbitkan. Ia menunjukkan peningkatan konduksi haba yang lebih tinggi berbanding cecair konvensional. Dalam kajian ini, satu kelengkapan coolant loop telah direka dan dibina untuk menilai kecekapan kadar peralihan dan turbulent heat transfer oleh air dan nanofluids berasaskan ethylene glycol. Simulasi perangkaan turut digunakan sebagai prosedur untuk menganggar dan meramal keputusan dalam kajian ini. Model two-phase mixture telah digunakan untuk simulasi aliran nanofluids dalam penukar haba annular bagi simulasi dua dan tiga dimensi.

Graphene Nanoplatelets (GNP) tersebar secara stabil dalam medium aqueous dengan ikatan kovalen dan bukan kovalen. Pada kepekatan yang sama, kekonduksian haba untuk ikatan kovalen nanofluids (GNP-COOH / air) adalah lebih tinggi berbanding ikatan bukan kovalen nanofluids (GNP-SDBS / air). Kekonduksian haba kedua-duanya adalah lebih tinggi berbanding air suling.

Pada fasa kedua kajian, Multi-walled carbon nanotubes (MWCNT) adalah berikatan kovalen dengan asid Aspartic (Asp) untuk mencapai bentuk MWCNT dengan dispersed colloidal suspension. Selepas penilaian kestabilan colloidal suspension melalui spektroskopi Uv-vis, penyejuk yang tersedia didapati mempunyai ciri-ciri yang dikehendaki iaitu kekonduksian haba yang lebih tinggi berbanding air. Selain itu, forced convection heat transfer coefficient dan penurunan tekanan turut disiasat pada tiga heat fluxes yang berlainan dan empat weight fractions. Kadar tinggi pemindahan haba, juga

kadar penurunan tekanan yang sedikit dalam kehadiran weight fractions yang berbeza menyediakan keadaan yang sesuai untuk penyejuk alternatif ini.

Sebagai fasa ketiga kajian, bagi tujuan meningkatkan kestabilan colloidal Graphene Nanoplatelets (GNP) di dalam medium aqueous, ikatan perlu terlebih dahulu dibentuk dengan tetrahydrofurfuryl polyethylene glycol dengan tindak balas penambahan electrophonic yang cepat. Untuk menangani isu ini, functionalization permukaan GNP telah dianalisis menggunakan Raman spectroscopy dan analisis Termogravimetri. Di samping itu, morfologi sampel yang telah dirawat dikaji menggunakan transmission electron microscopy (TEM). Hasil eksperimen dan simulasi kajian telah mengesahkan keupayaan penyejukan TGNP / air.

Fasa terakhir kajian merujuk kepada termofizikal dan prestasi pemindahan haba GNP nanofluid berikatan kovalen berasaskan air / ethylene glycol melalui saluran anulus. Selepas uji kaji untuk mengukur sifat termofizikal sampel dibuat, satu kajian dinamik bendalir telah dijalankan untuk mengkaji pemindahan haba dan penurunan tekanan oleh nanofluids yang well-dispersed dan stabil. Berdasarkan hasil siasatan ini, terdapat peningkatan yang ketara ke atas kadar pemindahan haba yang dikaitkan dengan loading well-dispersed GNP in base-fluid.

ACKNOWLEDGEMENTS

First, I would like to thank my parents for guiding me through my first steps of life and education. I would also like to thank my supervisors, Dr. Kazi Md. Salim Newaz and Dr. Ahmad Badaruddin at UM university, who have guided my academic and professional development for the past three years. I would also like to thank my love, my wife, Maryam, who has been supportive of me and my study throughout my graduate educations.

TABLE OF CONTENTS

LIST OF FIGURES

LIST OF TABLES

LIST OF SYMBOLS AND ABBREVIATIONS

Roman symbols

C_p	specific heat capacity at constant pressure (J/kg.K)
d_p	nanoparticle diameter (m)
h	heat transfer coefficient based on mean temperature (w/m^2k)
I	turbulent intensity
I_0	initial turbulent intensity
k	turbulence kinetic energy (m^2/s^2)
Nu	Nusselt number (h.D/k)
p	static pressure (N/m^2)
Pr	liquid Prandtl number
$q^{"}$	heat flux (w/m^2)
Re	Reynolds number $(\frac{\rho v_{in} D}{\mu})$
r,z	2-D axisymmetric coordinates (m)
S	rate of deformation (s^{-1})
T	temperature (K)
v	velocity (m/s)
SSA	Specific Surface Area

Greek letters

ε	performance
μ	dynamic viscosity (kg/m s)
μ_t	turbulent viscosity (kg/m s)

ρ	density (kg/m^3)
τ	shear stress (Pa)
β	friction coefficient($kg\ m^{-3}s^{-1}$)
κ	thermal conductivity (W/m K)
ν	kinematic viscosity
φ	mass fraction
γ	ratio of nanolayer thermal conductivity to particle thermal conductivity
λ	nanoparticle with interfacial shell

Subscriptions

eff	effective
f	fluid
p	particle phase
r	radial direction
s	solid
w	wall
x	axial direction
-	mean
0	initial

CHAPTER 1: INTRODUCTION

Recently almost all advances and developments in industrial technology are being focused on the reduction of system processes leading to higher power concentrations for a wide range of applications. Consequently the need to increase in cooling capacities has been vital for these compact thermal systems. The conventional methods for example using extension surfaces like fins or utilizing micro channels with high heat transfer surface availability to obtain this prompted cooling efficiency have been extensively employed and are restricted in effectiveness. On the other hand, the cooling fluid characteristics, have been investigated recently.

Due to low conductivity characteristic of fluids, they do not have the enough capability to be used in high heat transfer efficiency equipment. In other words, fluids with characteristically poor heat transfer in one hand and increasing needs to micro-scale thermal systems in today's world on the other, have forced the researchers to find the new techniques of heat transfer enhancement. Inevitably one possible solution to overcome this restriction can be obtained by the high heat transfer ability of solid metal particles which are suspended inside flowing fluid. Previously there have been some efforts to add micro-scale metal particles into conventional fluids. Although this way had caused some remarkable improvement but it led to some significant shortcomings. These micro-particles, could enhance the heat transfer rate while impose some negative effect such as increase of viscosity resulting in the need to a more pumping power. To solve all the aforementioned problems with micro structure-based fluids, nanofluids was proposed.

The study of convective heat transfer in nanofluids is gaining a lot of attention. The nanofluids have many applications in the industries since materials of nanometer size

have unique physical and chemical properties. Nanofluids are solid-liquid composite materials consisting of solid nanoparticles or nanofibers with sizes typically of 1-100 nm suspended in liquid. Nanofluids have attracted great interest recently because of reports of greatly enhanced thermal properties. For example, a small amount (< 1% volume fraction) of Cu nanoparticles or carbon nanotubes dispersed in ethylene glycol or oil is reported to increase the inherently poor thermal conductivity of the liquid by 40% and 150% respectively (Choi et al., 2001; J. A. Eastman et al., 2001). Conventional particle-liquid suspensions require high concentration (>10%) of particles to achieve such enhancement. However, problems of rheology and stability are amplified at high concentration, precluding the widespread use of conventional slurries as heat transfer fluids. In some cases, the observed enhancement in thermal conductivity of nanofluids is orders of magnitude larger than predicted by well-established theories. Other perplexing results in this rapidly evolving field include a surprisingly strong temperature dependence of the thermal conductivity (Patel et al., 2003) and a three-fold higher critical heat flux compared with the base fluids (Sakiadis, 1961; You et al., 2003). These enhanced thermal properties are not merely of academic interest. If confirmed and found consistent, they would make nanofluids promising for application in thermal management. Furthermore, suspensions of metal nanoparticles are also being developed for other purposes, such as medical applications including cancer therapy. The interdisciplinary nature of nanofluid research presents a great opportunity for exploration and discovery at the frontiers of nanotechnology. The application of high conductive fluids will collect entirely the accessible and usable energy of a system which will associate the reduction of negative environmental impacts of companies as well as their operating costs. One of the advantages of nanoparticles in nanofluids is that these nano-particles have great surface

area which contributes to the enhanced thermal conductivity than pure fluids (Ghobadian et al., 2011; Vishwanadula, 2008).

1.1 Motivation

Fluids flow in the annular channels and their convective heat transfer are important phenomena in the engineering systems due to their technological applications such as cooling core of nuclear reactors, electrical gas-insulated transmission lines, thermal insulation, gas-cooled electrical cables, cooling systems, compact heat exchangers, cooling of electronic devices, boilers, solar energy systems, aircraft fuselage insulation to underground electrical transmission cables and thermal storage systems (Eiyad Abu-Nada et al., 2009; Duka et al., 2007; Mohammed, 2008; Passerini et al., 2008). As a result, studies on the heat transfer enhancement in annular pipe heat exchangers are essential (Kashani et al., 2013).

1.2 Objective

This study is focused on a horizontal annulus formed between an inner heat generating solid circular cylinder and an outer isothermal cylindrical boundary undergoing transition and turbulent convection nanofluid flow for different conditions (i.e. nanoparticle volume fractions, inlet mass flux and wall heat flux). Moreover, three types of tests studies were performed on three types of carbon nanostructure-based nanofluids and various functionalization methods. Experimental and numerical investigations were performed to obtain thermal conductivity data, pressure drops and frictional coefficient in the presence of nanofluidss.

The objectives of the present study is presented as follows:

- To compare thermophysical properties and heat transfer enhancement of covalent and non-covalent nanofluids in an annular heat exchanger.
- To investigate thermophysical properties and heat transfer rate of covalently functionalized multi-walled Carbon nanoplateles in an annular heat exchanger.
- To analyse heat transfer performance of water-based tetrahydrofurfuryl polyethylene glycol-treated graphene nanoplatelets super-coolant in an annular heat exchanger.
- To investigate the thermophysical and heat transfer performance of stabilized graphene nanoplatelets-ethylene glycol/water nanofluids in an annular heat exchanger.

CHAPTER 2: LITERATURE REVIEW

2.1 Introduction

Nanofluids are nanoscale colloidal suspensions containing nanoscalematerials (nanoparticles, nanotubes, nanorods) with diameter sizes in the order of 1 to 100 nanometers suspended in heat transfer base fluids. Nanofluids have been found to possess enhanced thermophysical properties such as thermal conductivity, thermal diffusivity, viscosity, and convective heat transfer coefficients compared to those of base fluids like oil or water (Wei Yu et al., 2012). The thermal conductivity of working fluids is important to determine the efficiency of heat exchange systems. Since the size of heat exchange systems can be reduced with the highly efficient heat transfer fluids, the enhancement of the thermal conductivity will contribute to the cooling of miniature devices.

Several investigations have revealed that the thermal conductivity of the fluid containing nanoparticles could be increased by more than 20% in the case of very low nanoparticles concentrations. When nanofluids were explored by Choi and his group at the Argonne National Laboratory, they first tried to use metal oxide particles of nanometer size to suspend them in the common coolants (e.g., water, ethylene glycol) (Maxwell, 1904).

All the physical mechanisms are governed by a critical length scale below which the physical properties of materials are changed, therefore, particles smaller than 100 nm exhibit properties different from those of conventional solids. The properties of nanoscale materials come from the relatively high surface area or volume ratio, which is due to the high proportion of constituent atoms residing at the grain boundaries (Sarit K Das et al., 2007).

Production of nanoparticles materials used in nanofluids can be classified into two main categories: physical processes and chemical processes. Typical physical process includes the mechanical grinding method and the inert-gas-condensation technique. Chemical process for producing nanoparticles includes chemical precipitation, spray pyrolysis, and thermal spraying (Wenhua Yu et al., 2008).

2.2 Nanofluids Preparation

2.2.1 One-Step Method

To reduce the agglomeration of nanoparticles, Eastman et al. developed a one-step physical vapor condensation method to prepare Cu-ethylene glycol nanofluids (J. A. Eastman et al., 2001). Liu et al. synthesized nanofluids containing Cu nanoparticles in water through chemical reduction method (M.-S. Liu et al., 2006). The one-step process consists of simultaneously making and dispersing the particles in the fluid.

This method has some advantages, the processes of drying, storage, transportation, and dispersion of nanoparticles are avoided, so the agglomeration of nanoparticles is minimized, and the stability of fluids is increased, but disadvantage of this method is that only low vapour pressure fluids are compatible with the process. This limits the application of the method (Y. Li et al., 2009). One-step processes can prepare uniformly dispersed nanoparticles, and the particles can be stably suspended in the base fluid (Wei Yu et al., 2012).

2.2.2 Two-Step Method

This is the first and the most classic synthesis method of nanofluids, which is extensively used in the synthesis of nanofluids considering the available commercial nano-powders supplied by several companies. Nanoparticles such as metal or metal oxides, and other

nanostructures used in this method are first produced as dry powders by chemical or physical methods. Then, the nanosized powder is dispersed into a fluid in the second processing step with the help of intensive magnetic force agitation, ultrasonic agitation, high-shear mixing, and homogenizing. Two-step method is the most economic method to produce nanofluids in large scale, because nanopowders synthesis techniques have already been scaled up to industrial production levels. Due to the high surface area and surface activity, nanoparticles have the tendency to aggregate. The important technique to enhance the stability of nanoparticles in fluids is the use of nan-covalently functionalization (Wei Yu et al., 2012).

2.2.3 Stability

The stability of nanofluids is very important for practical applications. It is strongly affected by the characteristics of the suspended particles such as the particle morphology, the chemical structure of the particles and the basefluids (Hwang et al., 2007). Because of the attractive Van der Waals forces between the particles, they tend to agglomerate as they are dispersed in the liquids (especially if nanopowders are used); therefore, a means of separating the particles is necessary. Groups of particles will settle out of the liquid and decrease the conductivity of the nanofluid. Only by fully separating all the agglomerating nanoparticles into their individual particles in the host liquid will be well-dispersed, and with the sustainability of this dispersion the optimum thermal conductivity exists (Wong et al., 2010).

Nanoparticles used in nanofluids have been made of various materials, such as metals (Cu, Ag, Au), metals oxides (Al_2O_3, CuO), carbide ceramics (SiC, TiC) and carbon nanotubes. Metal oxides were tried mainly for ease of manufacturing and stabilization compared to the pure metallic particles, which are difficult to suspend without

agglomeration. Subsequently, many investigators have carried out experiments with the oxide particles, predominantly Al_2O_3 particles, as well as CuO, TiO_2, and stable compounds such as SiC (Sarit K Das et al., 2007).

Eastman et al. (1996) stated that an aqueous nanofluid containing 5% volume fraction CuO nanoparticles exhibited a thermal conductivity 60% greater than that of water. Additionally, they reported 40% greater thermal conductivity compared to water for an aqueous nanofluid containing 5% volume fraction of Al_2O_3 nanoparticles (J. Eastman et al., 1996). Lee et al. (1999) and Wang et al. showed that alumina and copper oxide nanoparticles suspended in water and ethylene glycol significantly enhanced the fluid thermal conductivity (X. Wang et al., 1999).

Xie et al. (2002) observed 21% increase in fluid thermal conductivity of water with 5 vol. % of alumina nanoparticles. Pang et al. (2012) demonstrated 10.74% improvement of the effective thermal conductivity at 0.5 vol. % concentration of Al_2O_3 nanoparticles and about 14.29% increment at the same volume concentration of SiO_2 nanoparticles.

Particle loading would be the main parameter that influences the thermal transport in nanofluids and that is investigated in almost all of the experimental studies. Most of the nanofluid thermal conductivity data in the literature exhibit a linear relationship with the volume fraction of particles (J. A. Eastman et al., 2001; S. Lee et al., 1999; H.-q. Xie et al., 2002; H. Xie et al., 2002). However, some exceptions have shown a non-linear relationship (T.-K. Hong et al., 2005; Murshed et al., 2005; Zhu et al., 2006). Kwak et al. (2005) in their investigation on CuO–ethylene glycol nanofluid, observed that substantial enhancement in thermal conductivity with respect to particle concentration is attainable only when particle concentration is below the dilute limit.

The particle material is an important parameter that affects the thermal conductivity of nanofluids, it seems that better enhancement in thermal conductivity can be achieved with the higher thermal conductivity particles. Eastman et al. (2001) investigated thermal conductivity enhancement of nanofluid consisting of copper nanometer-sized particles dispersed in ethylene glycol. The effective thermal conductivity is shown to be increased by up to 40% at 0.3 vol. % of Cu nanoparticles which is much higher than ethylene glycol containing the same volume fraction of dispersed oxide nanoparticles of Cu. However, the thermal conductivity of dispersed nanoparticles is not crucial to determine the thermal conductivity of nanofluids; some research show that particle type may affect the thermal conductivity of nanofluids in other ways. Hong et al. (2005) reported an interesting result that the thermal conductivity of Fe based nanofluid was higher than the one obtained for Cu nanofluids of the same volume fraction. This is opposite to the expectation that the dispersion of the higher thermal conductive material is more effective in improving the thermal conductivity.

The intrinsic properties of nano scaled materials become different from those of the bulk materials due to the size confinement and surface effect (Hong et al., 2005). From the previous researches it is observed that with using the same particle materials there are a discrepancy in the thermal conductivity results even for the same particle load. This discrepancy is attributed to variety of physical and chemical parameters, in addition to the volume fraction, and the species of the nanoparticles, the other parameters such as the size, the shape, pH value and temperature of the fluids and the aggregation of the nanoparticles, have been considered playing roles on the heat transfer characteristics of nanofluids.

2.3 Effective Parameters on Thermal Conductivity

2.3.1 Particle Size

It is expected that the thermal conductivity enhancement increases with decreasing the particles size, which leads to increasing the Specific Surface Area (SSA):

$$SSA = \frac{particle\ surface\ area}{particle\ volume} \tag{2-1}$$

For the sphere particles:

$$SSA = \frac{\pi d_p^2}{\pi / 6 d_p^3} = \frac{6}{d_p} \tag{2-2}$$

This is clearly indicating that a decrease in particle diameter (d_p) causes the SSA to increase, which giving more heat transfer area between the particles and fluid surrounding the particles. Lee et al. (1999) suspended CuO and Al_2O_3 (18.6 and 23.6nm, 24.4 and 38.4nm, respectively) in two different base fluids: water and ethylene glycol (EG) and obtained four combinations of nanofluids: CuO in water, CuO in EG, Al_2O_3 in water and Al_2O_3 in EG. Their results show that the thermal conductivity ratios increase almost linearly with volume fraction. Results suggested that not only particle shape but size of nanoparticle is considered to be dominant in enhancing the thermal conductivity of nanofluids.

Xie et al. (2002) demonstrated the nanoparticle size effect on the thermal conductivity enhancement; they measured the effective thermal conductivity of nanofluids (Al_2O_3 in ethylene glycol) with different nanoparticle sizes. They reported that an almost linear increase in conductivity was obtained with the increase of volume fraction, but the rates

of the enhancement ratios with the volume fraction was dependent on the dispersed nanoparticles. They stated that the enhancements of the thermal conductivities are dependent on the specific surface area (SSA) and the mean free path of the nanoparticles and the base fluid. With the decrease of the particle size the Brownian motion of nanoparticles enhances which dominates the nanoconvection. As a result, the effective thermal conductivity of nanofluids becomes higher.

Yoo et al. (2007) investigated the thermal conductivities of (TiO_2, Al_2O_3, Fe, and WO_3) nanofluids. It shows that the surface-to-volume ratio of nanoparticles is a key factor which influences thermal conductivity of nanofluids.

2.3.2 Particle Shape

Murshed et al. (2005) measured the effective thermal conductivity of rod-shapes (10nm x 40 nm; diameter by length) and spherical shapes (15nm) of TiO_2 nanoparticles in deionized water. The results show that the cylindrical particles present a higher enhancement which is consistent with theoretical prediction, i.e., Hamilton-Crosser (Hamilton et al., 1962) model.

Evans et al. (2008) investigated the effect of the aspect ratio on the enhancement of the thermal conductivity of nanofluids. They have compared the thermal conductivity enhancement of long fibers in flat plates at a specific concentration for different aspect ratios. The results suggest that the optimum design for nanofluids for thermal conductivity enhancement would involve the use of high-aspect-ratio fibers, e.g. carbon nanotubes, rather than spherical or ellipsoidal particles.

2.3.3 Base Fluid

Different types of fluids, such as water, ethylene glycol, vacuum pump oil and engine oil, have been used as base fluid in nanofluids. It is clearly seen that no matter what kind of nanoparticle was used, the thermal conductivity enhancement decreases with an increase in the thermal conductivity of the base fluid (Xie et al., 2011). Xie et al. (2002) investigated the thermal conductivity of suspensions containing nanosized alumina particles, for the suspensions using the same nanoparticles; the enhanced thermal conductivity ratio is reduced with increasing thermal conductivity of the base fluid. Liu et al. (2005) also investigated base fluid effect with MWCNT nanofluids; they used ethylene glycol and synthetic engine oil as base fluids in the experiments. 1 vol. % MWCNT/ethylene glycol nanofluid showed 12.4% thermal conductivity enhancement over the base fluid, whereas at 2 vol. % MWCNT/synthetic engine oil nanofluid, the enhancement was 30%. It was observed that higher enhancements was achieved with synthetic engine oil as the base fluid.

2.3.4 Temperature-Dependent Thermal Conductivity

In conventional suspensions of solid particles (with sizes in the order of millimeters or micrometers) in liquids, thermal conductivity of the mixture depends on temperature only due to the dependence of thermal conductivity of base liquid and solid particles on temperature (Özerinç et al., 2010). However, in case of nanofluids, change of temperature affects the Brownian motion of nanoparticles and clustering of nanoparticles (C. H. Li et al., 2008) which results in dramatic changes of thermal conductivity of nanofluids with temperature.

Das et al. (2003) discovered that the nanofluids have strongly temperature-dependent conductivity compared to base fluids. They measured effective thermal conductivities of

Al_2O_3 and CuO nanoparticles in water when the mixture temperature was varied between 21 to 51°C. It is observed that a 2 to 4 fold increase in thermal conductivity enhancement of nanofluids can be achieved over that range of temperature. Patel et al (2003) reported that the thermal conductivity enhancement ratios of Au nanofluids were enlarged considerably when the temperature increased.

Zhang et al. (2006) measured effective thermal conductivity of Al_2O_3-distilled water in the temperature range of 5-50°C, were in a good agreement to Das et al. (2003). However, in other experimental investigations, it showed different thermal conductivity enhancement behaviours. Yu et al., investigated the nanofluids containing GONs (Graphene Oxide Nanosheets), the thermal conductivity enhancement ratios remain almost constant when they tested by varying temperatures. This indicates that many factors may affect the thermal conductivity enhancement ratios. One of these factors is the viscosities of the base fluids. In their experiments, Ethylene Glycol was used as the base fluid and the viscosity value was high. On the other hand, GONs were large, so the effect of Brownian motion was not obvious (Wei Yu et al., 2009).

2.4 Mechanisms of Thermal Conduction Enhancement

Heat conduction mechanisms in nanofluids have been extensively investigated in the past decades to explain the experimental observations of the enhanced thermal conductivities. Keblinski et al. (2002) and Eastman et al. (2004) proposed four possible mechanisms, e.g., Brownian motion of the nanoparticles, molecular-level layering of the liquid at the liquid/particle interface, the nature of heat transport in the nanoparticles, and the effects of nanoparticle clustering. Other groups have started from the nanostructure of nanofluids. These investigators assume that the nanofluid is a composite, formed by the nanoparticle as a core, and surrounded by a nanolayer as a shell, which in turn is immersed

in the base fluid, and from which a three-component medium theory for a multiphase system is developed (X.-Q. Wang et al., 2008).

2.4.1 Brownian Motion

The Brownian motion of nanoparticles could contribute to the thermal conduction enhancement through two ways, a direct contribution due to motion of nanoparticles that transport heat, and an indirect contribution due to micro-convection of fluid surrounding individual nanoparticles. The studies of Wang et al. (1999) clearly showed that Brownian motion is not a significant contributor to heat conduction. Keblinski et al. (2002) concluded that the movement of nanoparticles due to Brownian motion was too slow in transporting heat through a fluid. To travel from one point to another, a particle moves a large distance over many different paths in order to reach a destination that may be apparently a short distance from the starting point. Therefore, the random motion of particles cannot be a key factor in the improvement of heat transfer based on the results of a time-scale study. Evans et al. (2006) suggested that the contribution of Brownian motion to the thermal conductivity of the nanofluids is very small and cannot be responsible for the extraordinary thermal transport properties of nanofluids.

Even though it stated that Brownian motion is not a significant contributor to enhance heat conduction, some authors showed the key role of Brownian motion in nanoparticles in enhancing the thermal conductivity of nanofluids. (Sarit K Das et al., 2007) Jang and Choi (2004) proposed the new concept that the convection induced by purely Brownian motion of nanoparticles at the molecular and nanoscale level is a key nanoscale mechanism governing their thermal behavior. In this mechanism, the thermal conductivity of nanofluids is strongly dependent on the temperature and particle size.

Patel et al. (2006) developed microconvection model for evaluation of thermal conductivity of nanofluids by taking into account nanoconvection induced by Brownian nanoparticles and their specific surface area. Koo et al. (2005) discussed the effects of Brownian motion, thermo-phoretic, and osmo-phoretic motions on the effective thermal conductivities. They found that the role of Brownian motion is much more important than that of the thermo-phoretic and osmo-phoretic motions. Furthermore, the particle interaction can be neglected when the nanofluids' concentration are low (< 0.5%). The contribution of Brownian motion for high aspect ratio nanotube dispersions may not be as important as that for spherical particle dispersions. Xie et al. (2003) pointed out from their experimental observations that the thermal conductivity of nanofluids seems to be very dependent on the interfacial layer between the nanotube and base fluids.

2.4.2 Molecular-level Layering

At the solid-liquid interface, liquid molecules could be significantly more ordered than those in the bulk liquid alone. In the direction normal to the liquid–solid interface, liquid density profiles exhibit oscillatory behavior on the molecular scale due to the interactions between the atoms in the liquid and the solid (C.-J. Yu et al., 1999; Wenhua Yu et al., 2008). The magnitude of the layering increases with the increase of the solid–liquid bonding strength, and the layering extends into the liquid over several atomic or molecular distances. In addition, with the increasing strength of the liquid–solid bonding, crystal-like order develops in the liquid in the lateral directions (L. Xue et al., 2004). Therefore, Choi et al. postulated that this organized solid/liquid interfacial shell makes the transport of energy across the interface effect (Choi et al., 2001).

There is no experimental data regarding the thickness and thermal conductivity of these nanolayers which is an important drawback of the proposed mechanism (Özerinç et al.,

2010). To develop a theoretical model by considering liquid layering around nanoparticles some authors assumed some values for the thermal conductivity and thickness of the nanolayer (W Yu et al., 2003).

Recently, Tillman and Hill (2007) proposed another theoretical way to calculate the thickness and thermal conductivity of the nanolayer. Their approach requires a prior assumption about the functional form of the thermal conductivity in the nanolayer and iterations of the calculation process are required. They used the classical heat conduction equation together with proper boundary conditions to obtain a relation between the radial distribution of thermal conductivity in the nanolayer and nanolayer thickness.

Lee (2007) proposed a way of calculating the thickness and thermal conductivity of the nanolayer by considering the formation of electric double layer around the nanoparticles. So, the thickness of nanolayer depends on the dielectric constant, ionic strength, and temperature of the nanofluid. The thermal conductivity of the nanolayer depends on the total charged surface density, ion density in the electric double layer, pH value of the nanofluid, and thermal conductivities of the base fluids and the nanoparticles (X.-Q. Wang et al., 2008).

Xue (2003) proposed a model of the effective thermal conductivity for nanofluids considering the interface effect between the solid particles and the base fluid of the nanofluids, his model is based on Maxwell theory and average polarization theory. The theoretical results on the effective thermal conductivity of nanotube/oil nanofluid and Al_2O_3/water nanofluid are in good agreement with the experimental data.

Among those studies, Xue et al. (2004) examined the effect of nanolayer by molecular dynamics simulations and showed that nanolayers have no effect on the thermal transport.

They said that despite the large degree of orderly appearance, these liquid layers are still more disordered than the crystals.

2.4.3 Clustering

Clustering is the formation of larger particles through aggregation of nanoparticles. Clustering effect is always present in nanofluids and it is an effective parameter in thermal conductivity (Özerinç et al., 2010). Figure (2-1) schematically shows aggregation. The probability of aggregation increases with decreasing of particle size at a constant volume fraction, because the average interparticle distance decreases, which makes the attractive van der Waals force more important (Sarit K Das et al., 2007). Aggregation will decrease the Brownian motion due to the increase in the mass of the aggregates, whereas it can increase the thermal conductivity due to the percolation effects in the aggregates, as highly conducting particles touch each other in the aggregate (Prasher, Phelan, et al., 2006). However, larger clusters tend to settle out from the base fluids and therefore decrease the thermal conductivity enhancement.

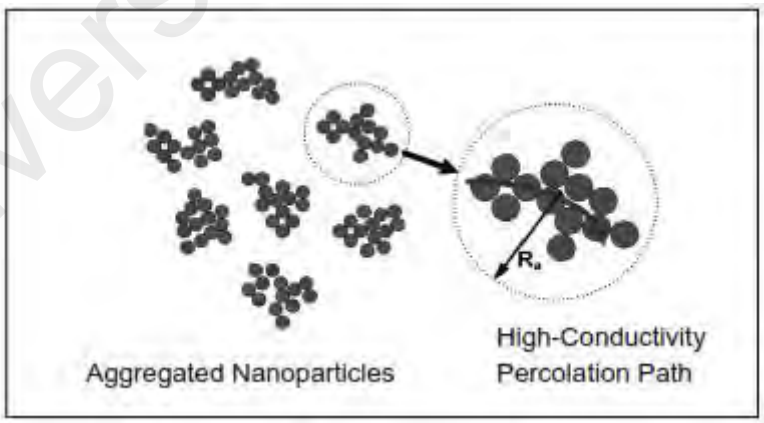

Figure 2.1: Schematic of Well-dispersed Aggregates.

A number of authors strongly suggested that nanoparticle aggregation plays a significant role in the thermal transport in nanofluids. Using effective medium theory Prasher et al.

(2006) demonstrated that the thermal conductivity of nanofluids can be significantly enhanced by the aggregation of nanoparticles into clusters. Hong et al. (2006) investigated the effect of the clustering of nanoparticles on the thermal conductivity of nanofluids. Large enhancement of the thermal conductivity is observed in Fe nanofluids sonicated with high powered pulses. The average size of the nanoclusters and thermal conductivity of sonicated nanofluids are measured as time passes after the sonication stopped. It has been observed that the reduction of the thermal conductivity of nanofluids is directly related to the agglomeration of the nanoparticles. Kwak and Kim (2005) demonstrated that larger thermal conductivity enhancements are accompanied by sharp viscosity increases at low (<1%) nanoparticle volume fractions, thus it is more effective to use small volume fractions than otherwise, in nanofluids. Lee et al. (2006) demonstrated the critical importance of particle surface charge in nanofluids thermal conductivity. The surface charge is one of the primary factors controlling the nanoparticle aggregation.

Furthermore, Putnam et al. (2006) and Zhang et al. (2006) and Venerus et al. (2006) have demonstrated that nanofluids exhibiting good dispersion do not show any unusual enhancement of thermal conductivity (Evans et al., 2008).

2.5 Carbon Nanotubes

The largest increases in thermal conductivity have been observed in suspensions of carbon nanotubes (CNT), which has very high aspect ratio (~2000), and very high thermal conductivity along their alignment axis, similar to the in-plane conductivity of graphite (2000 W/m K); but the conductivity perpendicular to the axis is similar to that for transplanar conduction in carbon. The first report on the synthesis of nanotubes was conducted by Iijima (1991).

CNTs are one-dimensional cylinder of carbon with single or multiple layers of carbon.. carbon is a densely packed single, hexagonal layer of carbon-bonded atoms that are rolled to form a cylindrical microstructure. The ends of the cylindrical microstructure can be capped with a hemispherical structure from the fullerene family or left open. Planner carbon sheets can be rolled in a number of ways. The orientation of rolling gives different possible structures of carbon nanotubes. Each type of CNT structure has their unique strength, electrical and thermal properties (Sarit K Das et al., 2007).

There are two main types of carbon nanotubes, single wall carbon nanotubes (SWCNT) and multi-wall carbon nanotubes (MWCNT). SWCNTs are composed of a single sheet of graphene rolled into a cylinder capped with one- half of a fullerene molecule at each end of the cylinder. Figure (2-2) A MWCNT consists of concentric sheets of rolled graphene that are either capped with one half of a fullerene molecule at each end or left open.

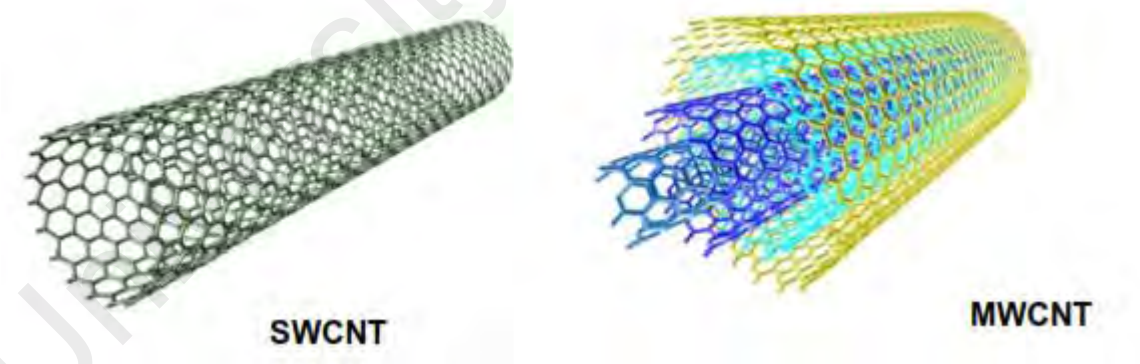

Figure 2.2: SWCNT and MWCNT

Recent studies reveal that CNTs have unusually high thermal conductivity (Berber et al., 2000; Hone et al., 1999). It can be expected that the suspensions containing CNTs would have enhanced thermal conductivity and their improved thermal performance would be applied to energy systems.

The first experimental observation of thermal conductivity enhancement was reported by Choi and co-workers for the case of MWNTs dispersed in poly- (α olefin) oil (Choi et al., 2001). They reported an enhancement of 160% at a nanotube loading of 1.0 vol. %. To get stable nanofluids, Xie et al. (2003) functionalized CNTs using concentrated nitric acid which reduced aggregation and entanglement of the CNTs. Functionalized CNTs were successfully dispersed into polar liquids like distilled water, ethylene glycol without the need of surfactant and into non polar fluid like decene (DE) with oleylamine as surfactant. Functionalized CNTs are stable in both water and ethylene glycol for more than two months. At 1.0 vol. % the thermal conductivity enhancements are 19.6%, 12.7%, and 7.0% for functionalized CNT suspension in DE, EG, and DW, respectively.

It is known that CNTs have a hydrophobic surface, which is prone to aggregation and precipitation in water in the absence of dispersant/surfactant (Zhang et al., 2004). The method of making a stable suspension includes physical mixing in combination with chemical treatments. The physical mixing includes magnetic force agitation and ultrasonic vibration. The chemical treatment is achieved by changing the pH value and by using surface activators and/or surfactant.

Various dispersion methods have been used to ensure a homogenous dispersion of the CNTs throughout the nanofluid (Ryglowski, 2009). The use of surfactants includes two-steps approach: dissolving the surfactant into the liquid medium, and then adding the selected carbon nanotube into the surfactant liquid medium with mechanical agitation and/or ultra-sonication (Zhang et al., 2004) All these techniques used in preparation process and the addition of surfactant, aim at changing the surface properties of suspended particles and suppressing formation of particles aggregation, so, nanofluids can keep stable without visible sedimentation of nanoparticles (Xuan et al., 2000).

Assael et al. (2004) measured the enhancement of the thermal conductivity of MWCNTs-water suspensions with 0.1 wt% Sodium Dodeycyl Sulfate (SDS) as a surfactant. The maximum thermal conductivity enhancement was 38% for a 0.6 vol. % suspension. Results showed that the additional SDS would interact with MWCNTs in which the outer surface was affected. Later, Assael et al. (2005) repeated the similar measurements using MWCNTs and double walled carbon nanotubes (DWNTs), but by using Hexadecyltrimethyl ammonium bromide (CTAB) and nanosphere AQ as dispersants. The maximum thermal conductivity enhancement was obtained 34% for a 0.6 vol. % MWCNTs –water suspension with CTAB. They also discussed the effect of surfactant concentration on the effective thermal conductivity of the suspensions and found that CTAB is better for MWCNTs and DWNTs.

Liu et al. (2005) tested nanofluids containing CNTs. They used ethylene glycol and synthetic engine oil as base fluids. N-hydroxysuccinimide (NHS) was employed as the dispersant in carbon nanotube–synthetic engine oil suspensions. It was found that in CNT/ethylene glycol nanofluids, the thermal conductivity was enhanced by 12.4% with 1 vol. % CNT, while in CNT/engine oil nanofluids; the thermal conductivity was enhanced by 30.3% with 2 vol. % CNT. Based on experimental observations of CNT–liquid and CNT–CNT interactions, CNT dispersed in base fluid; where CNT orientation and CNT–CNT contacts, can form extensive three-dimensional CNT network chain that facilitate thermal transport (Sastry et al., 2008).

Nanda et al. (2008) reported up to 35% enhancement in thermal conductivity for 1.1 vol. % CNTs (single wall) glycol nanofluid. Shaikh et al. (2007) used the modern light flash technique and measured the thermal conductivity of three types of nanofluids. They reported a maximum enhancement of 160% for the thermal conductivity of carbon

nanotube (CNT)-polyalphaolefin (PAO) suspensions. Ding et al. (2006) studied the heat transfer behavior of aqueous suspensions of multi-walled carbon nanotubes flowing through a horizontal tube. Wen and Ding found a 25% enhancement in the conductivity of carbon nanotubes suspended in water. The enhancement in the conductivity of the suspension increases rapidly with loading up to 0.2 vol. % and then begins to saturate, the measurements are taken up to 0.8 vol (Wen et al., 2004).

Significant enhancement of the convective heat transfer is observed and the enhancement depends on the flow conditions and CNT concentrations. They found that the enhancement is a function of the axial distance from the inlet of the test section and they proposed that particle re-arrangement, shear induced thermal conduction enhancement, reduction of thermal boundary layer thickness are due to the presence of nanoparticles, as well as the very high aspect ratio of CNTs are to be the possible mechanisms. Jiang et al. (2009) tested the thermal characteristics of CNT nanorefrigerants, where four kinds of CNTs employed in this research with different diameters and aspect ratios. The experimental results show that the thermal conductivities of CNT nanorefrigerants have increased significantly with the increase of the CNT volume fraction; the diameter and aspect ratio of CNT can influence the thermal conductivities of CNT nanorefrigerants, in which the smaller the diameter of CNT the larger the aspect ratio of CNT which provides the higher thermal conductivity of CNT nanorefrigerant. They reported that the influence of aspect ratio of CNT on nanorefrigerants' thermal conductivities is less than the influence of diameter of CNT.

Meibodi et al. (2010) investigated the stability and thermal conductivity of CNT/water nanofluids. They examined the affecting parameters including size, shape, and source of nanoparticles, surfactants, power of ultrasonic, time of ultra-sonication, elapsed time after

ultra-sonication, pH, temperature, particle concentration, and surfactant concentration. The work on CNTs containing nanofluids cited above clearly which indicates that nanotubes have a higher potential to be used in nanofluids.

2.6 Modeling Studies

The conventional understanding of the effective thermal conductivity of multiphase systems originates from continuum formulations which typically involve the particle size/shape and volume fraction and assume diffusive heat transfer in both fluid and solid phases. Researchers have proposed many theories to explain the anomalous behaviour observed in nanofluids. First attempt to explain the thermal improvement in nanofluids was made by using Maxwell theory (Maxwell, 1904). This theory is valid for diluted suspension of spherical particles in homogeneous isotropic material.

$$\frac{k_{eff}}{k_f} = \frac{k_p + 2k_f - 2\phi(k_f - k_p)}{k_p + 2k_f + \phi(k_f - k_p)} \tag{2-3}$$

The Maxwell equation takes into account only the particle volume concentration and the thermal conductivities of particle and liquid. Hamilton and Crosser (1962) developed this theory for non-spherical particles shapes their model allows calculation of the effective thermal conductivity (k_{eff}) of two component heterogeneous mixtures and includes empirical shape factor n given by $n=3/\psi$; (ψ is the sphericity defined as ratio between the surface area of the sphere and the surface area of the real particle with equal volumes),

$$\frac{k_{eff}}{k_f} = \frac{k_p + (n+1)k_0 - (n-1)(k_f - k_p)\phi}{k_p + (n-1)k_0 - (k_p - k_0)\phi} \tag{2-4}$$

where, k_p and k_0 are the conductivities of the particle material and the base fluid and ϕ is volume fraction of the nanoparticles Hamilton-Crosser theory takes into account the increase in surface area of the particles by taking the shape factor into account, but it does not consider the size of the particles. This is an obvious shortcoming of this theory. It was not surprising that both Maxwell's theory and HC theory were not able to predict the enhancement in thermal conductivity of nanofluids because it did not take into account the various important parameters affecting the heat transport in nanofluids like the effect of size of nanoparticle and modes of thermal transport in nanostructures. Other classical models include the effects of particle distribution developed by Cheng & Vachon (1969), and particle/particle interaction developed by Jeffrey (1973). Although they can give good predictions for micrometer or larger-size multiphase systems, the classical models usually underestimate the thermal conductivity increase of nanofluids as a function of volume fraction.

Keblinski et al. (2002) investigated the possible factors of increasing thermal conductivity of nanofluids such as the size, the clustering of the particles, Brownian motion of particles and the nanolayer between the nanoparticles and base fluids. Yu and Choi (2003) proposed a modified Maxwell model to account for the effect of the nanolayer by replacing the thermal conductivity of solid particles kp in Eq.(2-1) with the modified thermal conductivity of particles k_{pe}, which is based on the so called effective medium theory developed by Schwartz et al. (1995);

$$\frac{k_{eff}}{k_f} = \frac{2(1-\gamma)+(1+\beta)^3(1+2\gamma)\gamma}{-(1-\gamma)+(1+\beta)^3(1+2\gamma)} \qquad (2\text{-}5)$$

Where, $\gamma = k_{layer} / k_p$ is the ratio of nanolayer thermal conductivity to particle thermal conductivity and $\beta = h / r$ is the ratio of the nanolayer thickness to the original particle radius. This model can predict that the presence of very thin nanolayer, even though only a few nanometers thick, can measurably increase effective volume fraction and subsequently the thermal conductivity of nanofluids.

Xue (2006) proposed a model for calculating the effective thermal conductivity of nanofluids, which is expressed as

$$9(1-\frac{\nu}{\lambda})\frac{k_{eff}-k_f}{2k_{eff}+k_f}+\frac{\nu}{\lambda}\left[\frac{k_{eff}-k_{e,x}}{k_{eff}+B_{2,x}(k_{e,x}-k_{eff})}+4\frac{k_{eff}-k_{e,\mathrm{y}}}{2k_{eff}+(1-B_{2,x})(k_{e,y}-k_{eff})}\right]=0 \quad (2\text{-}6)$$

Where $k_{e,x}$ and $k_{e,y}$ are the thermal conductivity components of the complex elliptical particles along the x and y axes, respectively, ν and $\frac{\nu}{\lambda}$ are the volume fractions of the nanoparticles and the complex nanoparticles (nanoparticle with interfacial shell), respectively. His model is based on the Maxwell theory and average polarization theory, which includes the interfacial shell effect.

Shukla et al. (2005) developed a model for thermal conductivity of nanofluids based on the theory of Brownian motion of particles in a homogeneous liquid combined with the macroscopic Hamilton- Crosser model and predicted that the thermal conductivitydepends on the temperature and particle size. The model predicts a linear dependence of the increase in thermal conductivity of the nanofluid with their volume fraction of solid nanoparticles.

Xue and Xu (2005) derive an expression for the effective thermal conductivity of nanofluids with interfacial shells, the expression is not only dependent on the thermal conductivity of the solid and liquid and their relative volume fraction, but also dependent on the particle size and interfacial properties.

Patel et al. (2008) proposed a cell model to predict the thermal conductivity enhancement of nanofluids. Effects due to the high specific surface area of the mono-dispersed nanoparticles (in which, inter-particle interactions are neglected, as the particle–fluid heat transfer is expected to be much more significant compared to the particle–particle heat transfer), and the micro-convective heat transfer enhancement associated with the Brownian motion of particles are addressed in this model. In this model it is assumed that there are two paths for the heat flux, one corresponding to the heat conduction directly through the stationary liquid without involving the particle phase and the other in which heat passes from the liquid to the moving particle, propagates by conduction within the particle and finally returns to the liquid from particle phase, the convective resistance between the fluid and the particle due to particle motion and the conductive resistance through the particle are in series.

Akbari et al. (2011) proposed an expression for the effective conductivity of nanofluids; this model is based on Nan et al. model (Nan et al., 1997). It takes into consideration micro-convection between the liquid and the nanoparticles due to Brownian motion, the effect of particle clustering size and the effects of the interfacial thermal resistance.

In the last few years, attempts have been made to model the enhancement in thermal conductivity of CNT nanofluids using liquid layering scenario, fractal theory etc. Xue (1999) modeled the thermal conductivity of CNT nanofluids using field factor `approach,

with a depolarization factor and an effective dielectric constant. Hosseini et al. (2011) uses a set of dimensionless groups based upon the properties of the base fluid, the CNT-fluid interface, and characteristics of the nanotubes themselves, such as diameter, aspect ratio, and thermal conductivity. Patel et al. model (2008) is derived from Hemanth et al (2004), which is given for nanoparticle suspensions. The model considers two paths for heat to flow in a CNT nanofluid, one through the base liquid and the other one through the CNTs. These two paths are assumed to be in parallel to each other. Thus, two continuous media are considered here, participating in the conductive heat transfer mode. Usually, the aspect ratio of CNTs is very high and hence, a continuous net of CNTs available for heat transfer is a valid assumption.

2.7 Measurement of Thermal Conductivity of Liquids

There are three main methods commonly employed to measure the thermal conductivity of nanofluids: The transient hot wire method, the steady- state parallel plate and temperature oscillation.

2.7.1 Transient Hot Wire Method (THW)

In the ideal mode of the transient hot-wire apparatus, an infinitely long, vertical, line source of heat possessing zero heat capacity and infinite thermal conductivity is immersed in a sample fluid whose thermal conductivity is to be measured (Wakeham et al., 1991). The hot wire served both as a heating unit and as an electrical resistance thermometer. In practice, the ideal case is approximated with a finite long wire embedded in a finite medium. Because in general nanofluids are electrically conductive, a modified hot-wire cell and electrical system was proposed by Nagasaka et al. (1981) by coating the hot wire (typically platinum) with an epoxy adhesive which has excellent electrical insulation and heat conduction.

The wire is electrically heated, and the rise in temperature over the time elapsed is measured. Since the wire is essentially wrapped in the liquid, the heat generated will be diffused into the liquid. The higher the thermal conductivity of the surrounding liquid, the lower the rise in temperature will be. To calculate the thermal conductivity of the surrounding liquid, a derivation of Fourier's law for radial transient heat conduction is used (Sarit K Das et al., 2007). The differential equation for the conduction of heat is

$$\frac{\partial^2 T}{\partial x^2}+\frac{\partial^2 T}{\partial y^2}+\frac{\partial^2 T}{\partial z^2}=\frac{1}{\alpha}\frac{\partial T}{\partial t} \tag{2-6}$$

Using a solution presented by Carslaw and Jaeger (1959), the conductivity of a solution can be expressed as

$$k=\frac{q}{4\pi(T_2-T_1)}\ln\frac{t_2}{t_1} \tag{2.7}$$

Where, T_1 and T_2 represent the temperature of the heat source at time t_1 and t_2 respectively.

The transient hot wire method has been used widely to measure the thermal conductivities of nanofluids. However, Das et al. (2003) pointed that possible concentration of ions of the conducting fluids around the hot wire may affect the accuracy of such experimental results.

2.7.2 Steady-State Parallel-Plate Method

This method produces the thermal conductivity data from the measurement in a straightforward manner, the fluid sample is placed in the volume between two parallel

rounds copper plates (figure (2-3)). The two copper plates are separated by small spacers with a specific thickness. There are two heaters, one for upper plate which generates a heat flux to the lower plate and one for the lower plate so as to maintain the uniformity of the temperature in the lower plate. And there are heaters surrounding the whole system to eliminate the convection and radiation losses from the upper and lower plates. The heat supplied by the upper heater flows through the liquid between the upper and the lower copper plates. Therefore, the overall thermal conductivity across the two copper plates, including the effect of the spacers, can be calculated from the one-dimensional heat conduction equation (X. Wang et al., 1999). The disadvantages of steady- state methods are that heat lost cannot be quantified and may give considerable inaccuracy, and natural convection may set in, which gives higher apparent values of conductivity.

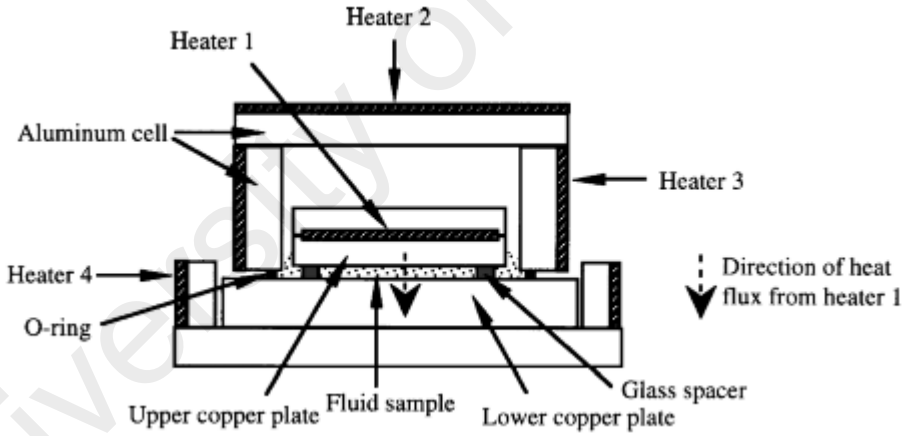

Figure 2.3: Steady State Parallel-plate Setup for thermal conductivity measurement

2.7.3 Temperature Oscillation Method

The apparatus used in this method (figure 2-4), consists of a hollow, insulating cylinder of which central hole is closed from both the sides (surface A and B) by two metal discs, leaving a central cylindrical (C) cavity available for the test fluid. At the surfaces A and B, periodic temperature oscillations are generated with a specific angular velocity.

Analytical solution for temperature distribution for one dimensional, transient heat conduction with periodic boundary condition is used to find the thermal conductivity of test fluid by measuring amplitude attenuation and phase shift in the temperature wave at the inner face of the disc and at the center of cavity. (Patel et al., 2010) The details of the technique are given by Das et al. (1999).

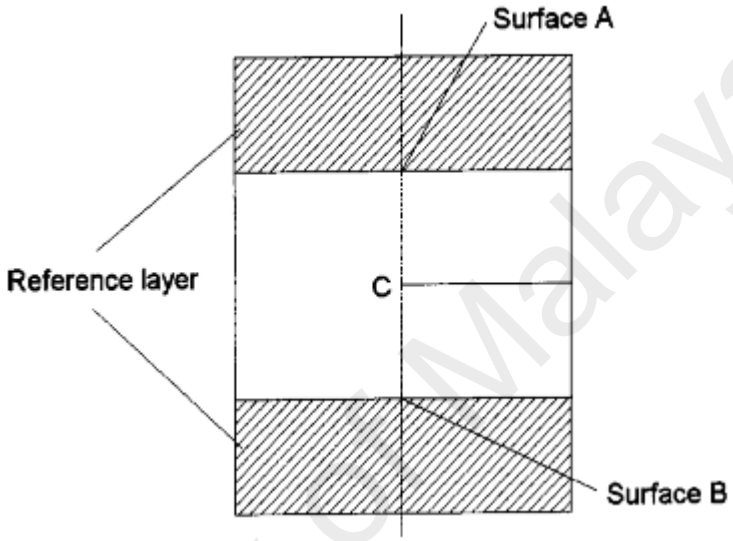

Figure 2.4: Temperature Oscillation Setup

2.8 Dynamic Thermal Test

2.8.1 Shear Flow Test

The primary interest in nanofluids is the possibility of using these fluids for heat transfer purposes. So, the nanofluids are expected to be used under flow condition. To know how these fluids will behave, more studies on its flow and heat transfer feature are needed. Shear rate is a parameter which can affect the thermal conductivity of nanofluid. Lee and Irvine investigated the effect of shear rate on the thermal conductivity of Non-Newtonian fluids (D.-L. Lee et al., 1997). They found that increasing the shear rate would increase the thermal conductivity of the fluid. Shin and Lee measured the thermal conductivity of suspensions containing micro particles (20-300μm) under Couette flow (Shin et al.,

2000). This study also showed that increasing the shear rate had increased the thermal conductivity of the fluids. Although neither of these studies used nanofluids, they are still relevant. Any practical application of nanofluids would subject them to shear. Understanding how they perform under shear, is therefore critical. A setup of similar to that used by Shin and Lee was used in this study to determine the effects of shear on nanofluids.

2.8.2 Pipe Flow Test

Convective heat transfer refers to heat transfer between a fluid and a surface due to the microscopic motion of the fluid relative to the surface. The effectiveness of heat transfer is described by the heat transfer Coefficient, h, which is a function of a number of thermo-physical properties of the heat transfer fluids, the most significant ones are thermal conductivity, k, heat capacity, Cp, viscosity, μ, density, ρ, and surface tension, σ. Although, measurement of the thermal conductivity provides an idea of how effective a nanofluid is as a thermal fluid, it does not show the entire picture. Recently, more tests have been performed to see how nanofluids perform in a convective situation. This is a more telling test because it is much more similar to practical applications, and shows what effects of particle size and viscosity might have on a nanofluid's performance. The majority of these studies have used a pipe flow set up (Anoop et al., 2009; Ding et al., 2006; Fotukian et al., 2010a, 2010b; Heris et al., 2006; Z.-H. Liu & Liao, 2010; Williams et al., 2008). These studies agreed that nanofluids heat transfer coefficient had significantly improved.

Anoop et al. (2009) found 25% increase in alumina nanofluids, with even greater increases in the entrance region. However, an increase in thermal conductivity does not necessarily imply an increase in heat transfer coefficient. Heris et al. (2006) found that

copper based nanofluids had provided an increase in thermal conductivity. However, aluminium based nanofluids showed greater increases in heat transfer coefficient. The authors suggested that the larger particle size and larger viscosity of the copper fluids caused them to perform worse in convection tests. Although these anomalies have been reported by others, there has been far too little testing done to offer conclusive explanations why some nanofluids offer small improvement in convection than in conduction.

2.9 Carbon nanostructure-based nanofluids

Shanbedi et al. (2013) investigated the performance of two-phase closed thermosyphon (TPCT) and multiwalled carbon nanotubes (MWCNT). They reported that presence of functionalized MWCNT leads to 11% improvement in the thermal efficiency of the TPCT. The researchers had reported that the thermo-physical properties such as the thermal conductivity of the nanoparticles played the key role in their applications in heat exchangers (Afshar et al., 2009; Garg et al., 2009; Mahian et al., 2013; Mehta et al., 2007). Graphene nanoparticles (GNP) have higher thermal conductivity than other carbon allotropes such as diamond, SWNT and MWNT (Azizi et al., 2013). As a result GNP has attracted researcher's attention in various scientific fields for manufacturing some items like sensors and batteries. A majority of these usages, however, cannot completely be realized due to poor interaction among GNP and other materials. Thus, in order to increase the interactivity of carbon nanostructures, covalent (aminoacids) and non-covalent (GA) functionalizations were proposed as the common solutions by the researchers (Amiri et al., 2012). Covalent and non-covalent functionalizations are two promising approaches to enhance the GNP dispersibility in aqueous/organic solvents. Non-covalent functionalization of carbon nanostructures is performed by engaging several surfactants

(Amiri et al., 2012; Arzani et al., 2015; Brege et al., 2007; Silvera-Batista et al., 2011; Suttipong et al., 2011). In order to enhance the dispersibility of carbon nano-structures in aqueous media, four common surfactants such as triton X-100, sodium dodecyl benzene sulphonate (SDBS), sodium dodecyl sulphonate (SDS) and gum Arabic (GA) are commonly applied. SDBS and triton X-100 have a benzene function, which produces the powerful **π**–**π** interactions with the surface of carbon nanostructures. It is noteworthy that SDBS has higher dispersibility than that of Triton X-100. This is attributed to the steric hindrance tip chains in triton X-100, which resulted in low concentration of triton on the carbon nanostructures surface (Islam et al., 2003). On the other hand, although GA can provide better condition for dispersion of carbon nanostructures in comparison with SDBS and triton X-100, but it significantly increases the viscosity of the suspension, which may cause numerous problems including increase in pressure drop in thermal equipment (Shanbedi et al., 2013).

2.10 Research gap

There are many theoretical and experimental works have been done on internal flow of nanofluids under different geometries and flow regimes,

- There are a few investigations considering annular pipes. Moreover, there is no comprehensive study on nanofluids flow and their functionalizations in annular pipes.
- Covalent and non-covalent functionalization are two possible methods to prepare carbon nanostructure-based nanofluids, but there is no investigation compare their thermophysical and heat transfer performance.
- Fouling and corrosion phenomena are major problems in heat exchangers

CHAPTER 3: METHODOLOGY

2.11 Experimental apparatus

In the field of heat transfer, the heat transfer coefficient (h) plays a key role in the rate of heat transfer and the performance of thermal equipment. The experimental setup for this work is shown in Figure 3-1. It contains a flow loop, measuring instruments, a cooler, a heating unit and a control unit. The flow loop includes a reservoir tank, a pump, a magnetic flow meter, a differential pressure transmitter, and an annulus test section. The nanofluids were pumped from a 7 Liter capacity stainless steel jacketed tank by a Cole-Parmer magnetic drive pump at a flow rate of 0–8 liter/min, and the pump flow was controlled by a Hoffman Muller inverter. The flow rate and the pressure loss were measured by a magnetic flow meter and a differential pressure transmitter, respectively.

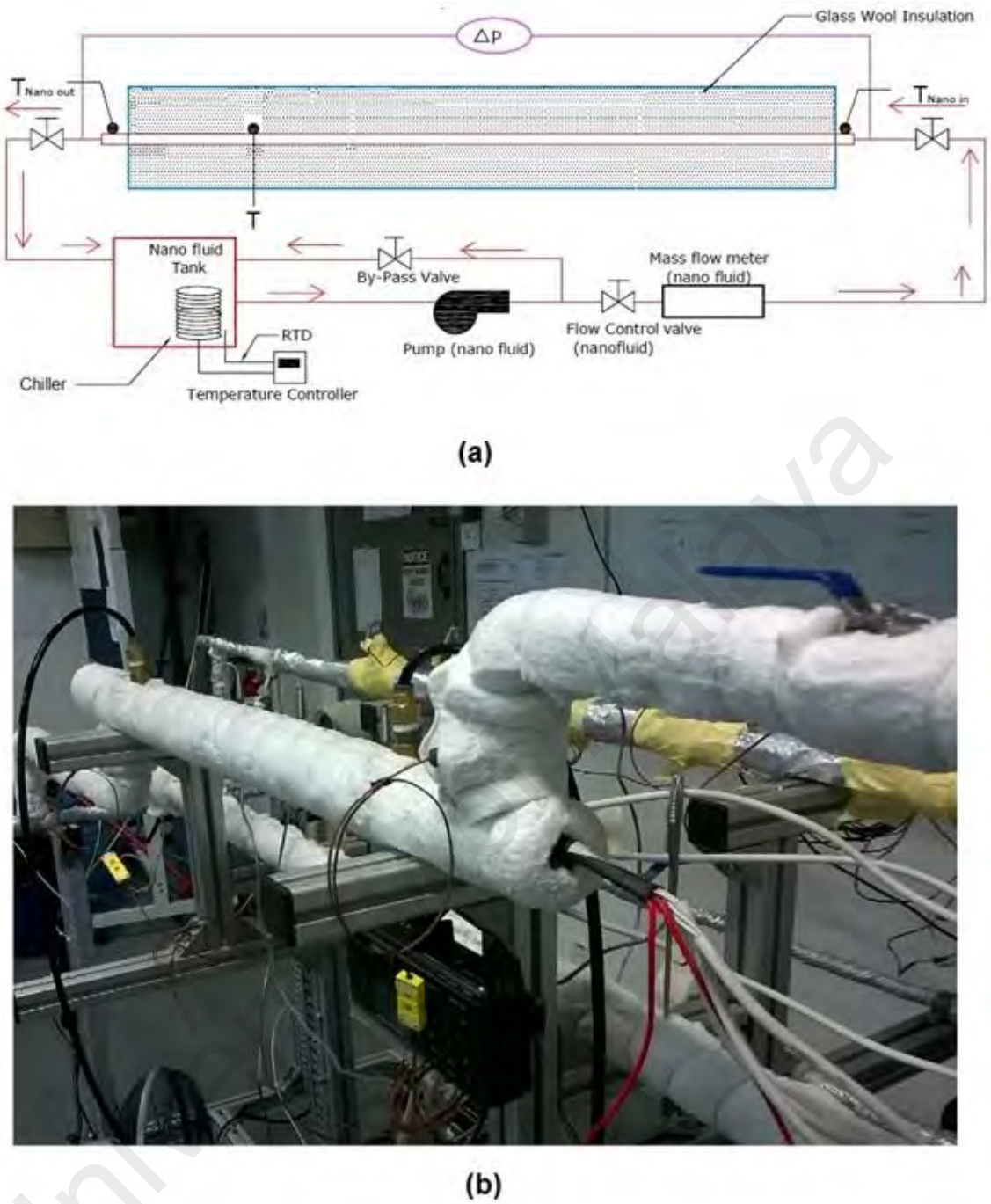

Figure 0.1: (a) Schematic diagram of the experimental setup (b) Experimental test Section for the measurement of the convective heat transfer coefficient.

A straight stainless steel horizontal annulus section formed with a length of 900 mm inner heat generating solid circular cylinder and an outer adiabatic cylindrical boundary with diameters of 15 mm and 26.7 mm, respectively (Figure 3-2). The test section was heated using an ultra-high-temperature heater (Omega, USA) at a maximum power of 3000 W, which was linked to a Variac transformer and a watt/amp meter. Three K type

thermocouples (Omega, Singapore) were embedded at the outer surface of the inner heat generating tube.

To measure the cold and hot nanofluid temperatures, two RTD (PT-100) sensors (Omega, Singapore) were inserted to measure the bulk temperatures at the inlet and outlet of the test section.

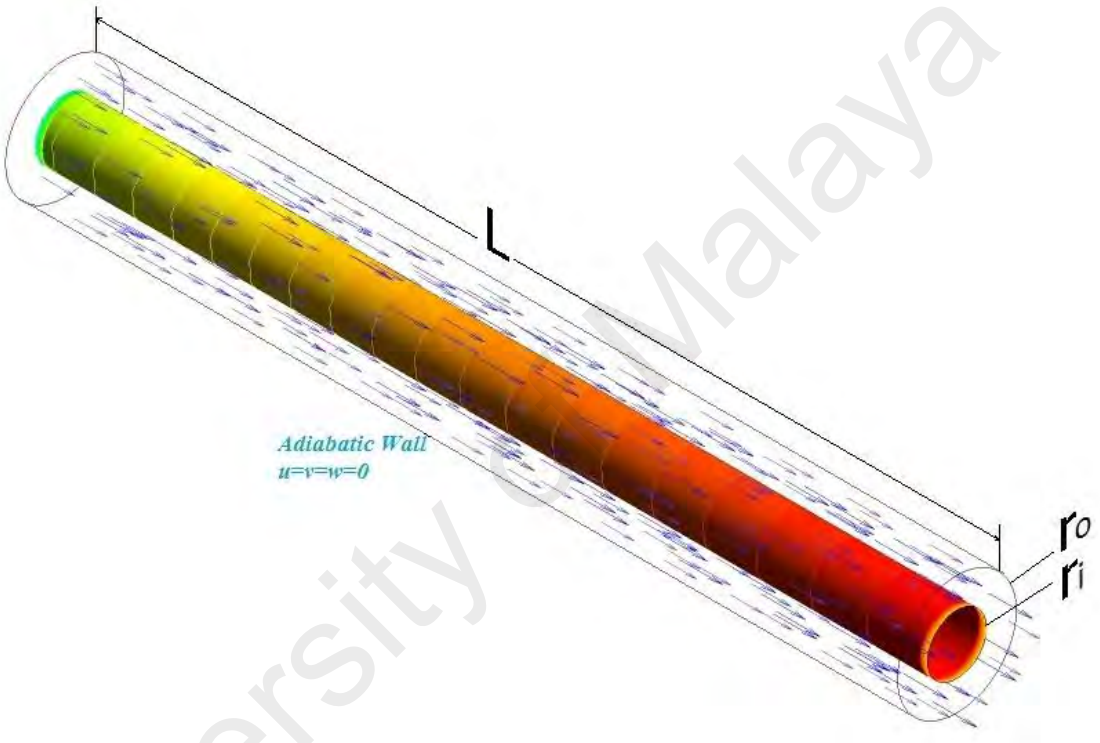

Figure 0.2: Geometrical configuration and boundary conditions of the present study.

Convective heat transfer coefficient is calculated from the measured temperature of surface and bulk by using Eq. (3-1), which is the Newton's cooling law:

$$h = \frac{q}{T_w - T_b} \tag{3-1}$$

Where, q, T_b and T_w, are heat flux, bulk temperature and wall temperature, respectively. Heat flux can be found by using Eq. (3-2).

$$q = \frac{VI}{A} \tag{3-2}$$

Where, V and I are representing the voltage and the current respectively. Internal surface area of the tube is defined as $A = \pi DL$. Three input powers (VI) were considered for the current study are 800, 1000 and 1200W. Also, the temperature profile between the thermocouples and the outer surface of the inner circular pipe were calculated by the Wilson plot method (Fernandez-Seara et al., 2007).

2.12 Numerical Study

The present study employs the mixture model by assuming that two phases are interpenetrating, meaning there is a velocity vector field of the primary phase and also a velocity vector field of the secondary phase, within any control volume each phase has its own volume fraction, and the connection between phases is strong, so nanoparticles closely follow the basefluid flow. The mixture method applications and its accuracy in calculation for nanofluids has been showed by several researchers such as Lotfi et al. (2010), Bianco et al. (2009), Akbarinia and Laur (2009); Mirmasoumi and Behzadmehr and his research group (2007, 2008a and 2008b).

As an alternative for applying the governing equations for each phase, the continuity, momentum and fluid energy equations for the mixture are employed. By looking at the forced convection heat transfer in the turbulent region for incompressible and Newtonian fluid, the governing equations can be presented by equations 3-3 to 3-5 (Shih, 1984):

a). Continuity equation:

$$\nabla.\left(\rho_{eff}\overline{V}\right) = 0 \tag{3-3}$$

b). Momentum equations:

$$\nabla.(\rho_{eff}\bar{V}\bar{V}) = -\nabla\bar{P} + \mu_{eff}\nabla^2\bar{V} - \rho_{eff}\nabla.(\overline{v'v'}) \tag{3-4}$$

c). Conservation of energy:

$$\nabla.(\rho_{eff}C_{p,eff}\bar{V}\bar{T}) = \nabla.((\mathrm{k}_{eff} + \mathrm{k}_t)\nabla\bar{T}) \tag{3-5}$$

In the equations of 3 to 5, the symbols $\bar{V}$, $\bar{P}$ and $\bar{T}$ represent the time averaged flow variables, while the symbol v' represents the fluctuations in the velocity. The term $\rho_{eff}\nabla.(\overline{v'v'})$ in the momentum equations illustrate the turbulent shear stress. The terms k_{eff} and k_t represent the effective molecular conductivity and the turbulent thermal conductivity respectively.

For modeling flow in the turbulent regime, the standard k-ε model can be employed based on the Launder and Spalding study (Launder et al., 1974), which is presented by equations 3-6 to 3-9.

$$\nabla.(\rho_{eff}kV) = \nabla.[(\frac{\mu_t}{\sigma_k})\nabla(k)] + G_k - \rho_{eff}\varepsilon \tag{3-6}$$

$$\nabla.(\rho_{eff}\varepsilon V) = \nabla.[\frac{\mu_t}{\sigma_\varepsilon}\nabla\varepsilon] + \frac{\varepsilon}{k}(C_{1\varepsilon}G_k - C_{2\varepsilon}\rho_{eff}\varepsilon) \tag{3-7}$$

$$G_k = \mu_t(\nabla V + (\nabla V)^T),\ \mu_t = \rho_{eff}C_\mu\frac{k^2}{\varepsilon} \tag{3-8}$$

$$C_{\mu} = 0.09, \sigma_k = 1.00, \sigma_{\varepsilon} = 1.30, C_{1\varepsilon} = 1.44, C_{2\varepsilon} = 1.92 \quad (3\text{-}9)$$

where, μ_{eff} and μ_t are the effective viscosity of nanofluid and coefficient of viscosity in turbulent regime, respectively.

2.12.1 Numerical implementation

Herein, the numerical method available in the commercial CFD package is ANSYS-Fluent, V15 which has been used. Fluent uses a finite volume approach to convert the governing partial differential equations into a system of discrete algebraic equations. Based on the discretization methods, a second-order upwind scheme has been selected for the momentum, turbulent kinetic energy and turbulent dissipation rate equations, whereas the second order upwind for energy equation is selected. For two-phase calculations, the phase momentum equations with the shared pressure are solved in a coupled and segregated fashion. The phase coupled SIMPLE (PC-SIMPLE) algorithm is employed for the pressure-velocity coupling. PC-SIMPLE is an extension of the SIMPLE algorithm to multiphase flows. The scaled residuals for the velocity components and energy are set equal to 10^{-8} and 10^{-9}, respectively.

A structured non-uniform grid distribution has been used to discretize the computational domain as shown in Figure 3-3. Finer grids have been used close to the inner wall where the temperature gradients are high. Several different grid distributions have been tested to ensure that the calculated results are grid independent. It is shown in Figure 3-4 that increasing the grid numbers does not change significantly the Nusselt numbers. Therefore, the total grid points and the elements employed in the whole tube are 147,358 and 395,977, respectively.

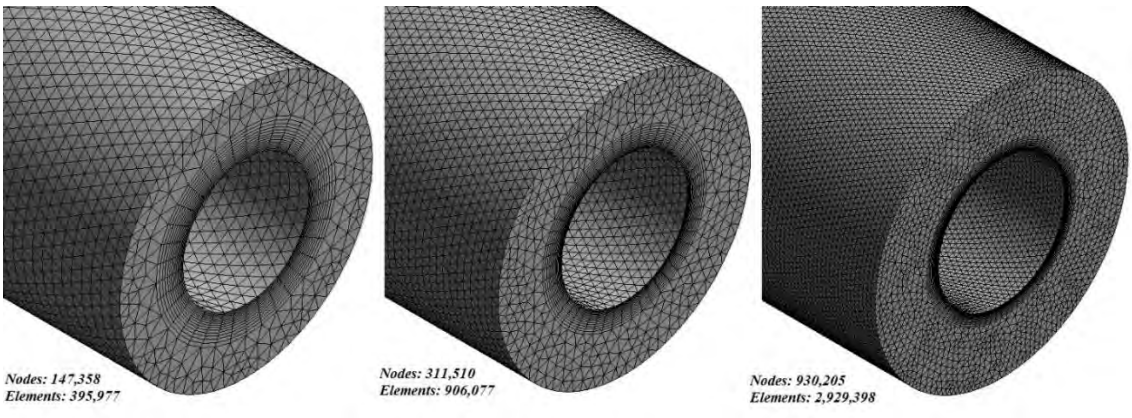

Figure 0.3: Mesh configuration of the present study.

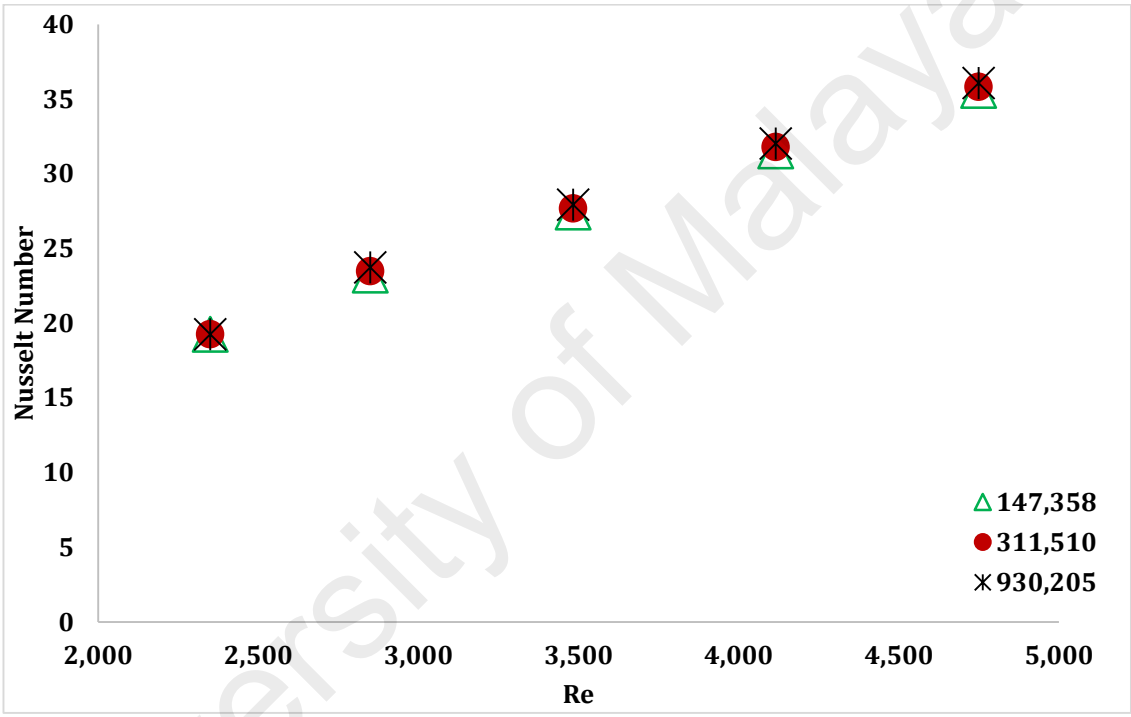

Figure 0.4: Comparison of Nusselt numbers versus Reynolds numbers for basefluid at three different grid distributions.

2.12.2 Accuracy

To evaluate the accuracy and reliability of the experimental and numerical systems before conducting systematic experiments with nanofluids, pure water was tested as the working fluid and compared with the standard empirical equations. Figure 3-5 panels (a) to (c) show a comparison between the Nusselt numbers obtained experimentally and numerically for distilled water and that calculated using theoretically validated equations e.g. the Dittus-Boelter correlation, which is shown in Eq. 3-10.

$$Nu_D = 0.023 Re_D^{4/5} Pr^4 \quad (3\text{-}10)$$

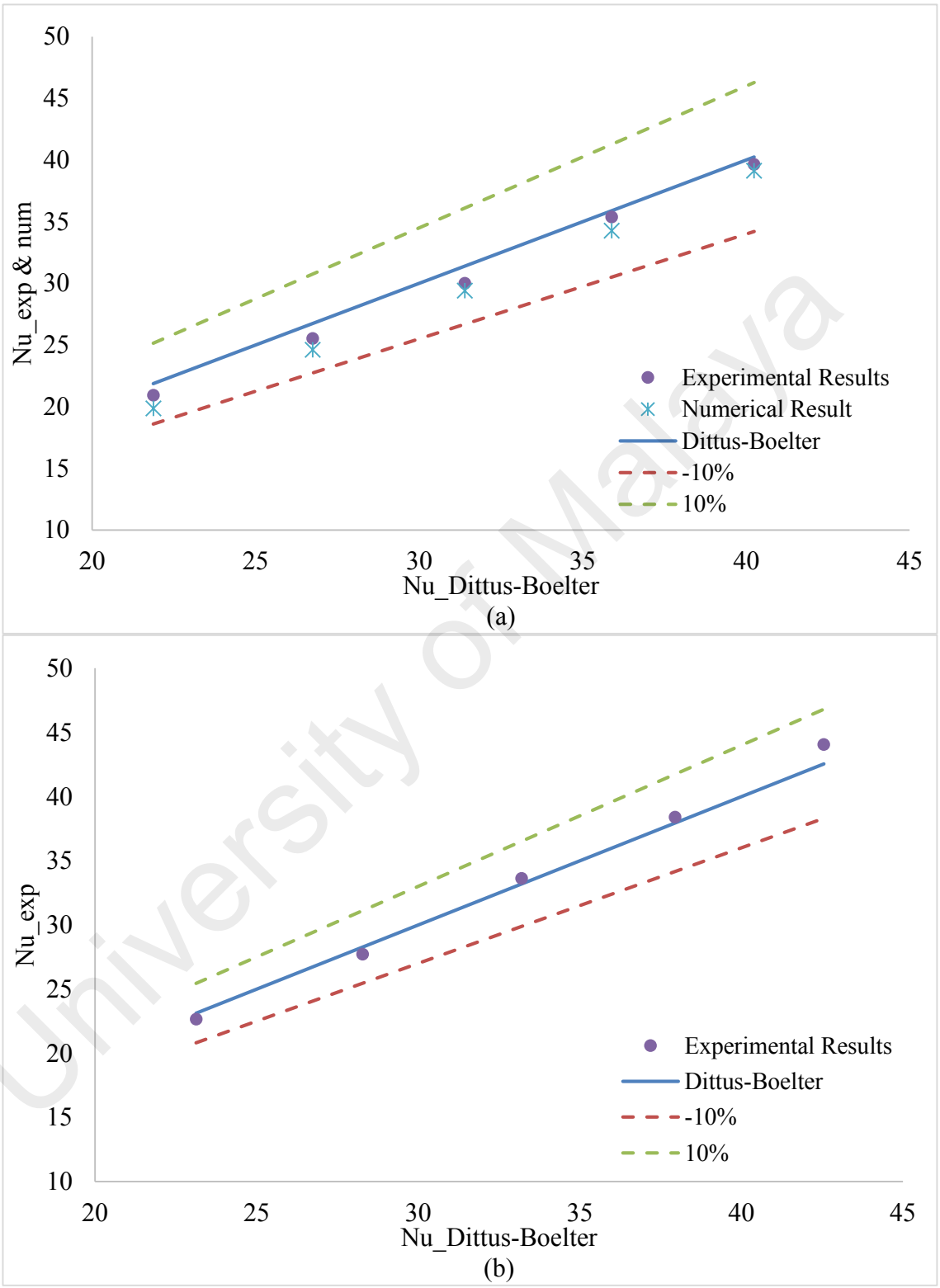

Figure 3.5, continued

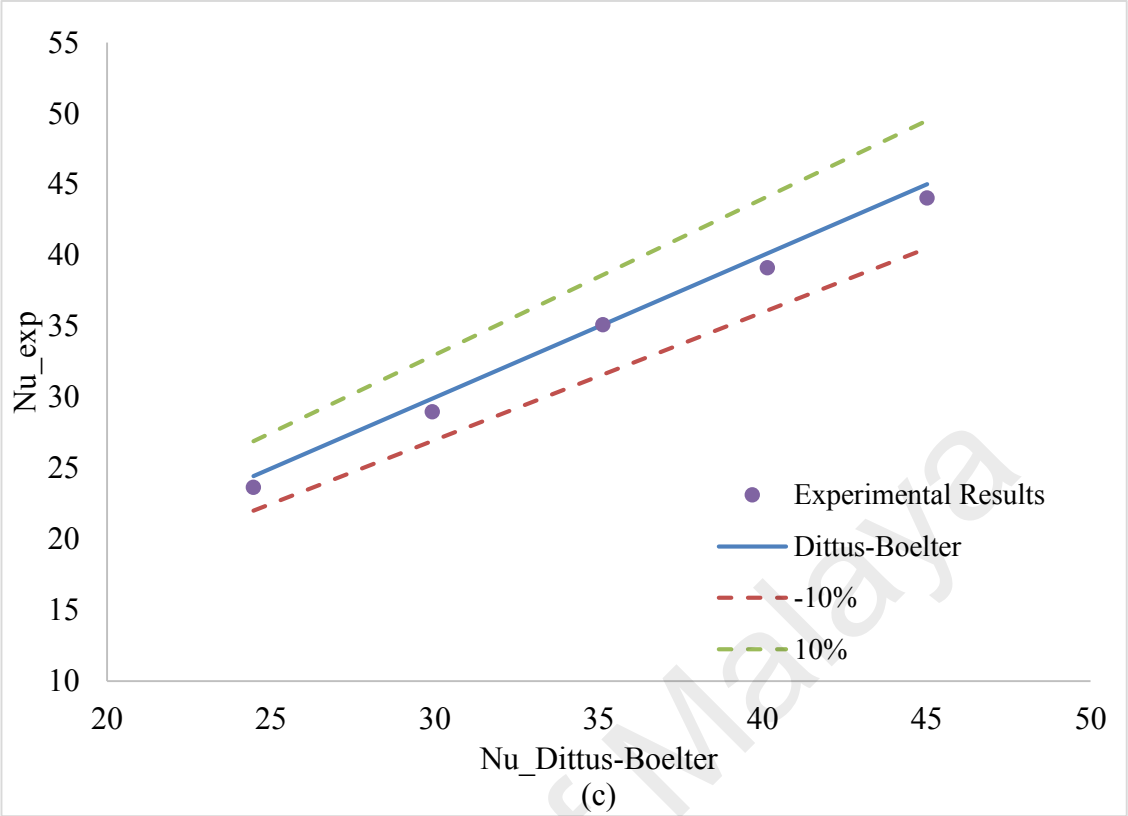

Figure 0.5: Comparison of the experimental Nusselt numbers for distilled water in relation to obtained by the Dittus-Boelter correlation at (a) 800W, (b) 1000W and (c) 1200W.

The deviation between the present prediction obtained from Eq. (3-10) and the experimental values obtained are found to be less than 5%. This indicates that the present test facility is correct and it can be used to evaluate the heat transfer characteristics of samples.

2.13 Physical Properties

Thermophysical properties of coolants such as thermal conductivity, viscosity, density and specific heat are the most important characteristics in the field of heat transfer. The prepared nanofluids were characterized in terms of thermo-physical properties. Specific heat capacities of the base fluid and the nanofluid were measured with a differential scanning calorimeter (DSC 8000, Perkin Elmer, USA) with an accuracy of ±1.0%. Thermal conductivities of the nanofluids were measured by the KD-2 pro device

(Decagon, USA) where KS-1 probe sensors were used having 6 cm and 1.3 mm length and diameter, respectively. The accuracy of the measured thermal conductivity is 5%.To ensure the equilibrium of the nanofluids, an average of 16 measurements were recorded during 4 h for each temperature and weight concentrations. Calibration of instrument with DI water was performed before starting of the measurements of nanofluids. The thermal conductivity of DI water at 30 °C was measured and a value of 0.61 W/mK was found. Also, the rheological properties of the samples were measured on a shear-rate controlled Anton Paar rotational rheometer (model Physica MCR301, Anton Paar GmbH). The densities of water and nanofluids were measured experimentally by Mettler Toledo DE-40 density meter. The accuracy of the density measurement is 10g/cm^3. For each temperature and sample, the measurements were recorded 3 times.

CHAPTER 4: THERMOPHYSICAL AND HEAT TRANSFER PERFORMANCE OF COVALENT AND NON-COVALENT FUNCTIONALIZED NANOFLUIDS IN AN ANNULAR HEAT EXCHANGER

About 24% maximal reduction of thermal resistance in gold-water and titanium dioxide-water nanofluids was presented by Buschmann and Franzke (2014). Shanbedi et al. (2013) investigated the performance of two-phase closed thermosyphon (TPCT) and multiwalled carbon nanotubes (MWCNT). They reported that presence of functionalized MWCNT leads to 11% improvement in the thermal efficiency of the TPCT. The researchers had reported that the thermo-physical properties such as the thermal conductivity of the nanoparticles played the key role in their applications in heat exchangers (Afshar et al., 2009; Garg et al., 2009; Mahian et al., 2013; Mehta et al., 2007). Graphene nanoparticles (GNP) have higher thermal conductivity than other carbon allotropes such as diamond, SWNT and MWNT (Azizi et al., 2013). As a result GNP has attracted researcher's attention in various scientific fields for manufacturing some items like sensors and batteries. A majority of these usages, however, cannot completely be realized due to poor interaction among GNP and other materials. Thus, in order to increase the interactivity of carbon nanostructures, covalent (aminoacids) and non-covalent (GA) functionalizations were proposed as the common solutions by the researchers (Amiri et al., 2012). Covalent and non-covalent functionalizations are two promising approaches to enhance the GNP dispersibility in aqueous/organic solvents. Non-covalent functionalization of carbon nanostructures is performed by engaging several surfactants (Amiri et al., 2012; Arzani et al., 2015; Brege et al., 2007; Silvera-Batista et al., 2011; Suttipong et al., 2011). In order to enhance the dispersibility of carbon nano-structures in aqueous media, four common surfactants such as triton X-100, sodium dodecyl benzene sulphonate (SDBS), sodium dodecyl sulphonate (SDS) and gum Arabic (GA) are

commonly applied. SDBS and triton X-100 have a benzene function, which produces the powerful **π–π** interactions with the surface of carbon nanostructures. It is noteworthy that SDBS has higher dispersibility than that of Triton X-100. This is attributed to the steric hindrance tip chains in triton X-100, which resulted in low concentration of triton on the carbon nanostructures surface (Islam et al., 2003). On the other hand, although GA can provide better condition for dispersion of carbon nanostructures in comparison with SDBS and triton X-100, but it significantly increases the viscosity of the suspension, which may cause numerous problems including increase in pressure drop in thermal equipment (Shanbedi et al., 2013).

The objective of the present chapter is abstracted in the synthesizing of the new kind of fluids, such as graphene nanopletelets-based water nanofluids at different weight concentrations, the experimental investigation of thermophysical properties of covalent and non-covalent nanofluids (GNP-SDBS- and GNP-COOH-based water nanofluids) and numerical simulation of annular heat exchanger in the presence of prepared nanofluids. To realize this goal appropriately, two-phase has been employed. The comparison of analytical and proposed result by simulation in two-phase method confirmed the validity of work. Then, the nanofluids flow in a two dimensional annular pipe has been investigated in different weight concentrations and ratio of heat flux. As a result, Nusselt number profiles and friction factor are measured for both of the synthesized nanofluids.

3.1 Covalent functionalization of GNP

To provide non-covalent nanofluids (GNP-SDBS-based water nanofluid) of known weight concentrations, the given amount of pristine GNP was first weighted, followed by pouring a weight ratio of SDBS/pristine GNP at 0.5:1 into a vessel filled with the given distillated water.

Regarding covalent nanofluid (GNP-COOH-based water nanofluids), based on the technique explained by Wang et al. (1999) with slight modification, carboxylation of GNP was performed. In order to generate carboxylated GNP, 1gr pristine GNP with a mixture of HNO_3 and H_2SO_4 (1:3 volume ratio) were first sonicated for 0.5 h at room temperature in a closed vessel. The GNP suspension was then poured into a Teflon reaction vessel and placed in an industrial microwave (Milestone MicroSYNTH programmable microwave system) with output power of 700 W and heated up to 90ºC for 15 min. The resulting suspension was cooled at room temperature and then diluted with 200mL deionized water to reduce the intensity of acids for filtration. The GNP suspension was filtered through 45 μm polytetrafluoroethylene (PTFE) membrane, and the filtrate was continually washed with the deionized water to remove any unreacted acids. The functionalized sample was dried overnight at 40 ºC in a vacuum. Then, the GNP-COOH produced after microwave phase were dispersed in the deionized water at room temperature. Dispersed concentration of 0.1 wt% was easily obtained in water in the presence of COOH groups on the surface of GNPs.

3.2 Thermophysical properties

3.2.1 Viscosity

The viscosities of GNP-SDBS- and GNP-COOH-based water nanofluids were investigated at different temperatures and concentrations, as presented in Table 4-1. Similar to other coolants, the rheological behaviour of GNP-SDBS and GNP-COOH-based water nanofluids show two essential characteristics: (i) an enhancement in the viscosity with increasing concentration, which means that the concentration of GNP increases, the viscosity increases, and (ii) a decrease in viscosity with increasing temperature, which is due to weakening of the intermolecular forces of the particles and

fluid itself. It can be seen that the enhancement in the viscosity of both synthesized nanofluids are not similar with increase in weight concentration, which obtained by higher viscosity of SDBS. In addition, the results are in agreement with Ko et al. (2007) and Aravind et al. (2011) where viscosity decreases with the increase of temperature.

Table 3-1: Dynamic viscosity of the GNP-SDBS and GNP-COOH-based water nanofluids as the functions of temperature and weight concentration at the shear rate of 140 s^{-1}.

Temp.	Water	GNP-SDBS/Water			GNP-COOH/Water		
		0.025%	0.05%	0.1%	0.025%	0.05%	0.1%
20	0.001002	0.0013	0.0014506	0.0015478	0.0010961	0.0011494	0.0012166
35	0.000761	0.00100985	0.0011418	0.0012785	0.0008407	0.0008639	0.0009264
50	0.000557	0.000789185	0.0009397	0.001118	0.0006293	0.0006757	0.0007313
65	0.000441	0.0006635	0.0008001	0.0009831	0.0004781	0.0005244	0.0006032
80	0.000353	0.000547265	0.000647	0.000835	0.000358	0.000406	0.000457

3.2.2 Density

Also, the densities of GNP-SDBS- and GNP-COOH-based water nanofluids are investigated as the functions of temperature and weight concentration, which are shown in Table 4-2. It could be seen that the density of GNP-SDBS- and GNP-COOH-based water nanofluids decline by increasing the temperature, which can be related to the enhancement in the volume of the liquid with enhancing the temperature. There is an upward trend between the density of GNP-SDBS- and GNP-COOH-based water nanofluids and their weight concentration.

Table 3-2: Densities of the GNP-SDBS- and GNP-COOH-based water nanofluids for different concentrations

Temp.	Water	GNP-SDBS/Water			GNP-COOH/Water		
		0.025%	0.05%	0.1%	0.025%	0.05%	0.1%
20 ºC	0.99823	0.99888	0.99901	0.99991	0.99858	0.99896	0.99966
30 ºC	0.99532	0.99668	0.99783	0.99899	0.99668	0.99733	0.99835
40 ºC	0.99222	0.99355	0.99594	0.99732	0.99323	0.99451	0.99543
50 ºC	0.98411	0.98794	0.98906	0.99134	0.98955	0.99063	0.98878

3.2.3 Thermal conductivity

Table 4-3 is presenting the thermal conductivity plots of GNP-SDBS- and GNP-COOH-based water nanofluids as the functions of temperature and concentration. One can clearly see that the thermal conductivities of GNP-SDBS- and GNP-COOH-based water nanofluids are higher than that of water. Also, it can be seen that a higher increase in the thermal conductivity of GNP-SDBS- and GNP-COOH-based water nanofluids as compared with water and with respect to the temperature. Thus, it confirms that fluid temperature play a key role in increasing the thermal conductivity of GNP-SDBS- and GNP-COOH-based water nanofluids. In comparison with water, the main mechanism of thermal conductivity enhancement with respect to the temperature is attributed to the Brownian motion of the nanoparticles suspended in the basefluid, which is a dominating function of temperature. For basefluids comprising of GNP, the formation of surface nanolayers play an important role in dominating the energy transfer. Liquid molecules can generate layers around the GNP, thereby enhancing the local order of the liquid layer at the interface region. Thus, the liquid layer at the interface would rationally be comprised of a higher thermal conductivity than the basefluid (S. S. J. Aravind et al., 2011; Jha et al., 2008), which announces the critical duty of the created nanolayer in increasing thermal conductivity of the GNP-SDBS- and GNP-COOH-based water nanofluids.

Table 3-3: Thermal conductivity of the GNP-SDBS- and GNP-COOH-based water nanofluids for different concentrations

Temp.	Water	GNP-SDBS/Water			GNP-COOH/Water		
		0.025%	0.05%	0.1%	0.025%	0.05%	0.1%
20 ºC	0.582	0.61	0.63	0.65	0.63	0.66	0.69
30 ºC	0.601	0.63	0.66	0.68	0.67	0.69	0.73
40 ºC	0.624	0.66	0.69	0.71	0.7	0.73	0.778
50 ºC	0.642	0.68	0.7	0.73	0.73	0.76	0.81

3.2.4 Specific heat capacity

The influence of temperature in a range of 25 to 65°C as well as weight concentration of GNP on the specific heat capacity of GNP-WEG coolant was also studied in this work. Table 4-4 shows that an increase in the weight concentrations of GNP-SDBS- and GNP-COOH-based water nanofluids have caused a drop in the specific heat capacities, but they are insignificant in magnitude.

Table 3-4: The specific heat capacity of the GNP-SDBS- and GNP-COOH-based water nanofluids for different concentrations

Temp.	Water	GNP-SDBS/Water			GNP-COOH/Water		
		0.025%	0.05%	0.1%	0.025%	0.05%	0.1%
20 ºC	4.18141	4.15242	4.10371	4.05532	4.16429	4.11031	4.0563
30 ºC	4.18001	4.15287	4.10416	4.05603	4.16497	4.11127	4.05693
40 ºC	4.17914	4.15245	4.10399	4.05587	4.16405	4.11095	4.05644
50 ºC	4.18009	4.15277	4.10409	4.05599	4.16477	4.11051	4.05667

3.3 Numerical study

A horizontal annulus formed between an inner heated solid circular cylinder and an outer isothermal cylindrical boundary undergoing a turbulent convection flow which is used for the numerical study.

At the inlet, temperature was set up to 308˚K and the tube wall was exposed to 50000 (W/m^2), which was uniform. The analyses were performed up to 1000 iterations until the calculated results reached the steady state.

The numerical study on the turbulent forced convection flow of non-covalent functionalized nanofluids (GNP-SDBS-based water nanofluids) and covalent functionalized nanofluids (GNP-COOH-based water nanofluid) in an annular tube have been performed at various Reynolds numbers and weight concentrations. There are 24

cases of simulations where weight concentrations of 0%, 0.025%, 0.05%, 0.1% and the Reynolds numbers of 5000, 8000, 10000, 13000, 15000 and 17000 have been selected.

Figures 4-1 and 4-2 are respectively presented the convective heat transfer coefficients and the average Nusselt numbers of pure water, GNP-SDBS- and GNP-COOH-based water nanofluids as a function of the Reynolds number. It can be seen that some lines with different slopes, which increased with increase in Reynolds number as well as concentration of both types of GNPs. This phenomenon can be attributed to the higher thermal conductivity of basefluid in the presence of GNPs. The maximum heat transfer coefficient enhancements for GNP-SDBS and GNP-COOH-based water nanofluids are 21.9% and 28.9% respectively for a weight fraction of 0.1% which indicates higher heat transfer rate of covalent functionalized nanofluid samples to non-covalent functionalized one. Amiri et. al. (2015) compared non-covalent and covalent nanofluids in the thermosyphon and achieved 35% and 68% respectively and it also confirms that covalent functionalized nanofluid shows higher heat transfer rate compared to non-covalent one.

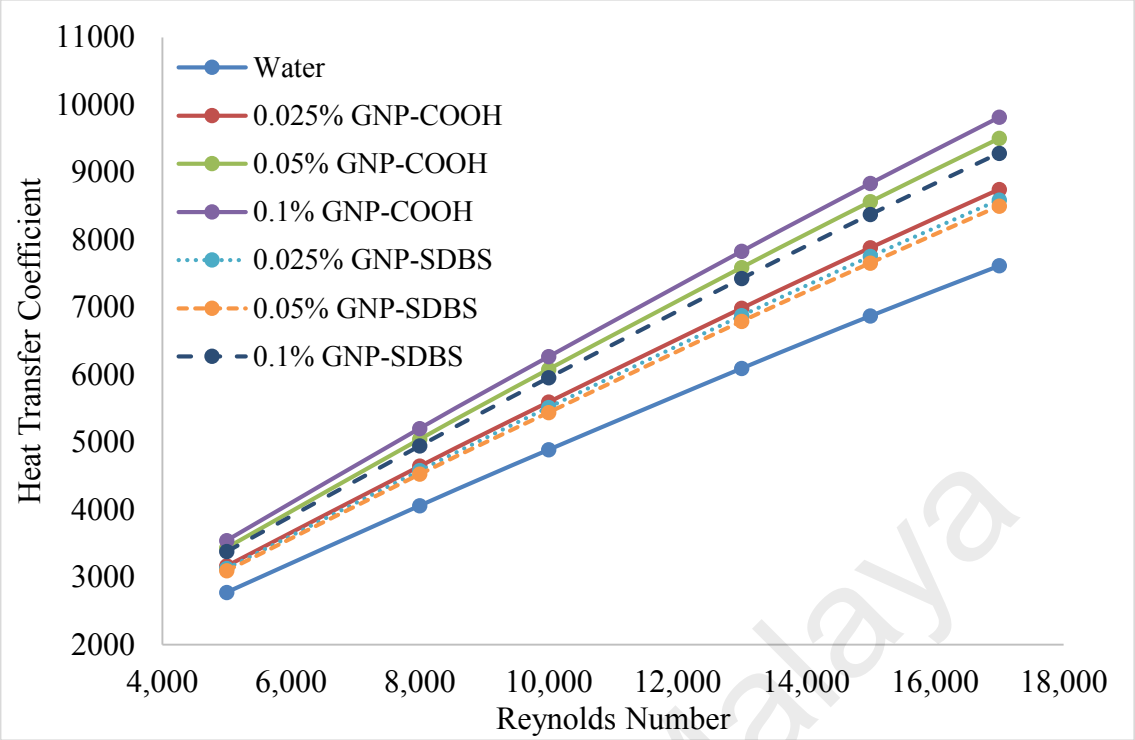

Figure 3.1: Average heat transfer coefficients of GNP-SDBS and GNP-COOH-based water nanofluids as a function of Reynolds numbers.

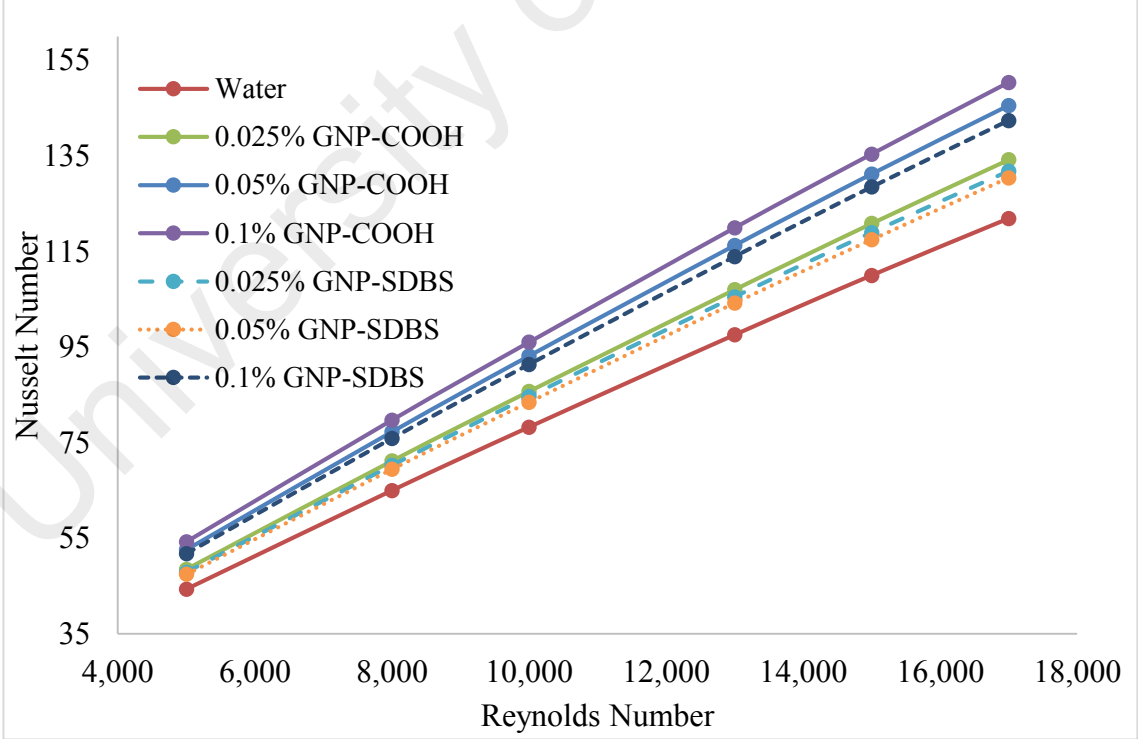

Figure 3.2: Average Nusselt numbers of GNP-SDBS and GNP-COOH-based water nanofluids as a function of Reynolds numbers.

The friction factor at different Reynolds number and weight concentrations of GNP-SDBS and GNP-COOH are shown in Figure 4-3. It can be seen that the friction factor decreases with increasing of the Reynolds number and/or volume flow rate at different concentrations. The friction factor also increases as the concentration of GNP increases in both the samples comprised of GNP-SDBS and GNP-COOH and the minimum value of friction factor is indicated for the basefluid.

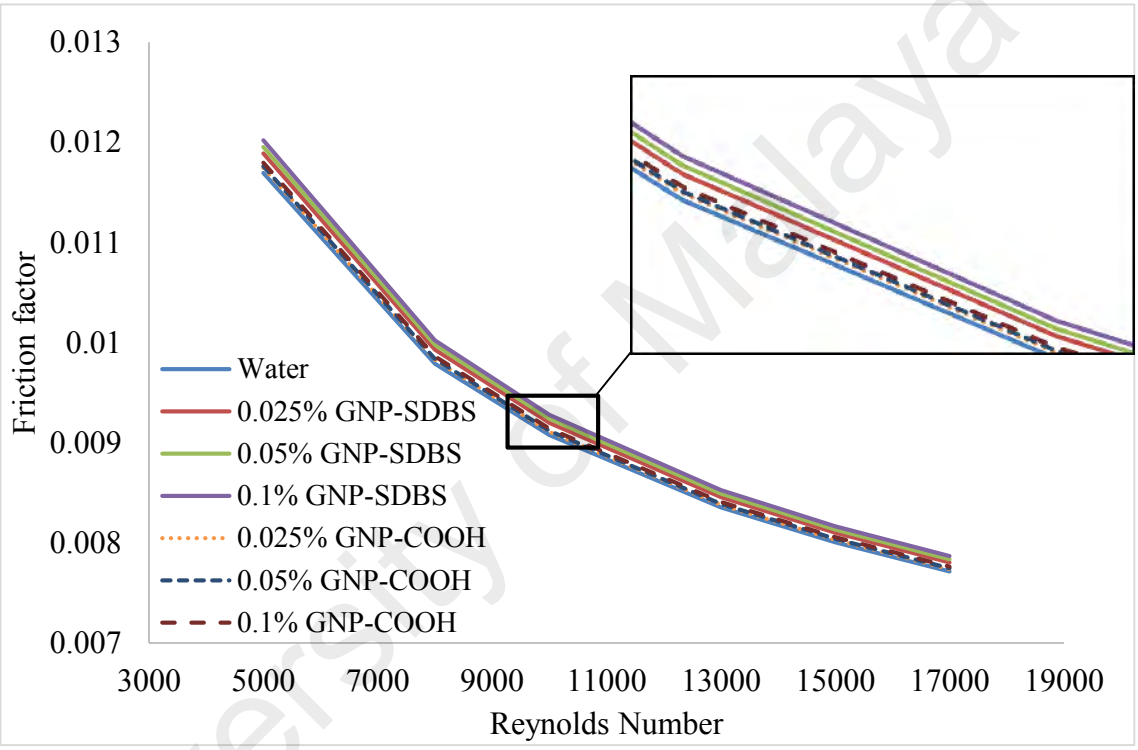

Figure 3.3: Friction factor of GNP-SDBS and GNP-COOH-based water nanofluids as a function of Reynolds numbers.

Also, as the Reynolds number increases, friction factor dependence on the concentration is not changed, implying more similarity to the data obtained for water. It is obvious that Brownian motion play an essential role in momentum transfer between the nanoparticles and basefluid molecules at low Reynolds numbers, resulting in an enhancement in the friction factor than that of the basefluid (Amiri et al., 2015; Amiri et al., 2012). However, this mechanism cannot be dominant at high Reynolds numbers. In summary, the viscosity of the working fluid has not played a key role in decreasing the friction factor at high

Reynolds numbers and the velocity can be considered as the most important parameter in increasing the friction factor compared to the basefluid results.

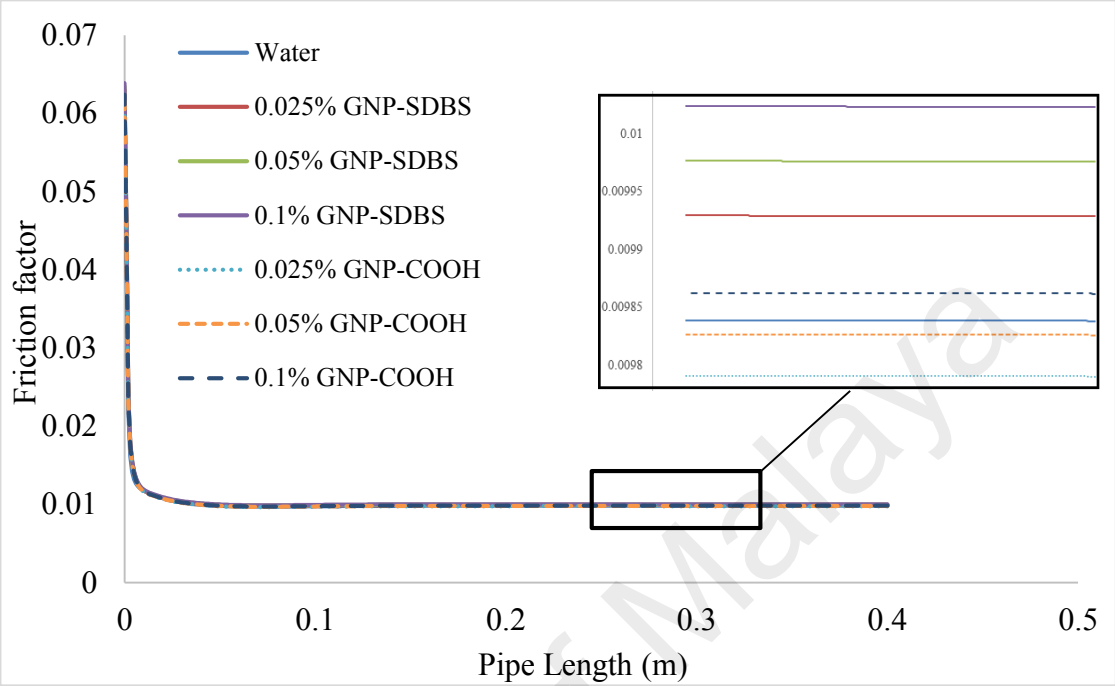

Figure 3.4: Friction factor throughout the tube for different concentrations of GNP-SDBS and GNP-COOH.

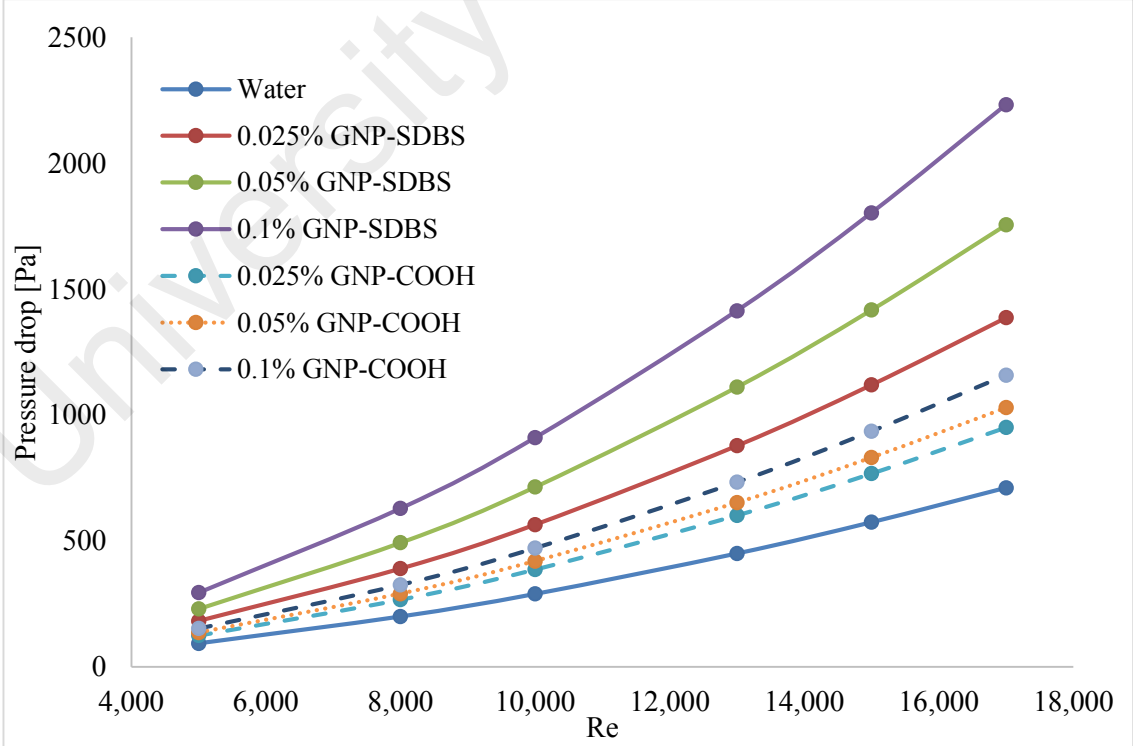

Figure 3.5: Relation between pressure drops along the annulus for various Reynolds numbers and concentrations.

The friction factor at different Reynolds number and weight concentrations of GNP-SDBS and GNP-COOH as function of axial positions are shown in Figure 4-4. The extent of friction factor remains same throughout the tube.

Figure 4-5 shows the measured pressure drop at different Reynolds numbers and concentrations of nanofluids. Figure 4-5 predicts that with the increase of the inlet velocity and concentration of nanofluids the pressure drop increases. The pressure drops for GNP-COOH/water nanofluids at various concentrations are not quit close to that for water. This observation confirms that the effect of GNP concentration on the viscosity of nanofluids and consequently on the pressure drop is significant, especially in the presence of GNP-SDBS. On the other hand, as the concentration of GNP-SDBS increases, the variation of pressure drop with the Reynolds number shows sharper slope. Thus the GNP-SDBS/water nanofluid at the mass fraction of 0.1% and Reynolds number of 17,000 shows the maximum pressure drop. Expectedly, the viscosity curves and the pressure drop curves have represented similar trends in the presence of covalent and non-covalent samples, which could have been caused from the direct connection between the viscosity and the pressure drop.

CHAPTER 5: INVESTIGATION OF THERMOPHYSICAL PROPERTIES AND HEAT TRANSFER RATE OF COVALENTLY FUNCTIONALIZED MWCNT IN AN ANNULAR HEAT EXCHANGER

Among the different nanostructures applied for creating nanofluids, carbon nanotubes (CNT) have enhanced the thermal efficiency of different setups due to promising thermal properties (Amiri et al., 2012; Shanbedi et al., 2013). The results reported by Azizi et al. (2013), Xue et al. (2006) and Liu et al. (2010) shown that nanofluids including nanoparticles with higher heat transfer coefficient like graphene and CNT can be more appropriate for heat transfer applications.

Azizi et al. (2013) studied the influence of graphene-water nanofluid on the heat transfer performance and resistance of two-phase closed thermosyphon (TPCT). They reported that increasing the volume fraction leads to the heat transfer enhancement of the TPCT. On the other hand, increase of the input power and nanoparticles' concentrations have caused a decrease in the thermal resistance of the TPCT. In two investigations, Shanbedi et al. (2013) considered influence of the covalent and noncovalent functionalization on the performance of TPCT. They concluded that functionalized carbon nanotubes with ethylene diamine had better heat transfer coefficient than the non-covalent functional groups. They also presented that covalent functionalization of CNT improved the thermal efficiency of the TPCT more than those functionalized by gum Arabic as a non-covalent group. In the field of functionalization, decreasing in the heat transfer efficiency was attributed to the non-covalent groups. Non-covalent functional groups cover around the carbon nanotubes surface and reduce the effective area which leads to less TPCT efficiency. Amiri et al. (2012) reported that the nature of covalent functional groups may also affect the thermal performance.

The objectives of the present chapter are abstracted in introducing a promising, potentially industrially scalable, cost-effective method for preparing highly-dispersive carbon nanotubes in aqueous media, and investigation of the thermophysical properties of the synthesized samples at different weight fractions. Accordingly, the experimental study on the convective heat transfer in an annular heat exchanger was performed. The obtained results were validated with the analytical results and confirmed the authenticity of the test rig. Then, the nanofluids flow through annular pipe was investigated for different weight fractions and Reynolds numbers. Here, the results of heat transfer coefficient, Nusselt number profiles, pressure drop and the pumping power were are evaluated for the synthesized nanofluids.

4.1 Functionalization procedure

To reach suitable colloidal suspension with multi-walled carbon nanotubes (MWCNT), covalent functionalization could be selected as one of the best methods. Therefore, aspartic acid as a hydrophilic group was selected to decorate on the surface of MWCNT. To reach highly-dispersive MWCNT in water, a pre-functionalization with carboxyl groups was done to make a bridge for attaching Asp molecules. So, pristine MWCNT was stirred with a mixture of H_2SO_4-HNO_3 acids in a volume ratio of 1:1 for 24 h at 60°C. After filtering and simultaneously rinsed with deionized water, the filtrate cake was dried. Then, 1gr oxidized MWCNT and 1gr aspartic acid in 200ml DMF and 10ml toluene was kept under ultrasonic for 2 hours and then stirred for 12 hours. To increase reaction rate, $ZrCl_4$ (5% mol) as catalyst was used for doing direct amidation (Allen et al., 2012). Eventually, the resulting suspension was filtered, rinsed with deionized water, DMF and THF to delete non-reacted aspartic acid and dried in the oven for 48h at 50°C.

4.2 Preparation of nanofluid

Anton Paar rheometer (Physica MCR 301, Anton Paar GmbH) was employed to investigate the rheological behavior of the suspensions. The experiment was performed three times in order to approve the accuracy of the data measured by rheometer. With a KD2 thermal properties analyzer based on the transient hot-wire method, thermal conductivity of the suspension was measured. For synthesizing MWCNT-Asp/water nanofluids, the MWCNT-Asp was first dispersed in the given amount of water for 1 hr by a probe ultrasonic with the power of 600 W and 20 kHz (Sonics & Materials, Inc., USA). Next, the abovementioned MWCNT-Asp/water nanofluids were prepared for the measurements of their thermophysical properties.

4.3 Dispersibility

Figure 5-1 shows the quantitative analysis of the dispersion state and the long-term stability of the MWCNT-Asp/water coolants in UV–Vis spectroscopy for different weight fractions. Here the absorbance at the wavelength of 264 nm was measured during 30 days for different weight concentrations. It can be seen that the relative concentration of MWCNT-Asp decrease insignificantly over time. As a result, the maximum sediment of about 20% was obtained for highest weight concentration of 0.1, which confirmed the suitable dispersibility of MWCNT-Asp in water.

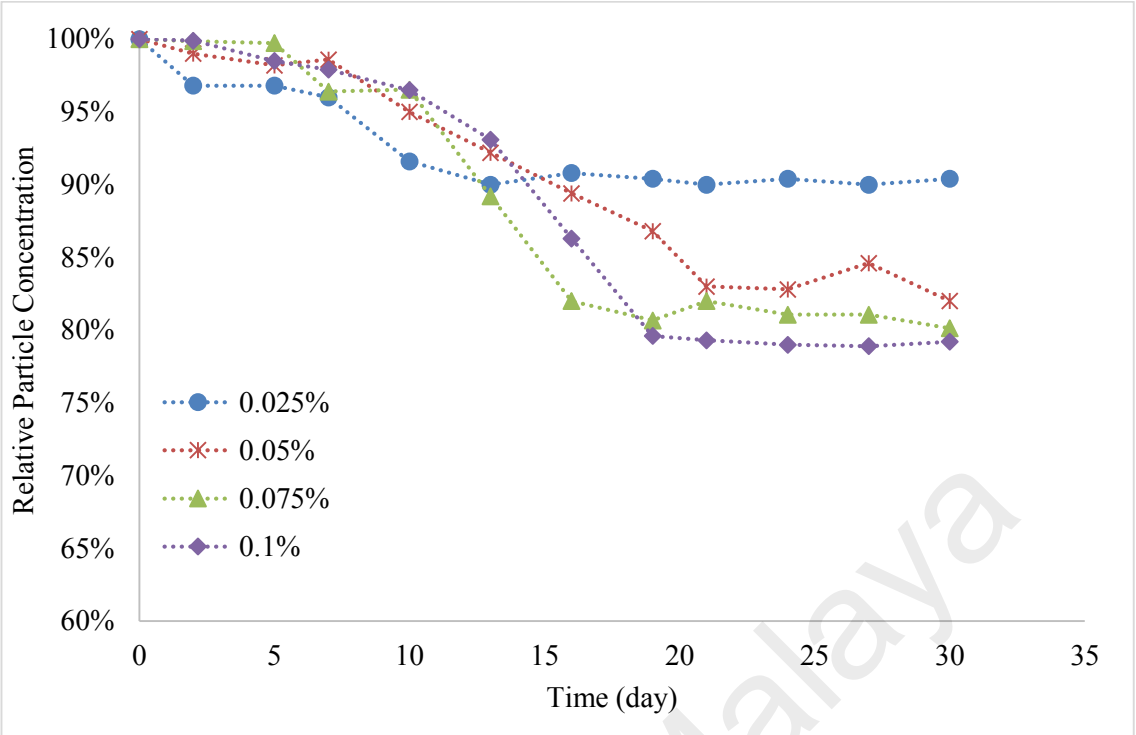

Figure 4.1: Colloidal stability of the MWCNT-Asp/water as a function of time at different volume fractions.

4.4 Functionalization analysis

Raman spectroscopy indicates necessary information in order to estimate the covalent functionalization of the MWCNT and has been regarded as one of the main characterization method for examining functionalization (Amiri et al. 2015). This method can establish a great sensitivity to the disordered band on the structure depending on the optical skin depth (Amiri et al., 2011). The Raman spectra of the pristine MWCNT and MWCNT-Asp are presented in Figure 5-2, indicating the D and G bands at 1343 and 1576 cm^{-1}, respectively. The G band at 1576 cm^{-1} is related to the motion in opposite direction of two high carbon atoms of graphitic sheet. The respective pattern can denote the presence of the crystalline graphitic carbon in MWCNT. On the other hand, the D band around 1343 cm^{-1} is associated to the amorphous carbon, which occurred by adding functional groups to the backbone.

The intensity ratios of D and G bands ($I_{D/G}$) can be employed for assessing the amount of amorphous carbon relative to graphitic carbon (Amiri et al., 2011). It can be observed in Figure 5-2 that the $I_{D/G}$ ratio of MWCNT-Asp are more than pristine MWCNT, because of the increase in the structure defects, indicating effective functionalization of the MWCNT with target groups. Here, the remarkable fact is that the higher the $I_{D/G}$ value, the higher extent of covalent amidation will be.

Also, TGA curve of the pristine MWCNT and MWCNT-Asp are indicated in Figure 5-3. While no weight loss is observed in the curve of pristine MWCNT, a sharp weight loss is obvious in the temperature range of 100–250ºC for the MWCNT-Asp.

The surface morphology of the MWCNT-Asp was investigated by TEM for more evidence. Figure 5-4 indicates the TEM images of the MWCNT-Asp. After functionalization, some of the nanotubes lost their caps. So, opening end of MWCNT was ascribed to the acid treatment part, demonstrating that nitric acid may decrease the length and open end-caps of MWCNT (Amiri et al. 2015).

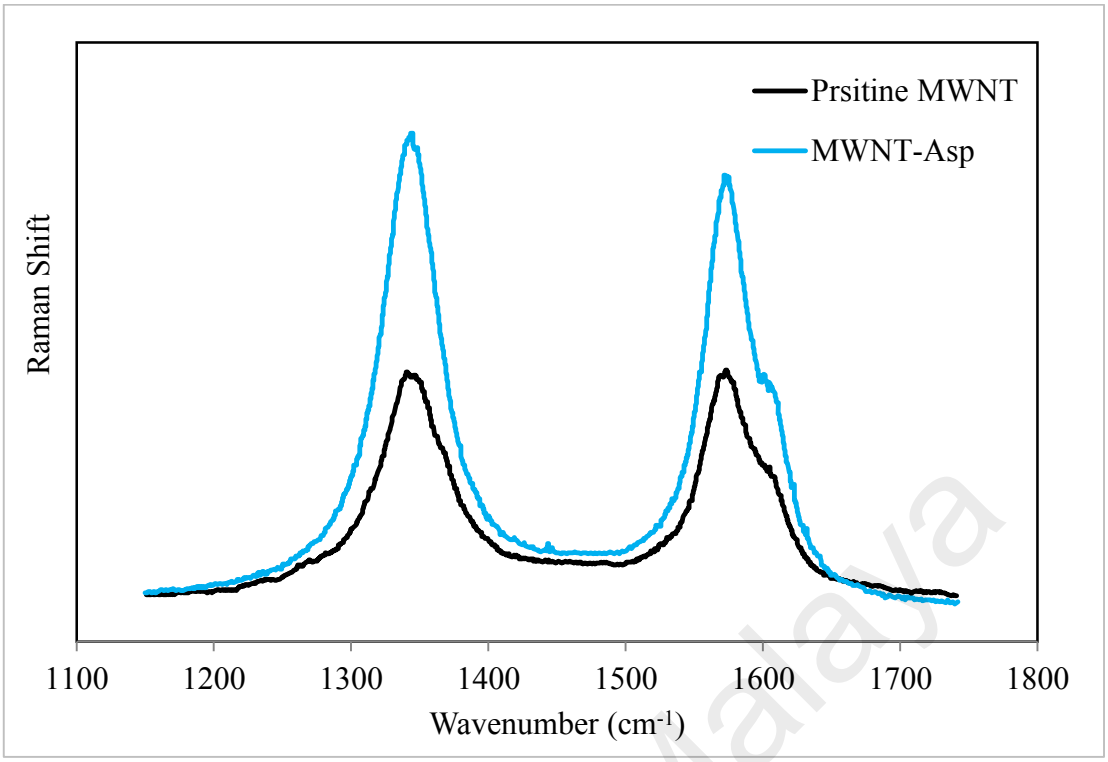

Figure 4.2: Raman Spectra of pristine MWCNT and Asp-treated MWCNT.

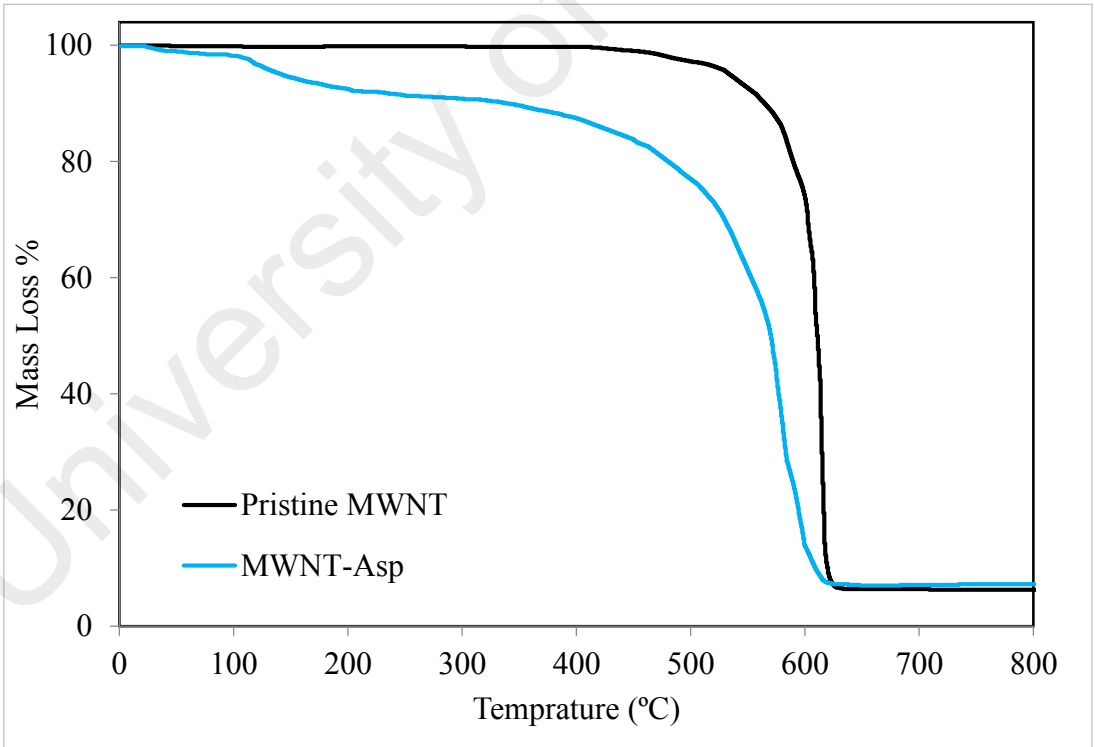

Figure 4.3: TGA curves of pristine MWCNT and Asp-treated MWCNT.

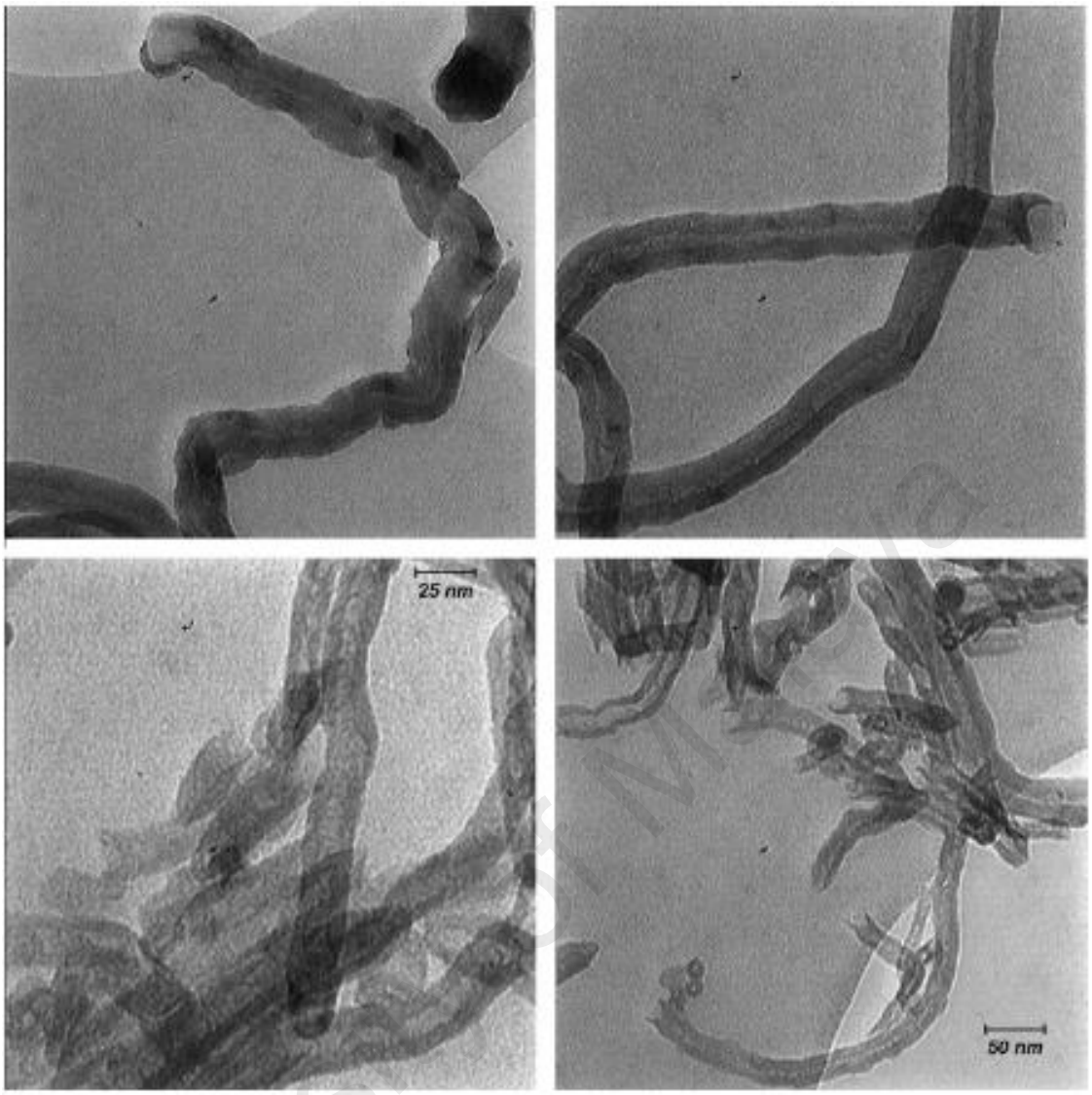

Figure 4.4: TEM images of MWCNT-Asp.

4.5 Physical Properties

Thermophysical properties of coolants such as thermal conductivity, viscosity and density are the most important characteristics in the field of heat transfer. Experimental results about thermophysical properties of MWCNT-Asp/water was compared with pure water, which are shown in Figures 5-5 to 5-7. Figure 5-5, 5-6 and 5-7 show the experimental data of the density, viscosity and thermal conductivity at different temperatures of 20, 40, 60 and 80°C, respectively. Density is one of the thermophysical properties of fluids that can affect the convective heat transfer coefficient. Experimentally measured densities of

the MWCNT-Asp/water for different weight concentrations and water are shown in Figure 5-5 for different temperatures. The results show that the density of prepared coolants increases with increasing temperature and concentration, and expectedly they are higher than those of base fluids.

Viscosity is a crucial parameter in the dynamic design of nanofluids for heat transfer applications, especially in systems including pressure drop. By loading nanoparticles into the water, viscosity increases slightly. With increasing concentration, the viscosity of nanofluids increases and opposite trend obtains for increasing temperature. At all the temperatures and concentrations, the highest viscosity was for the nanofluid with weight concentration of 0.1%.

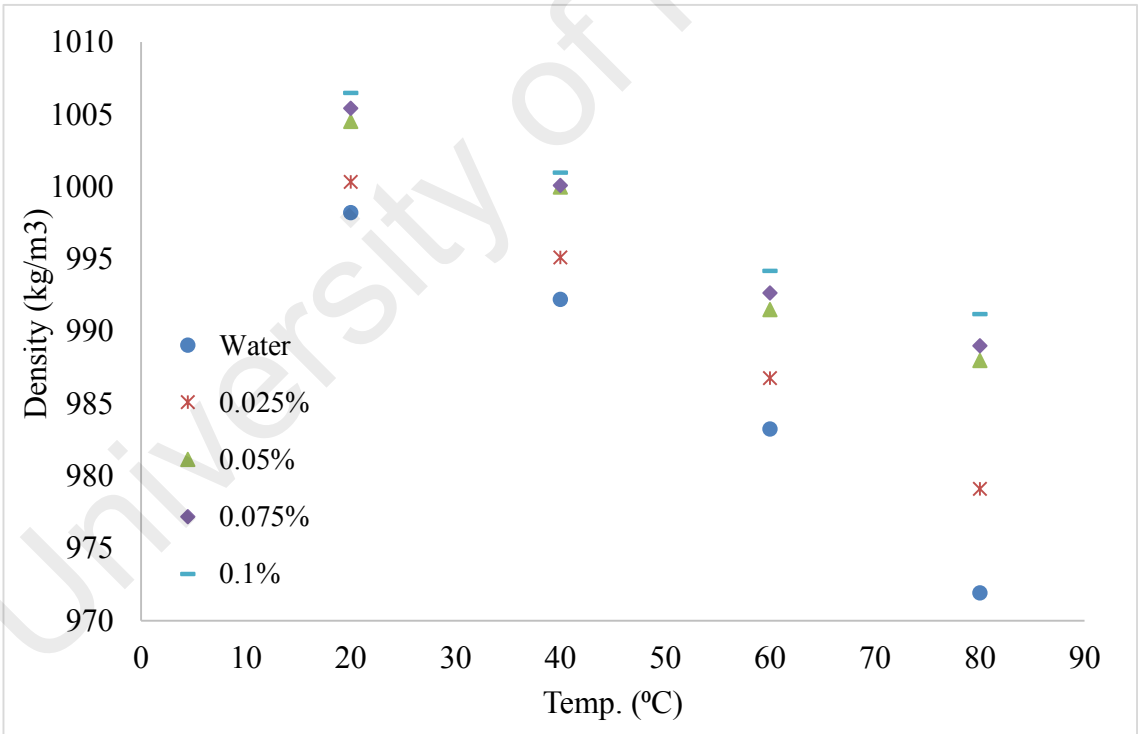

Figure 4.5: Densities of the MWCNT-Asp/water and water for different weight concentrations (kg/m^3) as a function of temperature.

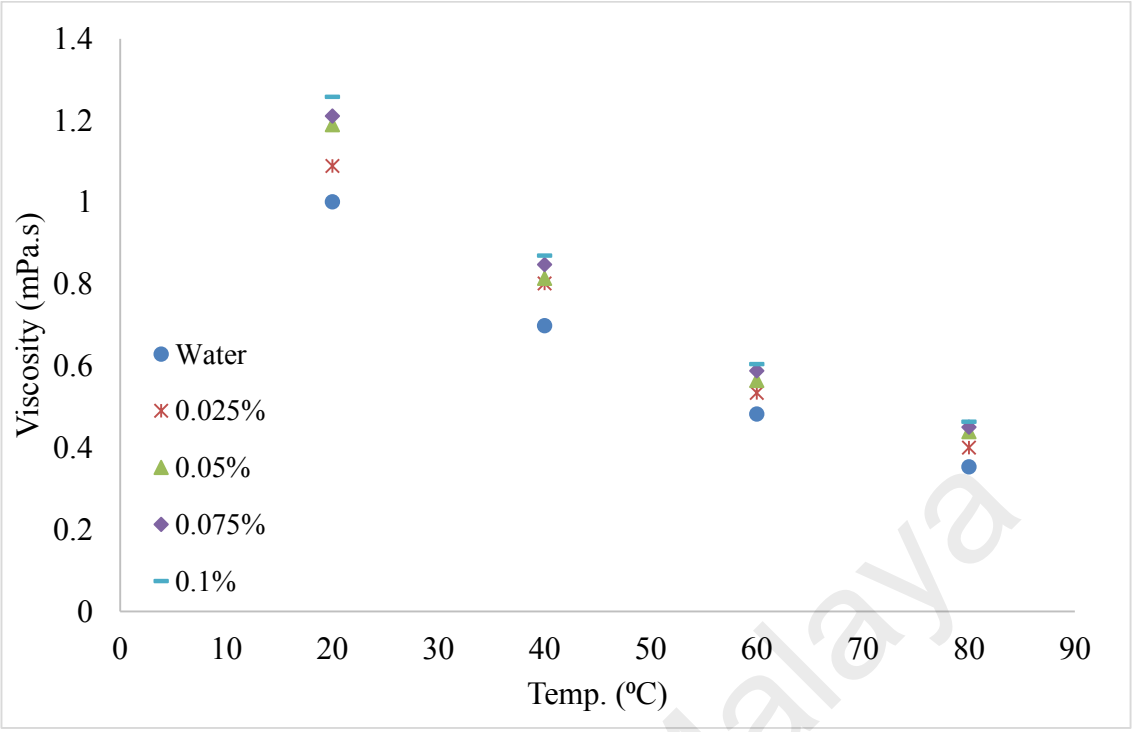

Figure 4.6: Dynamic viscosity of the MWCNT-Asp/water and water as a function of temperature and weight concentration at shear rate of 140 s^{-1} (mPa.s).

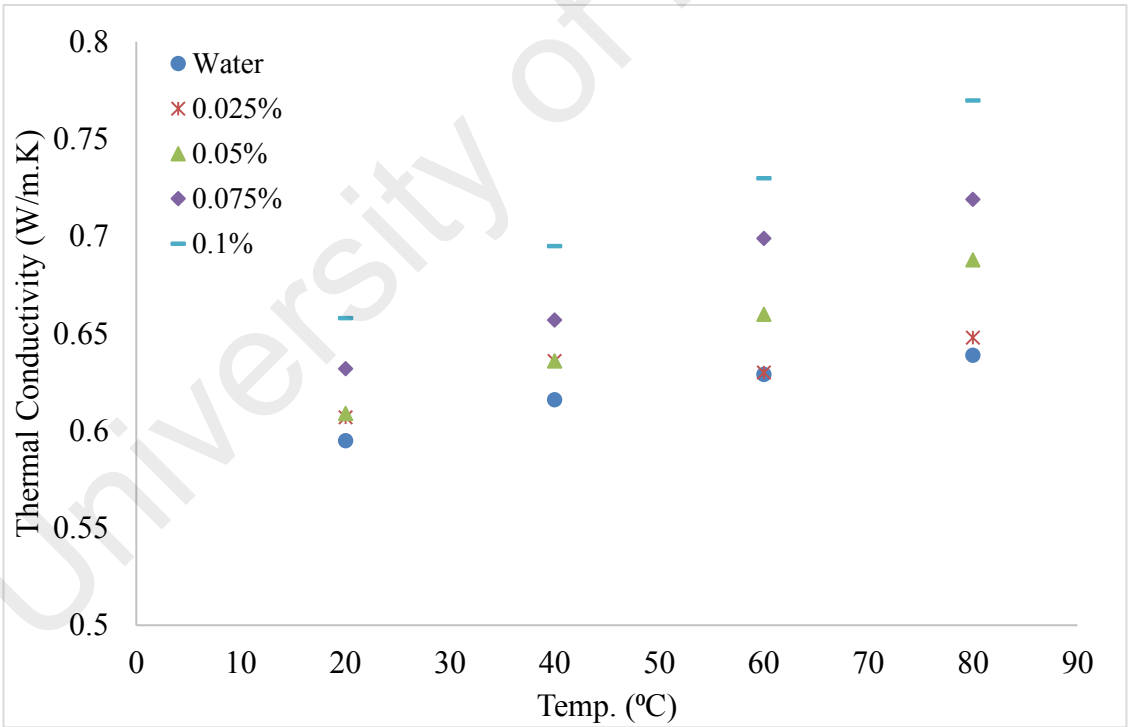

Figure 4.7: Thermal conductivity of MWCNT-Asp/water and pure water (W/m.K) as a function of temperature.

Thermal conductivity of working fluid is one of the key parameters in evaluating heat transfer rate of heat exchangers. It can be seen that the thermal conductivities of nanofluids were experimentally obtained and shown in Figure 5-7. The results show that the thermal conductivities of the nanofluids improve with increasing MWCNT-Asp and is definitely higher than pure water. Also, as the temperature increases, the thermal conductivity increases, which is more significant at higher concentration.

4.6 Thermal analysis

MWCNT-Asp/water was tested for the Reynolds numbers range of 2440± 20 to 6800± 20, four weight concentrations (0.025, 0.05, 0.075 and 0.1%) and three input powers to the test section (800, 1000 and 1200W). Figure 5-8(a-c) shows the heat transfer coefficient plots of MWCNT-ASP as a function of Reynolds number and weight concentrations. In addition, the comparison between the measurements and the predicted results are illustrated in Figure 5-8(a) and 5-9(a). The experimental results were in a good agreement with the numerical with a deviation percentage of 4.6%. It is realized that the enhancement of heat transfer coefficient of MWCNT remarkably exceeded those of the thermal conductivity improvements for different weight concentrations. The maximum heat transfer coefficient at concentration of 0.1%, Reynolds number of 6,807 and input power of 1200W is 22.4%. According to Aravind et al. (2013 and 2011), applying a simple analogy that the convective heat transfer is proportional to $k/\delta t$, where δt is the boundary thickness of thermal boundary layer. Therefore, increasing k and/or decreasing δt lead to an increase in the heat transfer coefficient. Noticeably, as reported by some researchers (Aravind et al., 2013; Ding et al., 2006), carbon nanostructures such as graphene and CNTs decrease thickness of thermal boundary layer. As a result heat transfer coefficient improves significantly compared to that of thermal conductivity.

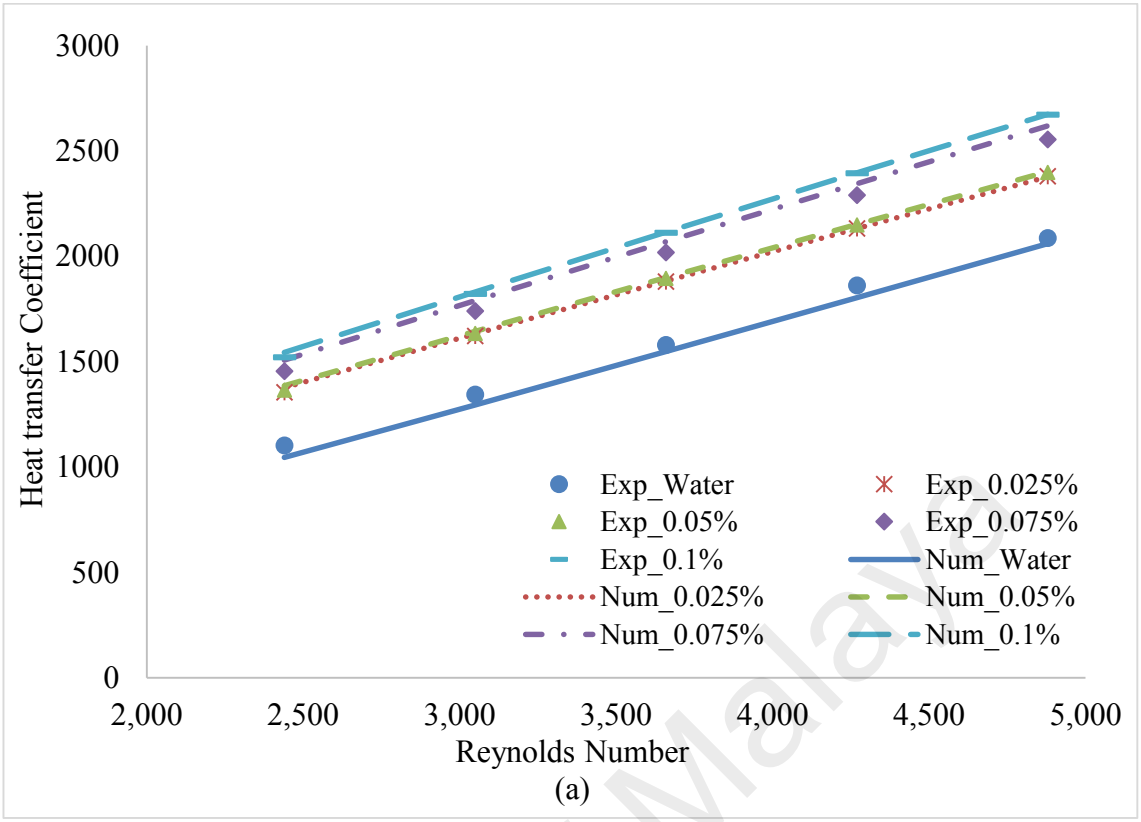

(a)

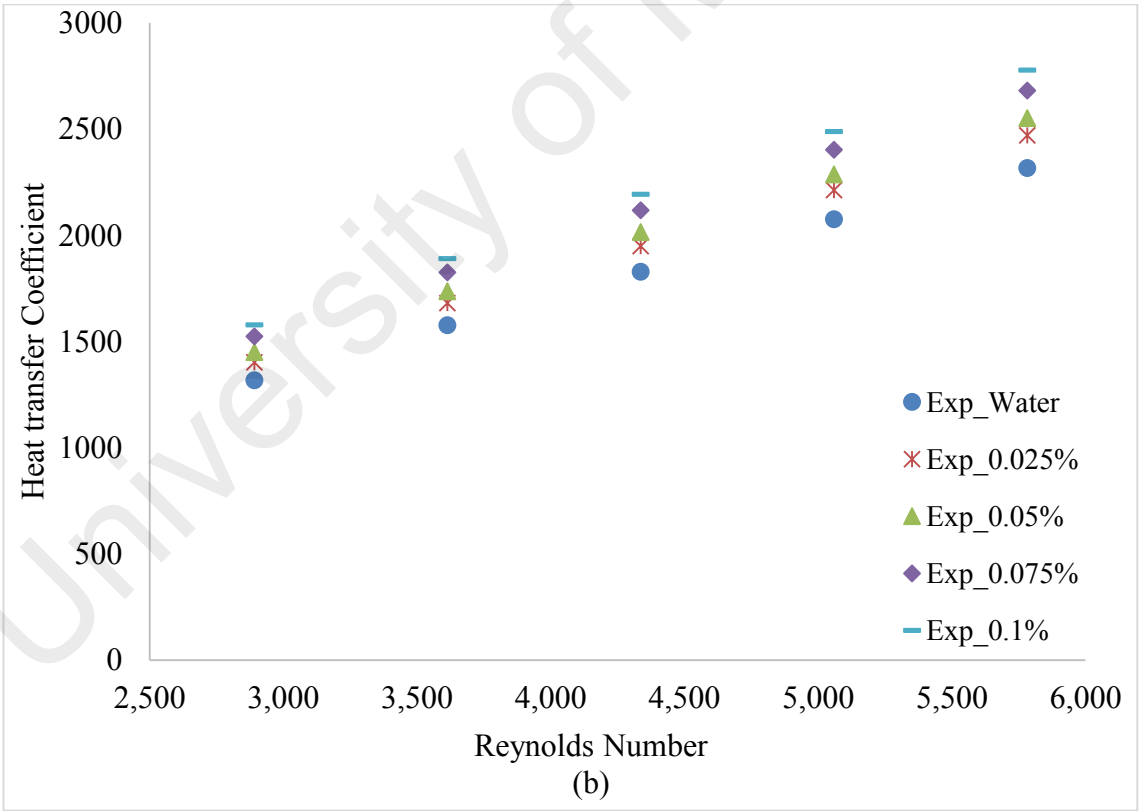

(b)

Figure 5.8, continued

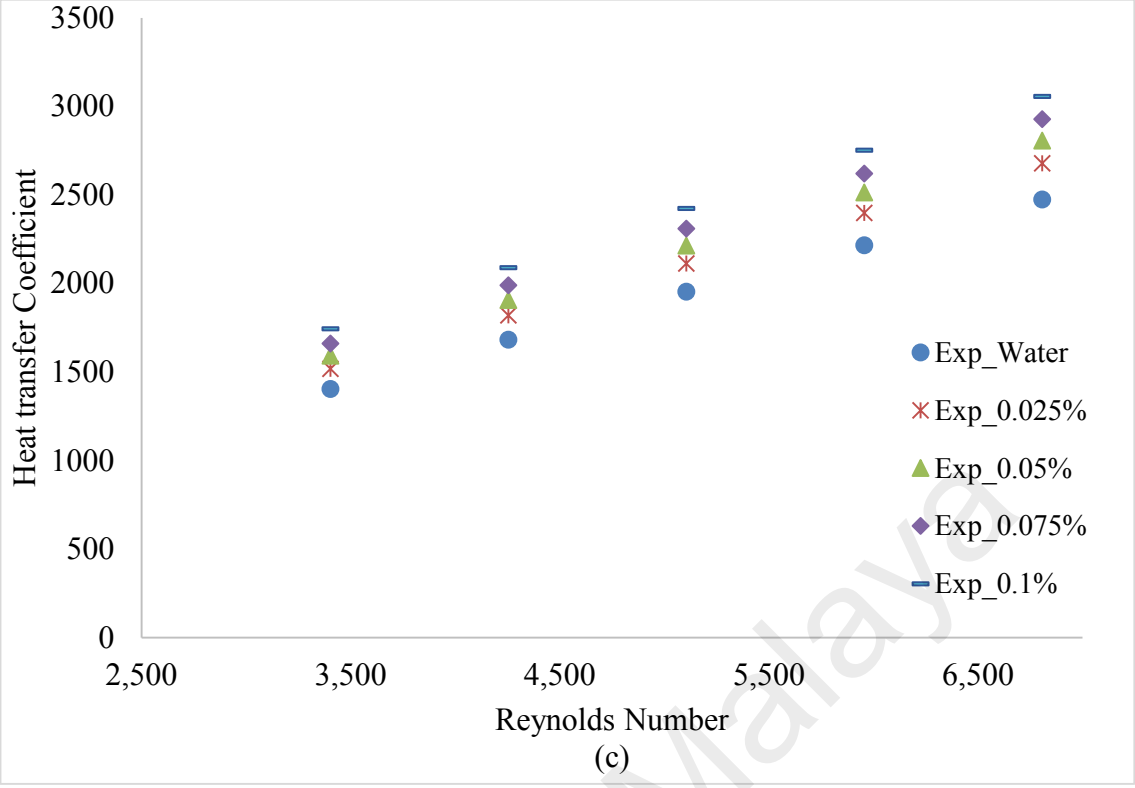

Figure 4.8: Comparison of the heat transfer coefficient obtained for distilled water and MWCNT-Asp/water nanofluid for different weight concentrations at (a) 800W, (b) 1000W and (c) 1200W.

Figures 5-9(a-c) show the average Nusselt numbers of MWCNT-Asp/water nanofluids for various weight concentrations and Reynolds numbers. To evaluate the ratio of convective to conductive heat transfer of MWCNT-Asp/water coolants, Nusselt number plots have been employed. The results suggest that the Nusselt number increases remarkably in the presence of treated samples in comparison to the applied basefluid. The MWCNT-Asp loading in basefluid improves the thermal conductivity of basefluid, which leads to the lower temperature difference between the bulk fluid and the tube wall, indicating higher Nusselt numbers and subsequently heat transfer rate. Figure 5-10 illustrates heat transfer performance of the MWCNT-Asp/water coolant at different heat fluxes for a constant weight concentration of 0.1%, where Nusselt number increases with the enhancement of Reynolds number. It could also be noted that the Nusselt number increases with the increase of heat fluxes to the test section.

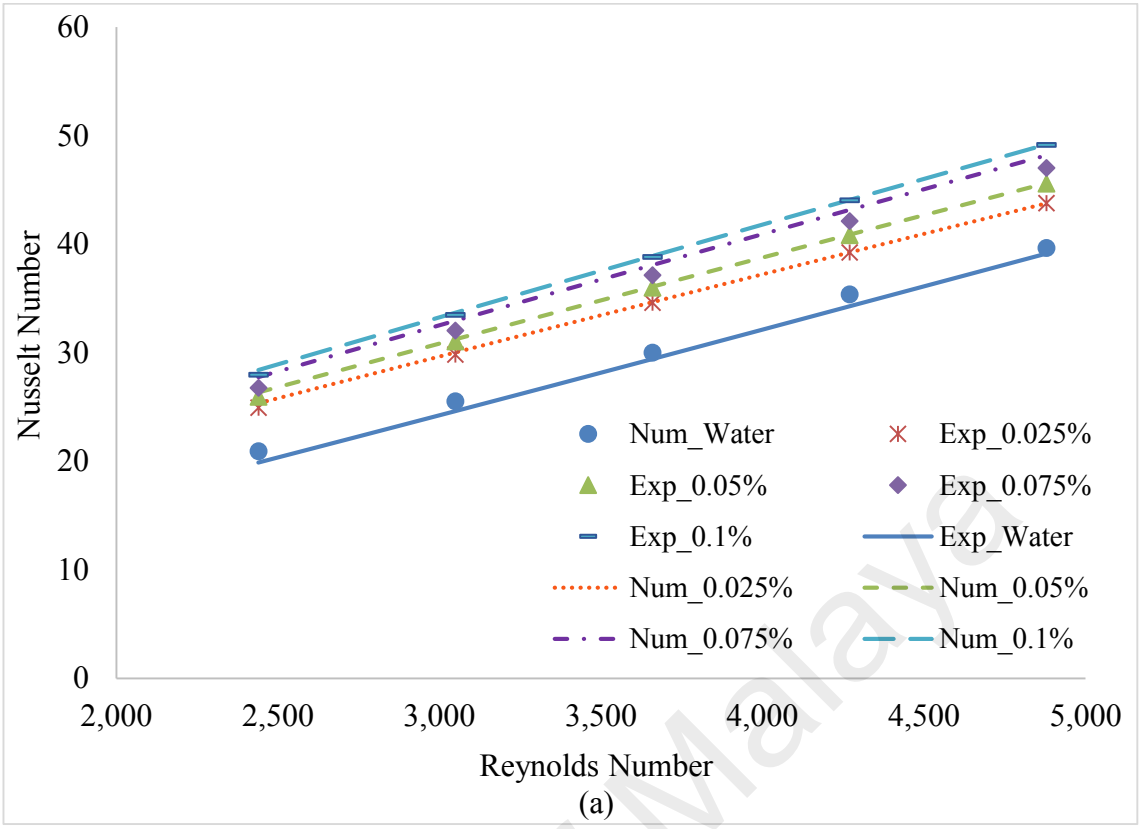

(a)

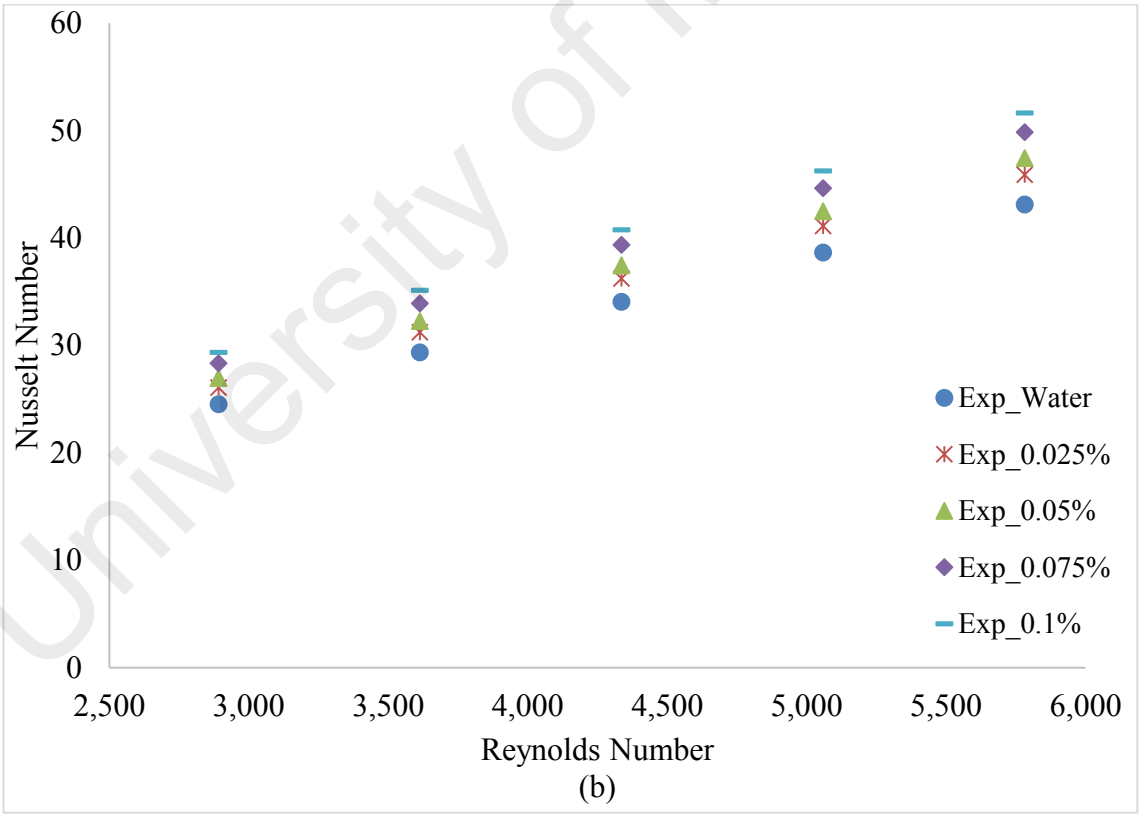

(b)

Figure 5.9, continued

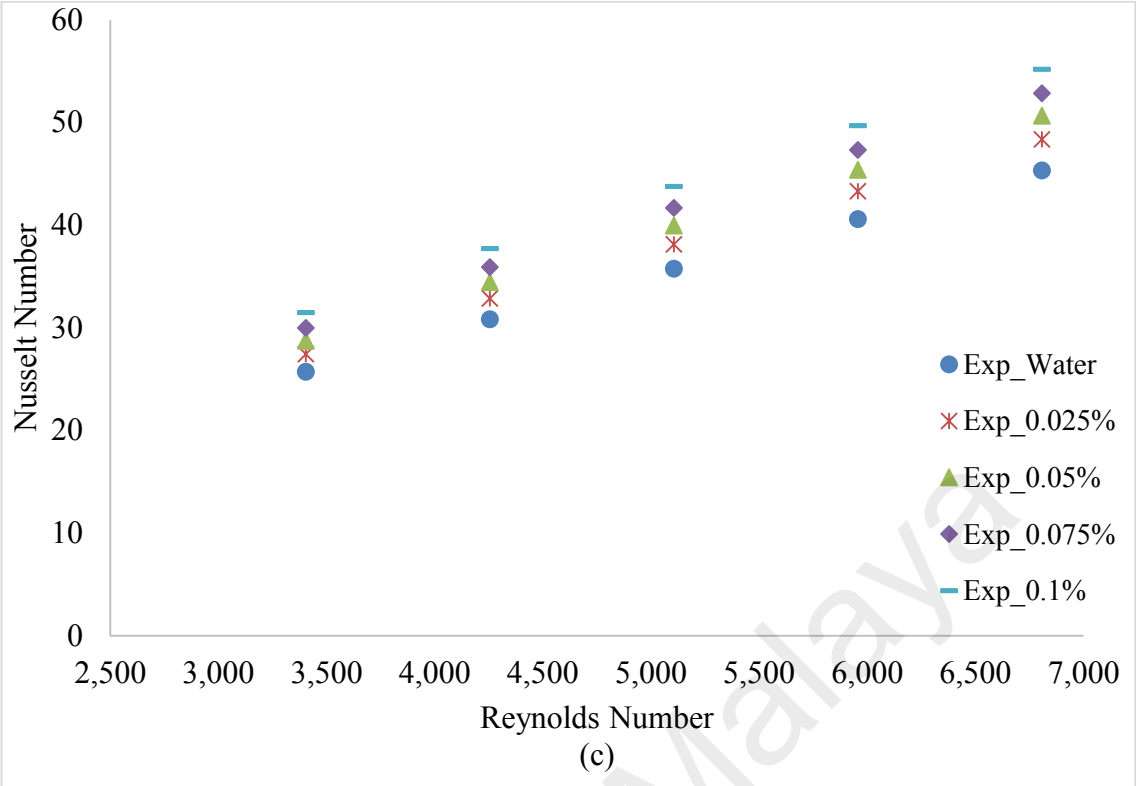

Figure 4.9: Comparison of Nusselt numbers obtained for distilled water and MWCNT-Asp/water for different weight concentrations at (a) 800W, (b) 1000W and (c) 1200W.

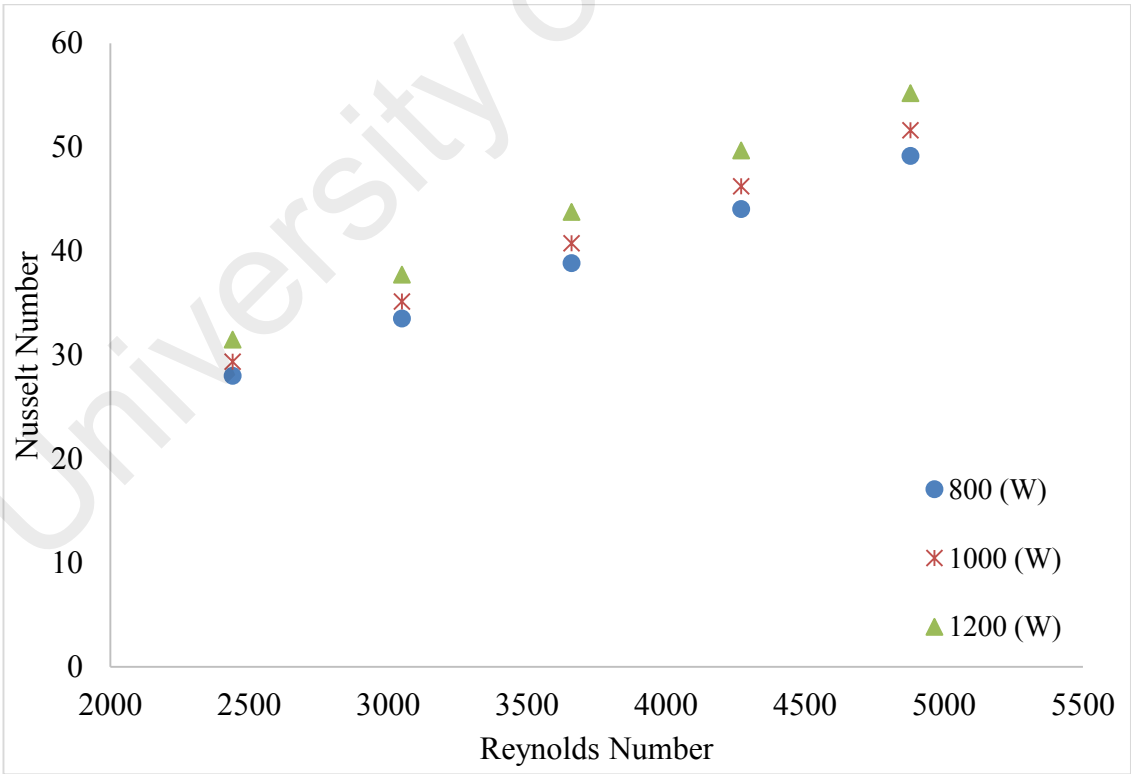

Figure 4.10: Comparison of Nusselt numbers of MWCNT-Asp/water for different heat fluxes at 0.1% weight concentration.

4.7 Pressure drop

The experimental and numerical results for the pressure drop of the fluid flow between the inlet and outlet of the test section as a function of Reynolds number for various weight concentrations are shown in Figure 5-11. The maximum deviation between the present prediction and the experimental values obtained are found to be less than 15%. It can be seen that the pressure drop of MWCNT-Asp/water increases continuously with increasing of the MWCNT-Asp concentration and Reynolds number, in which the dependence of the pressure drop on Reynolds number is almost linear. According to the results, the working fluid showed a pressure drop of average, 38% greater than that of the base fluid, which emphasizes that the viscosity of these samples resulted an increase of 31% compared with that of distilled water. The highest increase in pressure drop of MWCNT-Asp/water is obtained at the weight concentration of 0.1%, Reynolds number of 4880 and input power of 800W. As compared to the pure water, the maximum increase in the pressure drop in the presence of MWCNT-Asp is about 62%. Thus the higher weight concentration of MWCNT-Asp in the base fluids means the higher viscosity is implying more pressure drop.

In order to evaluate influence of temperature on pressure drop of MWCNT-Asp/water coolants, experiments were performed for different input powers (800, 1000 and 1200W) at the constant weight concentration of 0.1% in a range of inlet velocities and the pressure drops are evaluated and presented in Figure 5-12. This figure shows that for the MWCNT-Asp/water coolants the pressure drop decreases significantly with the increase of circulation temperature. It is also noteworthy that the pressure drop and viscosity curves exhibit similar trends, which can be attributed to the direct relationship between pressure drop and viscosity.

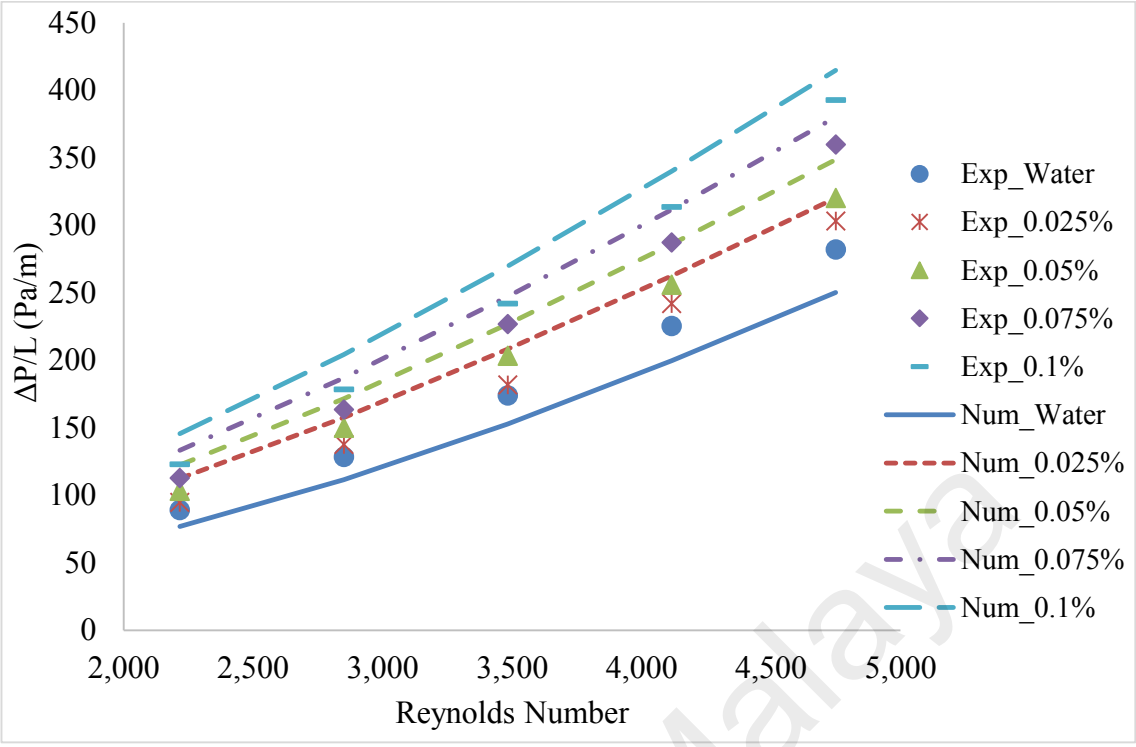

Figure 4.11: Test section pressure gradient versus Reynolds number for all samples at input power of 800W.

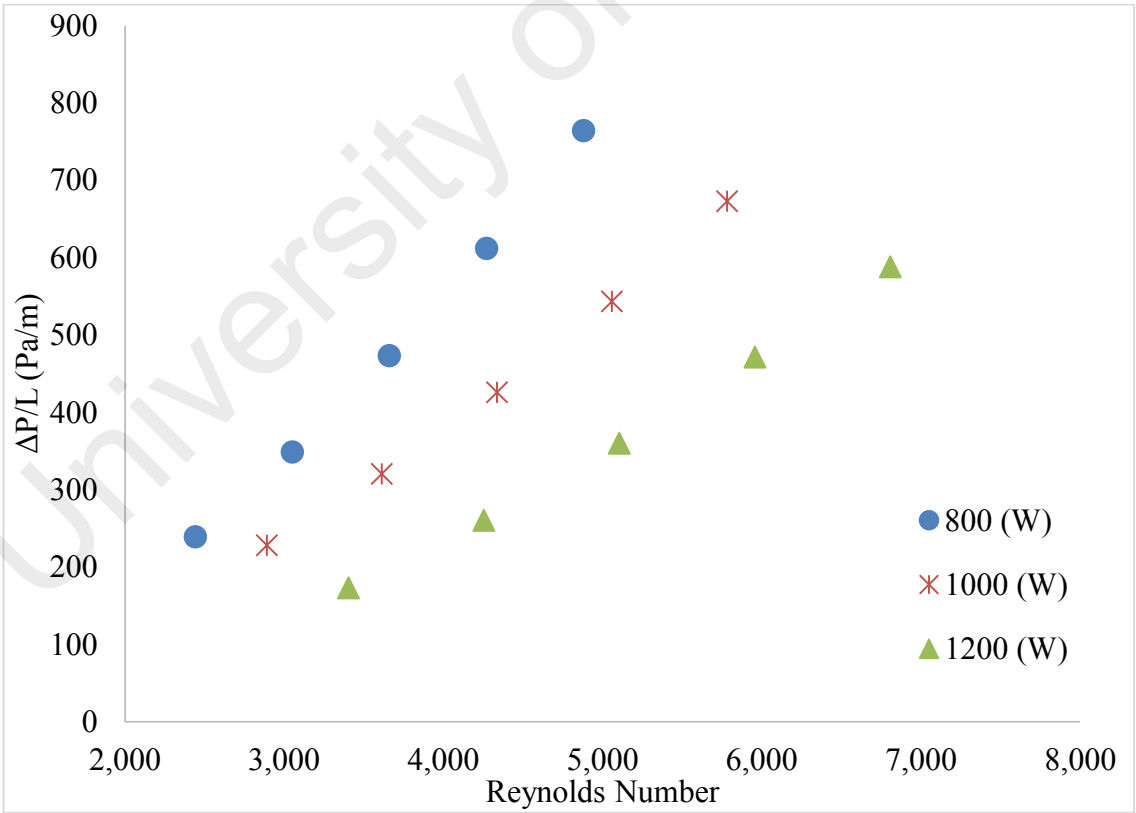

Figure 4.12: Test section pressure gradient versus Reynolds number for three different hear fluxes at concentration of 0.1%.

Power consumption and pumping characteristics in a loop is a critical parameter in terms of economy as well as energy-saving. Pumping power can be considered as an economic performance indicator in a loop system for evaluating the operability of fluid and performance of power plant. Figure 5-13 compares the pumping power of the annular heat exchanger at various concentrations of MWCNT-Asp for different temperatures with the pumping power data of the basefluid. This figure shows that there is a slight increase in the pumping power with the MWCNT-Asp/water loading. Interestingly, the pumping power of all the samples at all the concentrations are greater than 1, indicating the effectiveness of the prepared coolant in annular tube for different conditions. It could be noted that the pumping power decreases with the increase of heat fluxes to the test section.

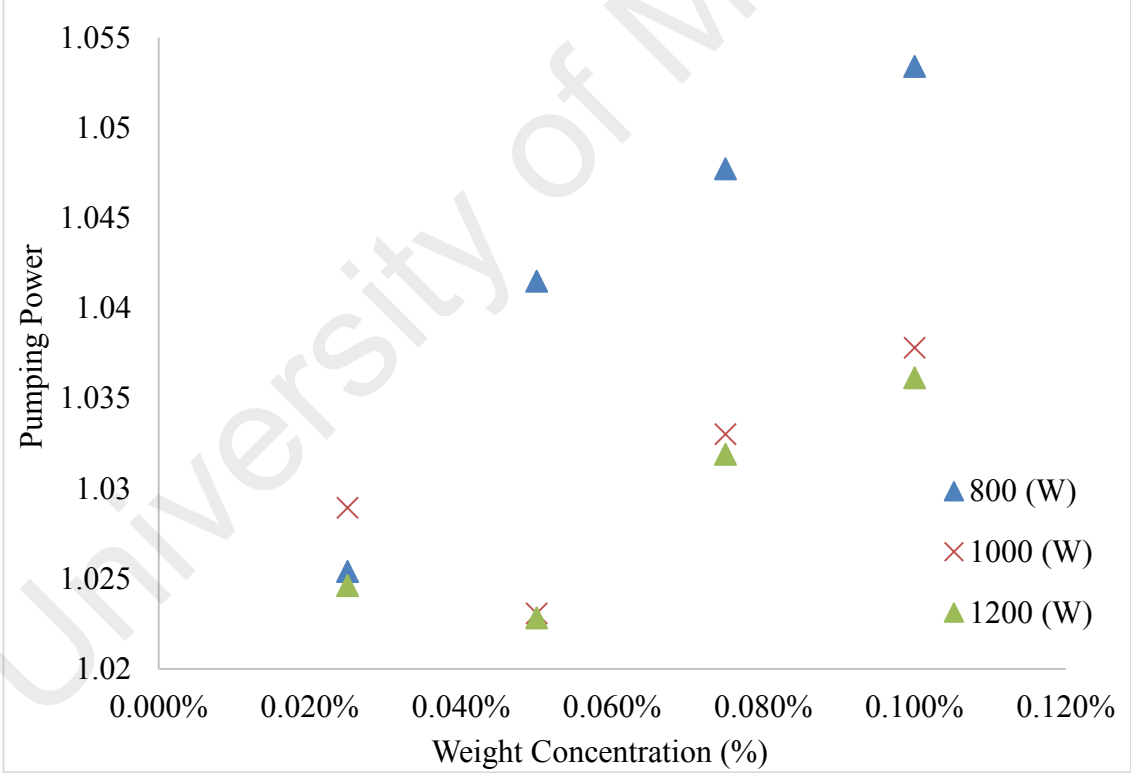

Figure 4.13: Pumping power as a function of weight concentrations of the MWCNT-Asp samples at different heat fluxes to the test section.

CHAPTER 6: HEAT TRANSFER PERFORMANCE OF WATER-BASED TETRAHYDROFURFURYL POLYETHYLENE GLYCOL-TREATED GRAPHENE NANOPLATELETS SUPER-COOLANT

The main problem with applying surfactants are the reduction of specific surface area of carbon nanostructures, implying a significant decrease in thermal properties of nanofluids. So, to avoid this issue and removing foaming in the flow-systems, covalent functionalization was suggested. However, most of the covalently functionalization procedures are complex and multi-step (Amiri et al., 2011). As some new studies in this field, Sun et al. (2010) and our group (Amiri, 2015) employed in situ diazonium formation procedure to functionalize thermally expanded graphite with 4-bromophenyl. They reported higher solubility for the chemically-assisted exfoliated graphene sheets than pristine graphene without any stabilizer additive. Sarsam et al. (2016) also reported a novel synthesis procedure for preparing triethanolamine-treated graphene nanoplatelets with different specific areas (SSAs). Using ultrasonication, the covalently functionalized graphene nanoplatelets with different weight concentrations and SSAs were dispersed in distilled water to prepare a new version of nanofluids.

Here, a quick and efficient covalent route is employed to synthesize tetrahydrofurfuryl polyethylene glycol-treated Graphene Nanoplatelets (TGNP). To prove functionalization, the TGNP sample was subjected to morphological and chemical characterization. The treated sample was then added to the pure water as a base fluid to synthesis the TGNP nanofluid and its thermo-physical properties were investigated. Finally, the convective heat transfer coefficient and pressure drop of the prepared supercoolants were studied in an annular heat exchanger.

5.1 Functionalization procedure and preparation of coolants

To synthesize TGNP, the pristine GNP (7 g) and $AlCl_3$ as a Lewis acid (129.8 g) were poured into an agate mortar and were grounded for several minutes. This mentioned mixture and 400 mL TFPEG were then poured into a vessel and stirred for 30 min at room temperature until a homogeneous suspension was produced. Then, 0.5 mL concentrated hydrochloric acid was added drop by drop. The mixture was then sonicated at 100ºC for 36 hrs. The resulting mixture was then cooled to the room temperature, centrifuged in ethanol, methanol and water for 9 times to remove any unreacted materials, and finally the sample was dried at 60ºC.

To synthesize the TGNP/water coolant, the given amount of TGNP was sonicated with water as a basefluid for 10 min at power of 480W. The TGNP/water coolants were synthesized at the weight concentrations of 0.025%, 0.05%, 0.075% and 0.1%.

The mechanism of the reaction can be summarized as follows:

With a Lewis acid ($AlCl_3$) as a catalyst and a trifle amount of concentrated hydrochloric acid (HCl) to protonate tetrahydrofurfuryl polyethylene glycol, electrophilic addition reactions were carried out between tetrahydrofurfuryl polyethylene glycol and GNPs through a sonication method. The reaction resulted in the attachment of tetrahydrofurfuryl polyethylene glycol and hydroxyl groups on the surface of the GNP (Tian et al., 2008).

5.2 Functionalization and Morphology

Raman characterization is a strong measurement for analyzing structure, having sp^2 and sp^3 hybridized carbon atoms in carbon-based materials and functionalization by following alterations in holes. The Raman spectra of the pristine GNP, and TGNP are presented in

Figure 6-1. While the pristine GNP is weak in terms of D band intensity, the fairly strong D band in the TGNP sample can be seen at 1343 cm^{-1}. The ratio of the intensities of the D-band to that of the G-band ($I_D/_G$) was considered to be the amount of disordered carbon (sp^3-hybridized carbon) relative to graphitic carbon (sp^2-hybridized carbon). In functionalization studies of GNP, the higher intensity ratio of $I_D/_G$ indicates a higher disruption of aromatic π-π electrons, implying partial damage of the graphitic carbon produced by covalent functionalization. The $I_D/_G$ ratio of TGNP is relatively higher than that of pristine GNP, which confirmed the successful functionalization via an electrophilic addition reaction under microwave irradiation. A significant increase in $I_D/_G$ can also confirm that the present method is completely successful for functionalization of GNP without acid-treatment phase.

As a further evidence, thermogravimetric analysis (TGA) was conducted to investigate functionalization of GNP with tetrahydrofurfuryl polyethylene glycol. TGA is a technique for thermally analysis in which alterations in the structure of materials are measured as a function of temperature. Figure 6-2 presents the TGA curve of the pristine GNP and TGNP. It can be seen that the TGA results of the pristine sample illustrate no mass loss up to 600ºC. However, there is an obvious weight loss in the temperature range of 100–200ºC in the TGNP curve. This mass loss was attributed to the functionality of tetrahydrofurfuryl polyethylene glycol as an unstable organic part on the surface of the GNP.

Figure 6-3 panels (a) and (b) display the TEM images of TGNP, where all the images reveal the presence of some multi-layer structure of GNPs. Images of the TGNP sample provide layer's surface full of wrinkles. Although TEM images are not able to show minute functional groups, some changes in morphology and surface deterioration can be

considered as an evidence for covalent functionalization. The wrinkles (waviness) seen in the TEM images are attributed to the inherent instability of 2D structures, which is increased during the ultrasonication process, resulting from appropriate flexibility of graphene flakes after treatment. Undoubtedly, TGNP can increase the wettability of GNP layer's surface, implying higher tendency for wrinkling during ultrasonication and/or drying process in preparing TEM samples. Consequently, higher dispersion stability was obtained as a result of higher wettability of the GNP layer's surface, which will be discussed in UV-vis study in depth.

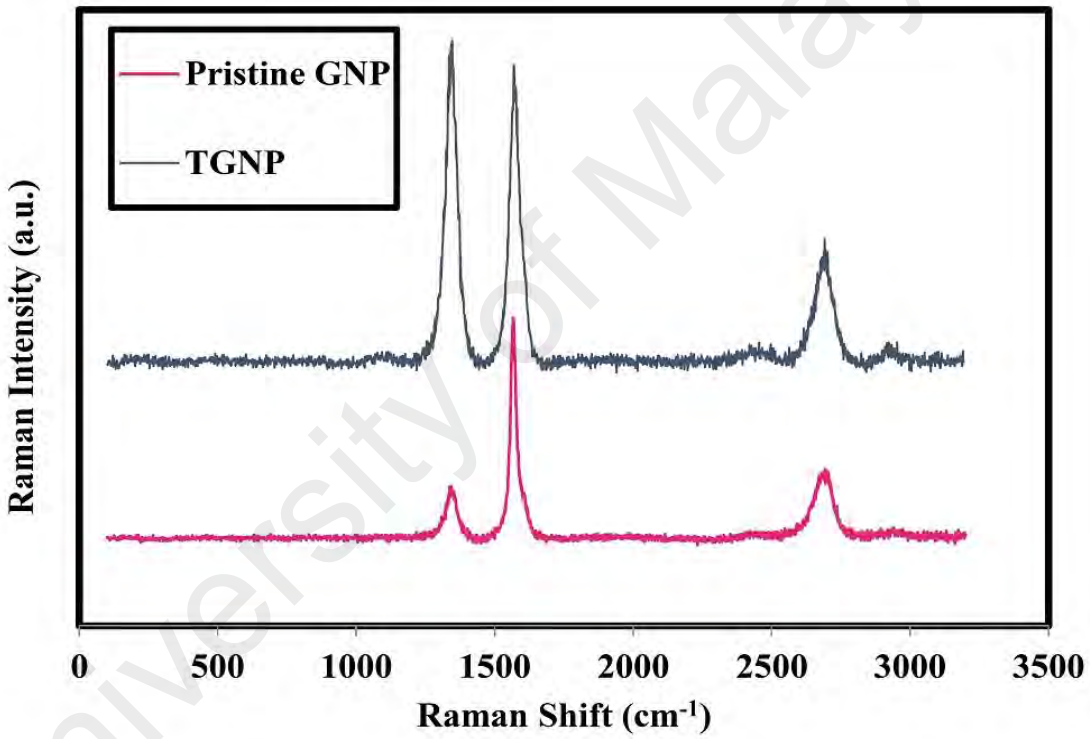

Figure 5.1: Raman analysis of the pristine GNP and TGNP.

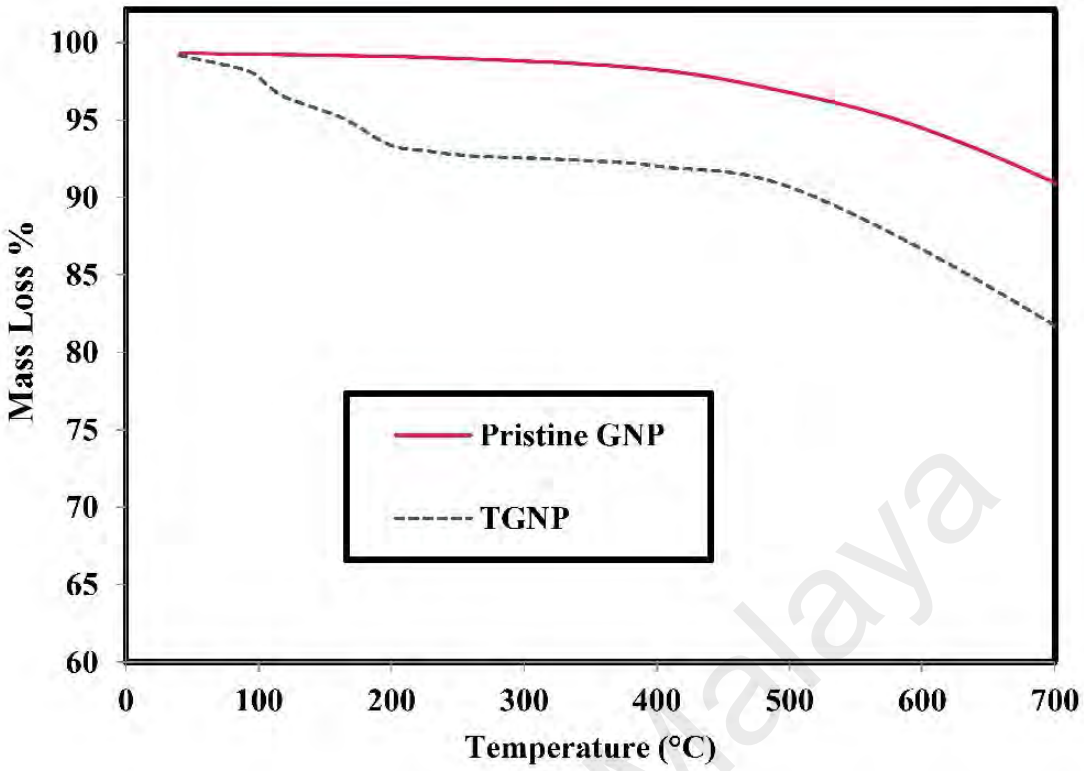

Figure 5.2: TGA analysis of the pristine GNP and TGNP.

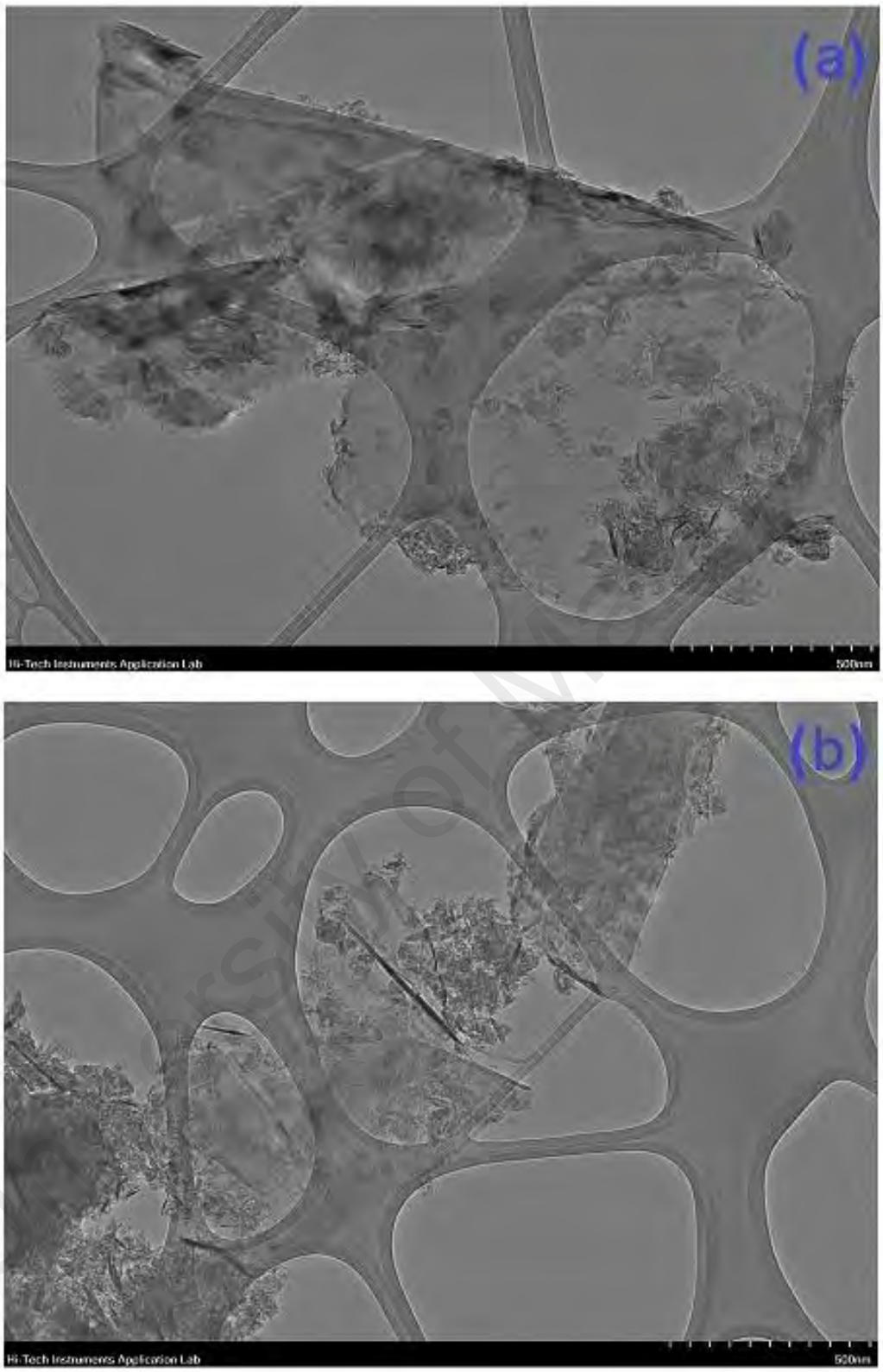

Figure 5.3: Panels (a) and (b) display the TEM images of TGNP.

5.3 Dispersibility

The UV–vis spectrum for the water-based TGNP nanofluids with different weight concentrations is presented in Figure 6.4(a), from which it can be realized that the peak value of absorbance for all samples due to the presence of TGNP lies almost at 268 nm. Photometric analysis of the UV–vis spectrometer was used to track the weight concentration of all the samples that were prepared at different times for 30 days. To this end, a standard curve was prepared for each nanofluid sample relating its weight concentration with the value of absorbance. Also, Figure 6.4(b) shows the quantitative analysis of the dispersion state and the long-term stability of the TGNP/water coolants in UV–Vis spectroscopy for different weight fractions. It can be seen that the relative concentration of TGNP/water nanofluid decrease insignificantly over time. As a result, the maximum sediment of about 15 % was obtained for highest weight concentration of 0.1, which confirmed the suitable dispersibility of TGNP in water as the basefluid.

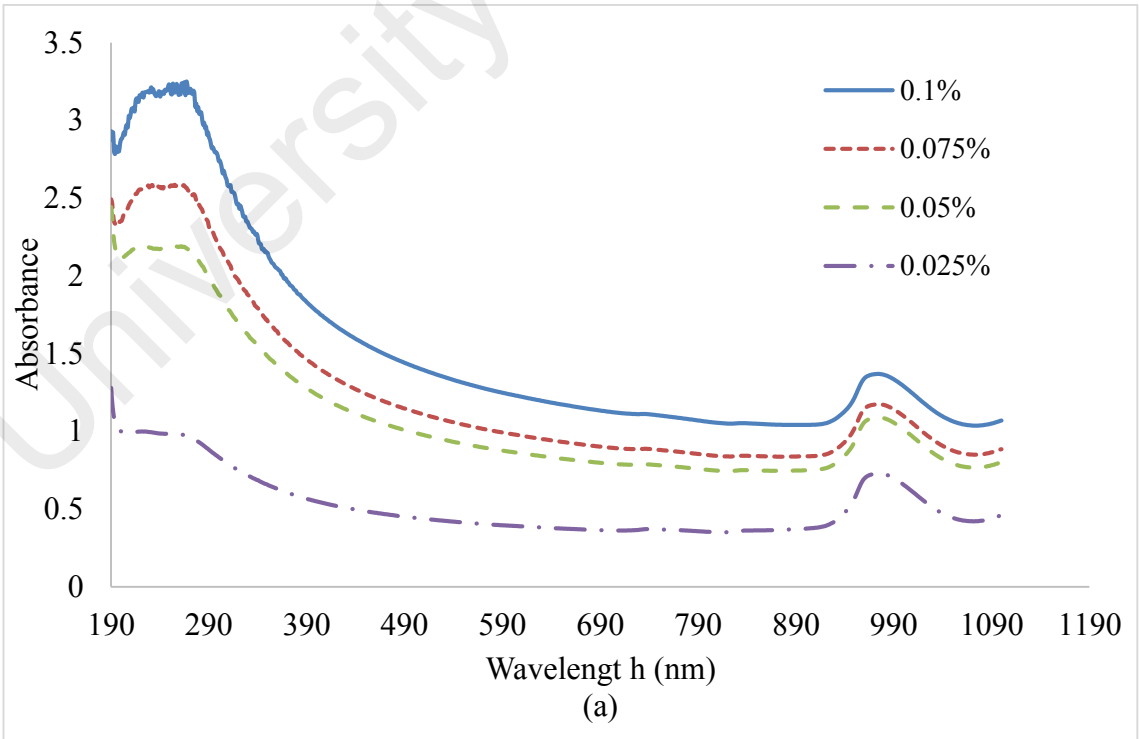

Figure 6.4, continued

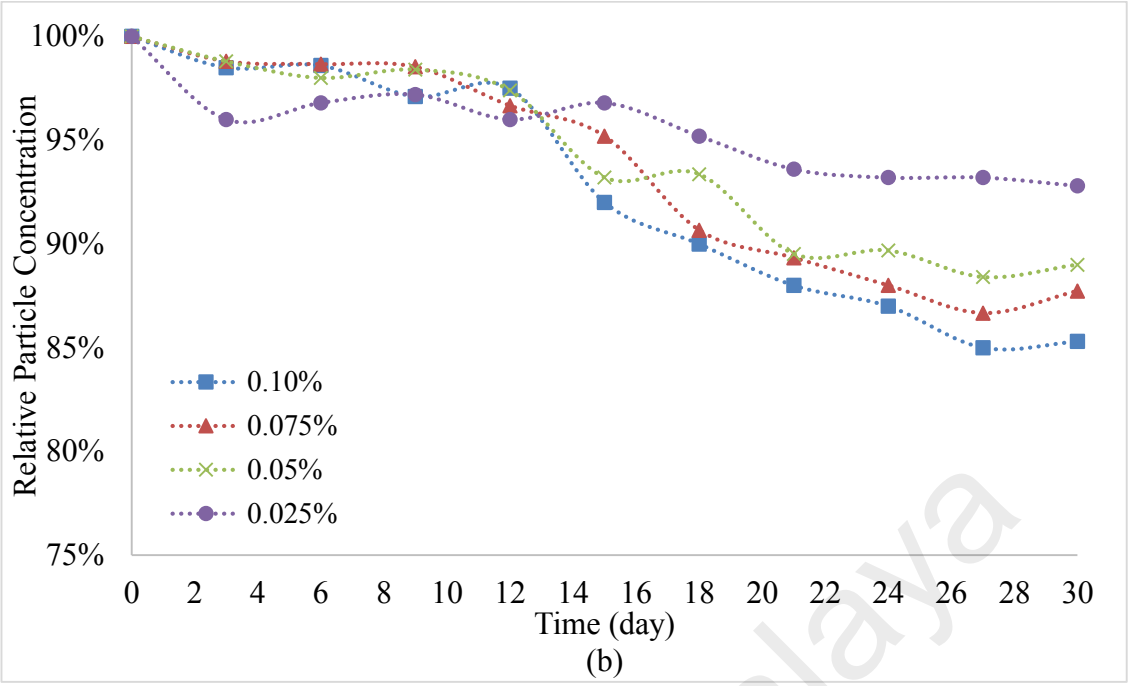

Figure 5.4: (a) UV–vis absorbance spectrum for the four different weight concentration of the water-based TGNP nanofluids and (b) colloidal stability of the TGNP/water as a function of time at different weight concentrations.

5.4 Physical Properties

Thermophysical properties of coolants such as thermal conductivity, viscosity, density and specific heat are the most important characteristics in the field of heat transfer. The prepared TGNP/water nanofluid was characterized in terms of thermo-physical properties. The prepared samples are studied with the differential scanning calorimeter (Perkin Elmer Diamond DSC) for measuring the specific heat capacities of samples. The thermal conductivity of TGNP/water samples at different concentrations were obtained by a KD2 Pro-thermal analyzer (Decagon Devices, USA). Also, the rheological properties of samples were measured on a shear-ratecontrolled Anton Paar rotational rheometer (model Physica MCR301, Anton Paar GmbH). The densities of water and nanofluids were measured experimentally by Mettler Toledo DE-40 density meter. The accuracy of density measurement is 10g/cm^3. For each temperature and sample, the measurements were recorded 3 times.

Experimental results about thermophysical properties of TGNP/water nanofluid were compared with pure water, which are shown in Figures 6.5 to 6.8. Figure 6.5, 6.6, 6.7 and 6.8 show the experimental data of the density, specific heat, viscosity and thermal conductivity at different temperatures of 20 to 60°C. Density is one of the thermophysical properties of fluids that can affect the convective heat transfer coefficient. Experimentally measured density of the GNP/water nanofuids at different weight concentrations as well as basefluid are shown in Figure 6.5 as a function of temperature. The results show that the density of the prepared coolants decreases with temperature and increases with concentration, and expectedly are higher than that of the basefluid.

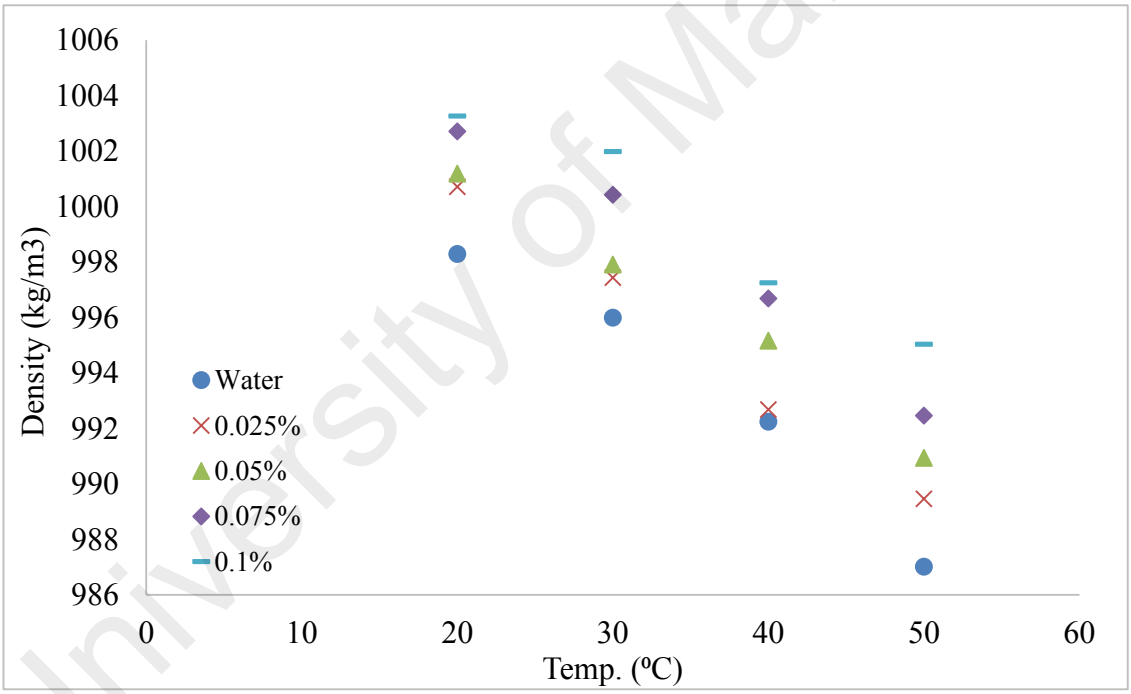

Figure 5.5: Densities of the TGNP/water and water for different weight concentrations (kg/m^3).

As another thermo-physical property, the specific heat capacity plot of TGNP as the functions of temperature and weight concentration of TGNP is illustrated in Figure 6.6. The results suggest that an increase in the weight concentration of TGNP leads a drop in the specific heat capacity. Also, the specific heat capacity of all samples increases gradually with the temperature, which is sharper in coolants including TGNP. It is

noteworthy that the drop in the specific heat capacity of nanofluids is due to the lower specific heat capacity of TGNP than that of the basefluid.

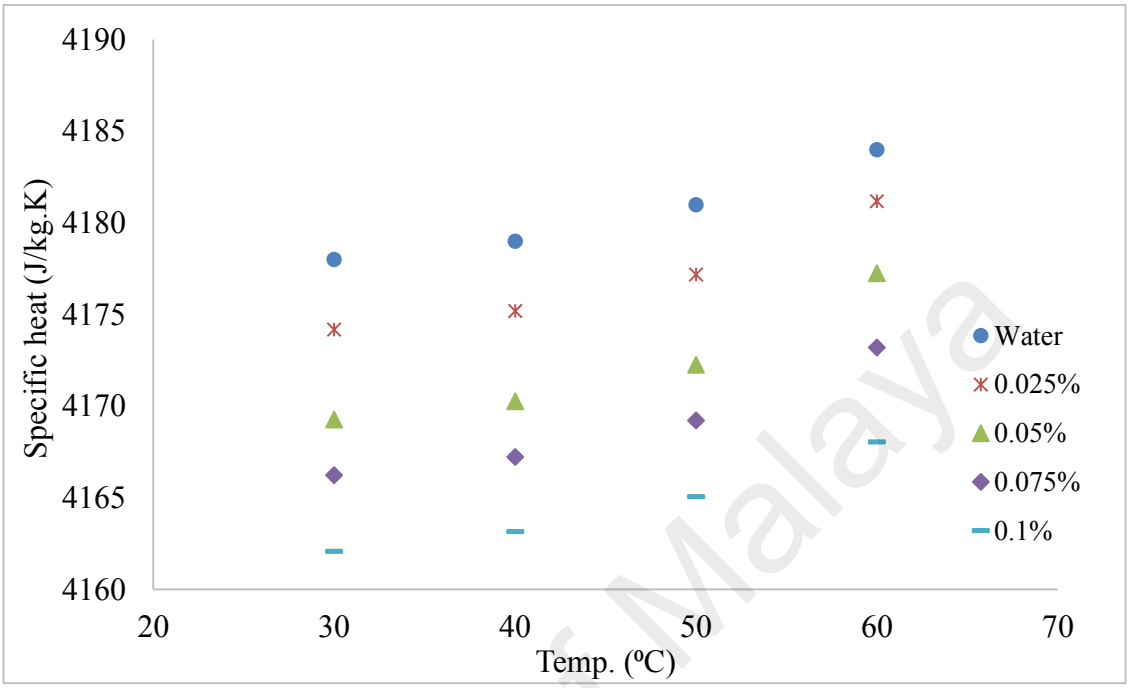

Figure 5.6: Specific heat capacity of the TGNP/water and water for different weight concentrations (J/kg.K) as a function of temperature.

Viscosity is a crucial parameter in the dynamic design of nanofluids for heat transfer applications, especially in the systems incurring pressure drop. By loading nanoparticles into the water, viscosity increases commonly (Figure 6-7). With increasing concentration, the viscosity of nanofluids increases and the opposite trend is obtained for increasing of temperature. In all the temperatures and concentrations, the highest viscosity was for the nanofluid with highest weight concentration (0.1%).

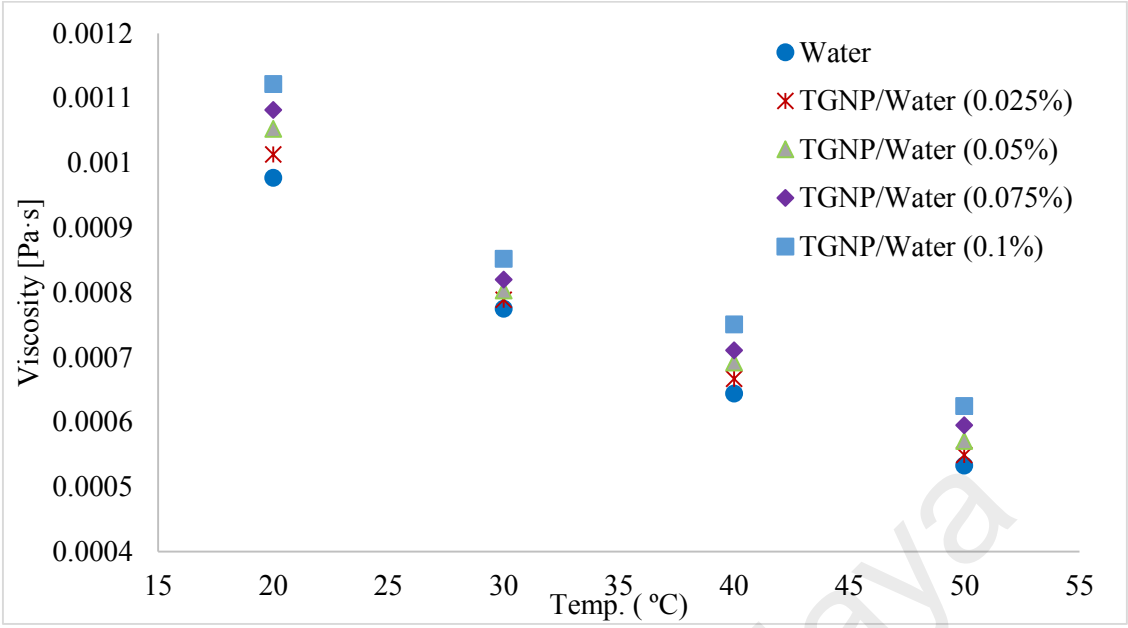

Figure 5.7: Dynamic viscosity of the TGNP/water and water as the functions of temperature and weight concentration at shear rate of 140 s^{-1} (mPa.s).

Thermal conductivity of working fluids is one of the key parameters in evaluating heat transfer rate of heat exchanger. Figure 6-8 represents the thermal conductivity of nanofluids and water as a function of temperature. The results show that the thermal conductivity of nanofluids improves with the loading of TGNP in the basefluid and they are higher in comparison to the water. Also, as the temperature increases, thermal conductivity increases, which is more significant at higher concentration.

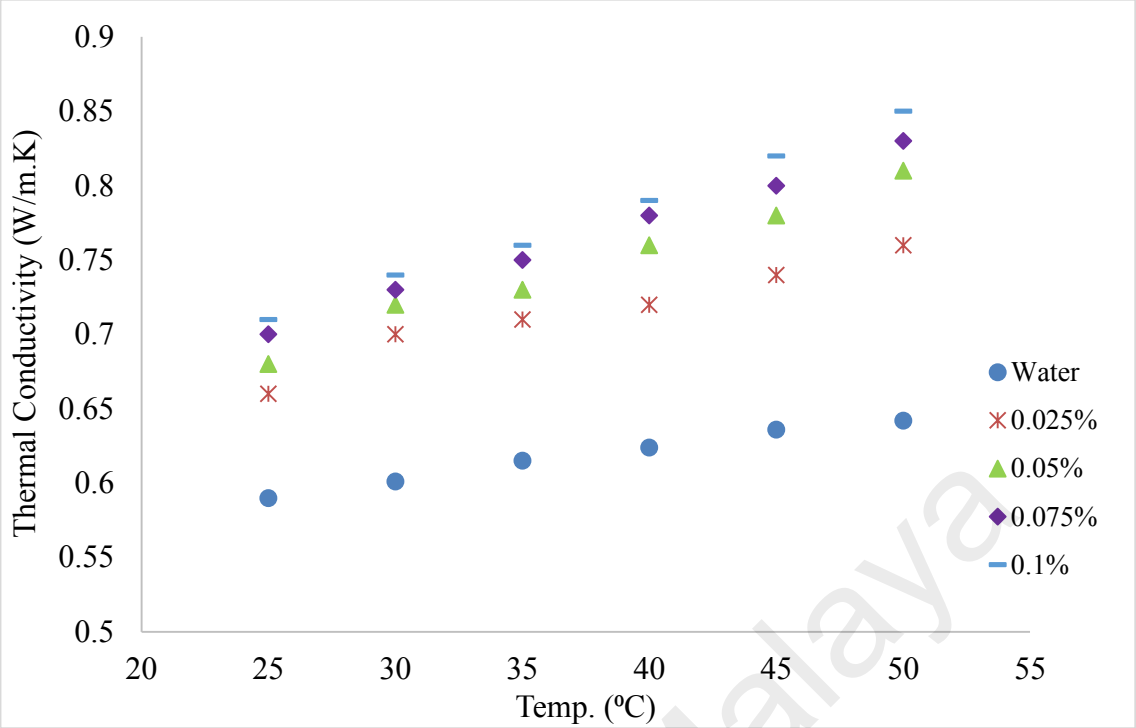

Figure 5.8: Thermal conductivity of TGNP/water and pure water (W/m.K) as a function of temperature and concentrations.

5.5 Thermal analysis

TGNP/water was tested for the Reynolds numbers range of 2220±20 to 7000±20, three weight concentrations (0.025, 0.05, 0.075 and 0.1%) and three input powers to the test section (800, 1000 and 1200W). Figure 6.9(a-c) shows the heat transfer coefficient plots of TGNP/water as the functions of Reynolds number and weight concentration. It is realized that the enhancement of heat transfer coefficient of TGNP/water remarkably exceed those of the thermal conductivity improvements for different weight concentrations in both numerical and experimental results. The maximum heat transfer coefficient at concentration of 0.1%, Reynolds number of 7000 and input power of 1200W is 25.6%.

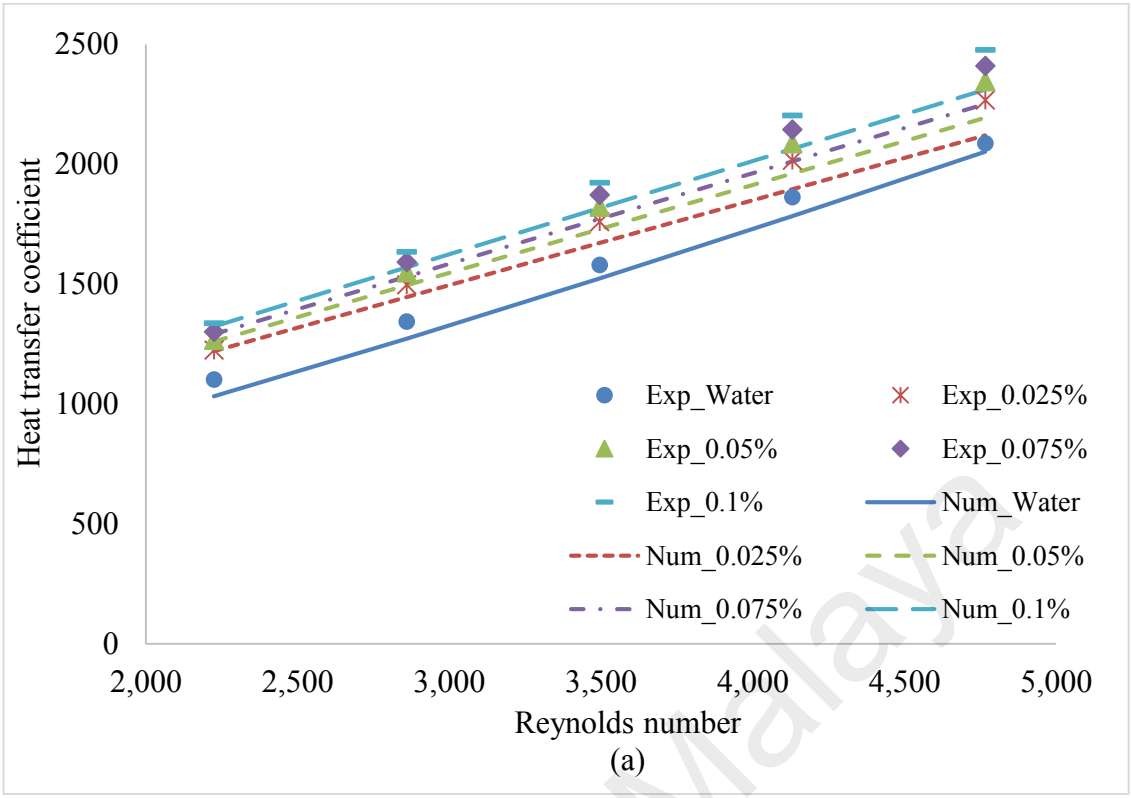

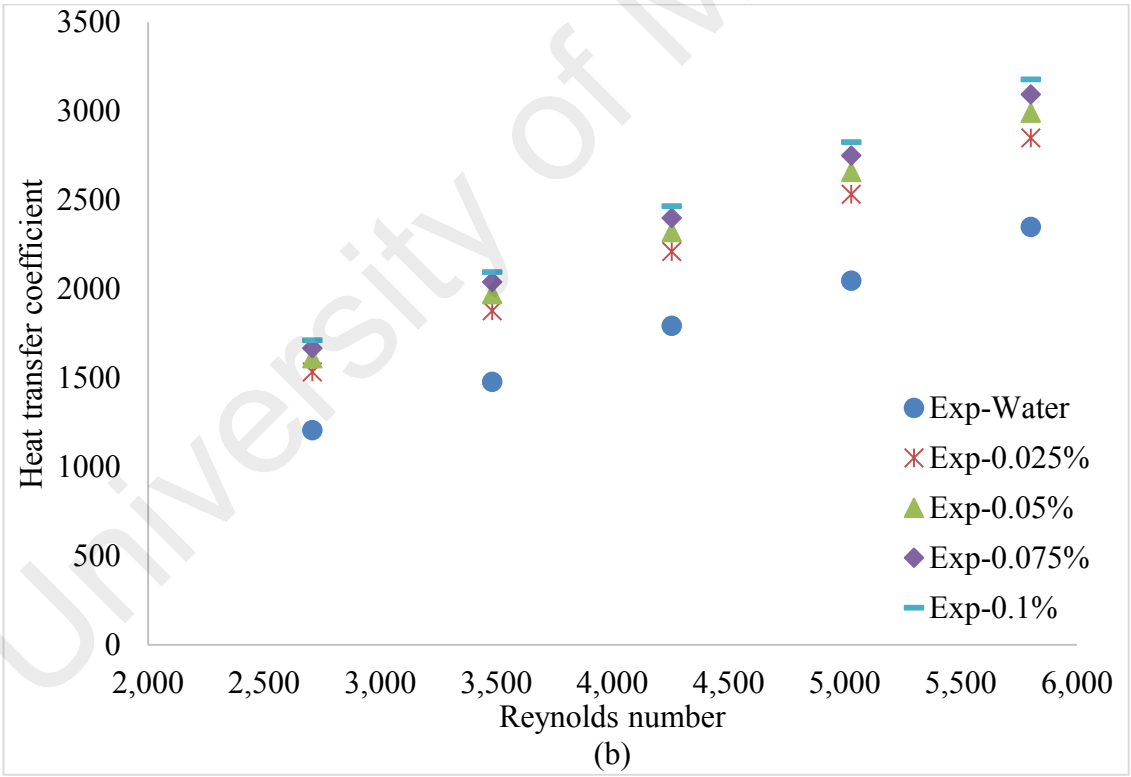

Figure 6.9, continued

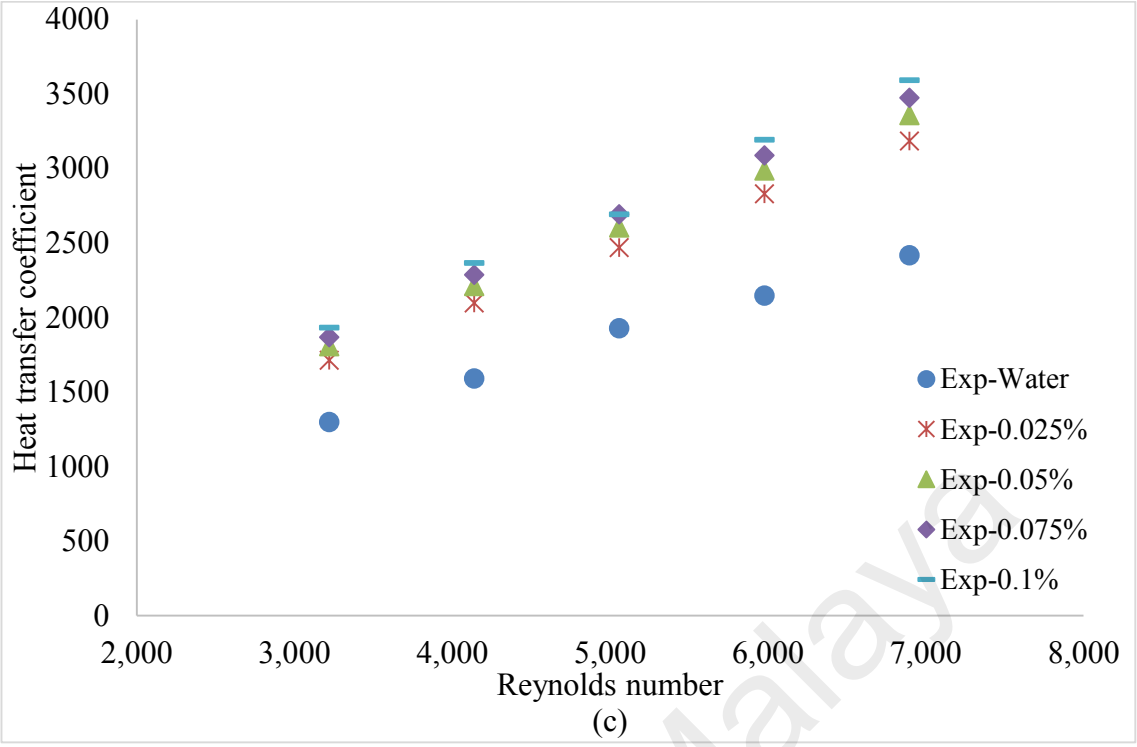

Figure 5.9: Comparison of the heat transfer coefficient obtained for distilled water and TGNP/water for different weight concentrations at different heat fluxes of (a) 800W, (b) 1000W and (c) 1200W to the text section.

Figure 6-10(a-c) shows the average Nusselt numbers of GNP/water nanofluid for various weight concentrations and Reynolds numbers. To evaluate the ratio of convective to conductive heat transfer of GNP/water coolants, Nusselt number plots have been employed. The results suggest that the Nusselt number increases remarkably in the presence of treated samples in comparison to the applied basefluid. The TGNP loading in basefluid improves the thermal conductivity of the basefluid, which leads to the lower temperature difference between the bulk fluid and wall tube, indicating higher Nusselt numbers or the heat transfer rate. The comparison between the measurements and the predicted results are illustrated in Figures 6.9(a) and 6.10(a). The experimental results were in a good agreement with numerical results, indicating a deviation percentage of 6.58.

Figure 6.11 illustrates the heat transfer performance of the TGNP/water coolant at different heat fluxes and at constant weight concentration of 0.1%, where increase in Reynolds number increases the Nusselt number (heat transfer performance) of the working fluid.

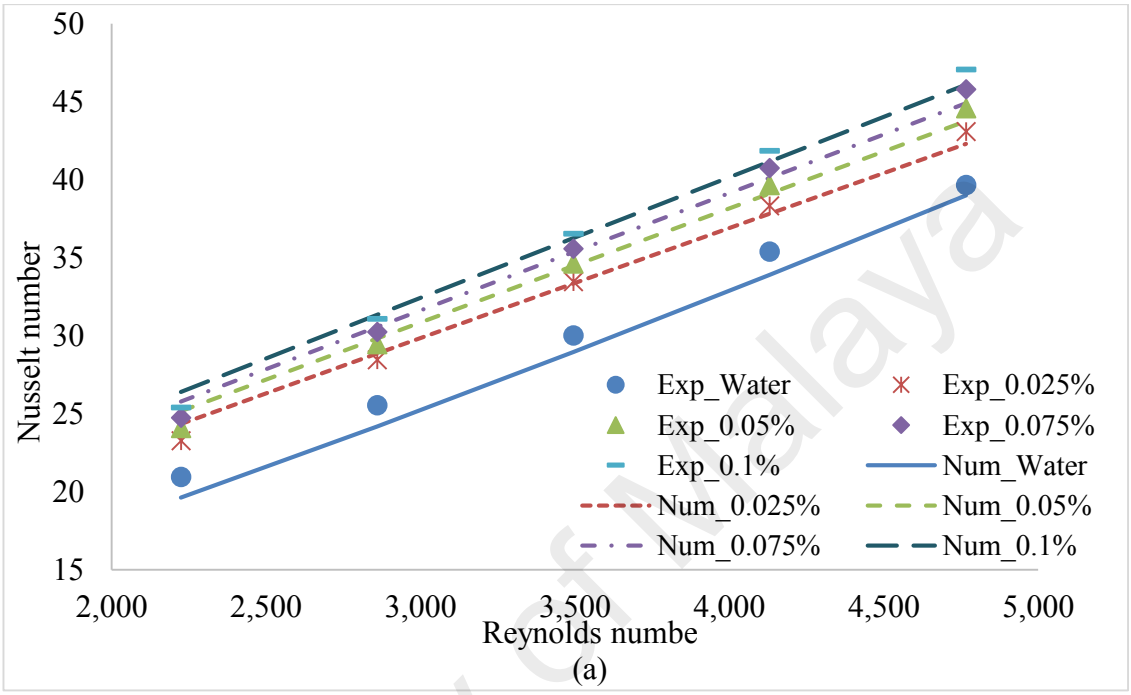

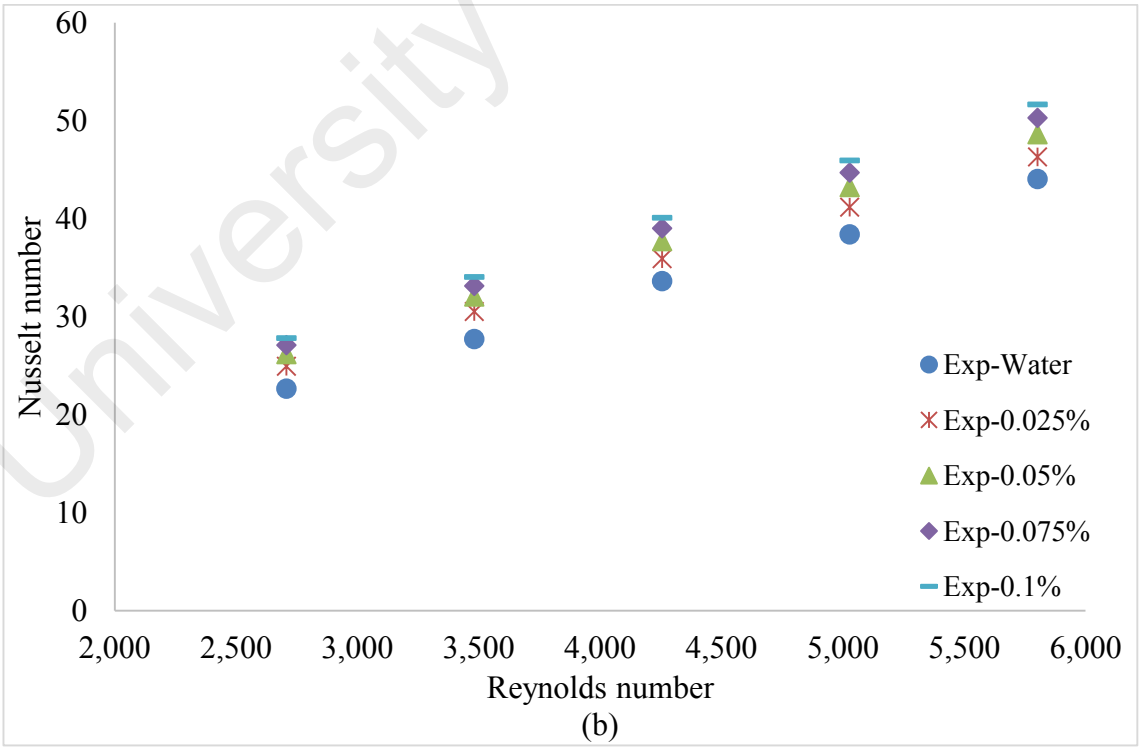

Figure 6.10, continued

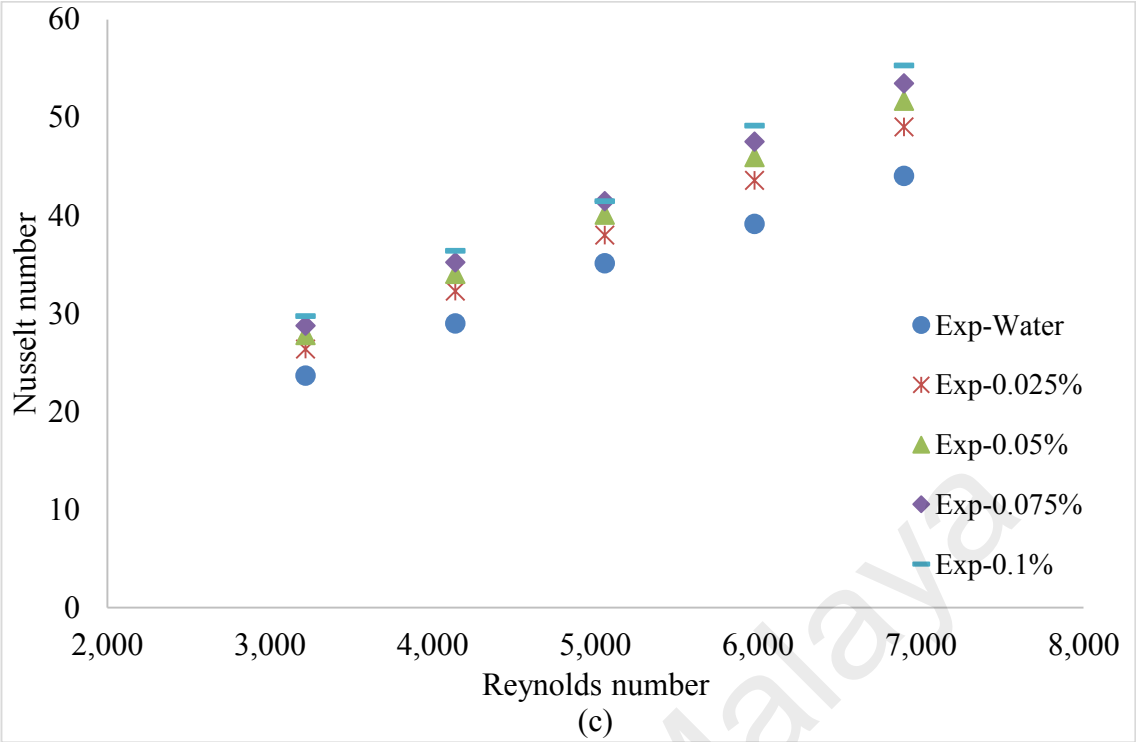

Figure 5.10: Comparison of Nusselt numbers obtained for distilled water and TGNP/water for different weight concentrations and at different heat fluxes (a) 800W, (b) 1000W and (c) 1200W to the test section.

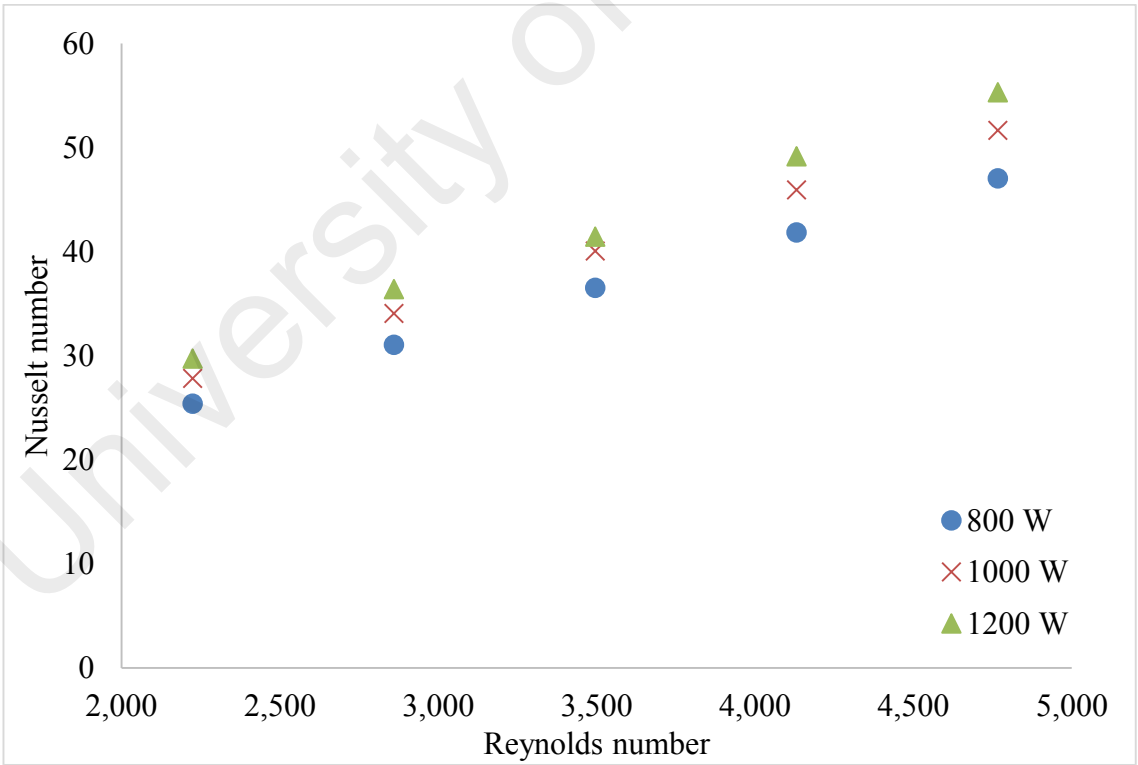

Figure 5.11: Comparison of Nusselt numbers of TGNP/water for different heat fluxes at weight concentration of 0.1%.

5.6 Pressure drop

The pressure gradient between inlet and outlet of the pipe is depicted in Figure 6.12. The pressure drop increases dramatically with the increment of the Reynolds number in both numerical and experimental results. The increasing rate of the pressure drop at the concentration of 0.1% with respect to pure water appears nearly 39.3% higher at Reynolds number of 4760 and the power supply of 800W to the test section. This value is considerably low in comparison with the increasing rate of the heat transfer.

In order to evaluate influence of temperature on pressure drop of TGNP/water coolants, experiments were performed for different input powers (800, 1000 and 1200W) at the constant weight concentration of 0.1% where the inlet velocities and the pressure drops are evaluated and presented in Figure 6.13. This figure shows that the pressure drop decreases significantly by increase the heat fluxes for the TGNP/water coolants. It is also noteworthy that the pressure drop and viscosity curves exhibit similar trends, which can be attributed to the direct relationship between pressure drop and viscosity and density.

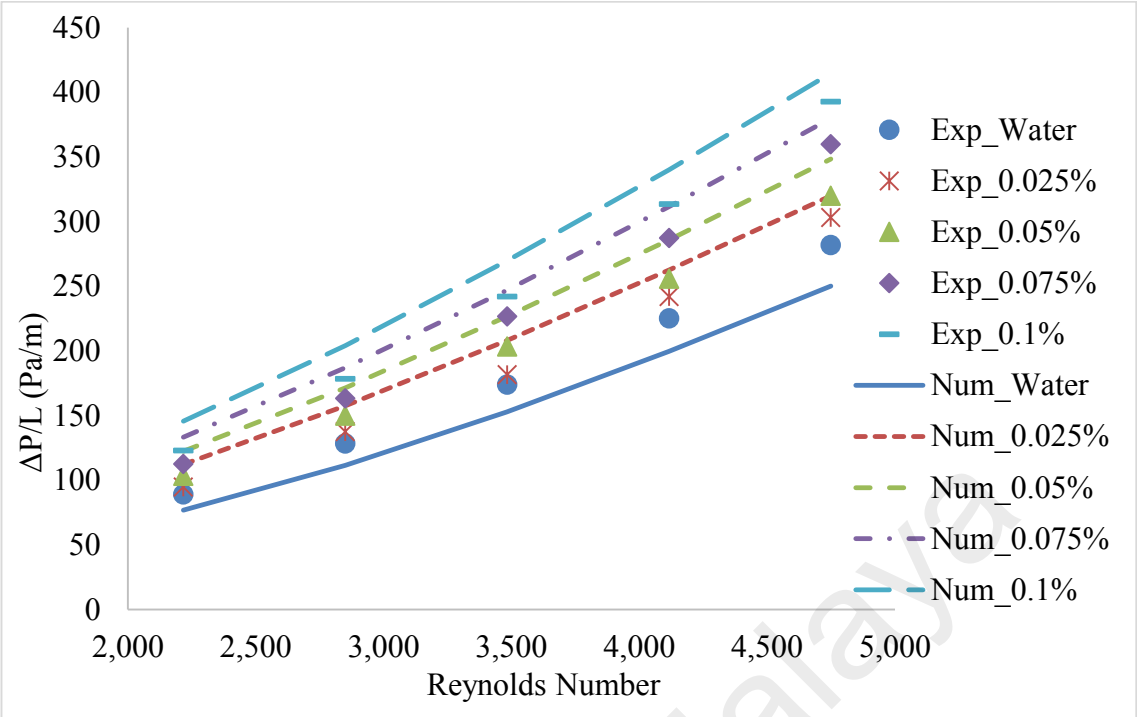

Figure 5.12: Test section pressure gradient versus Reynolds number for all the samples at the input power of 800W.

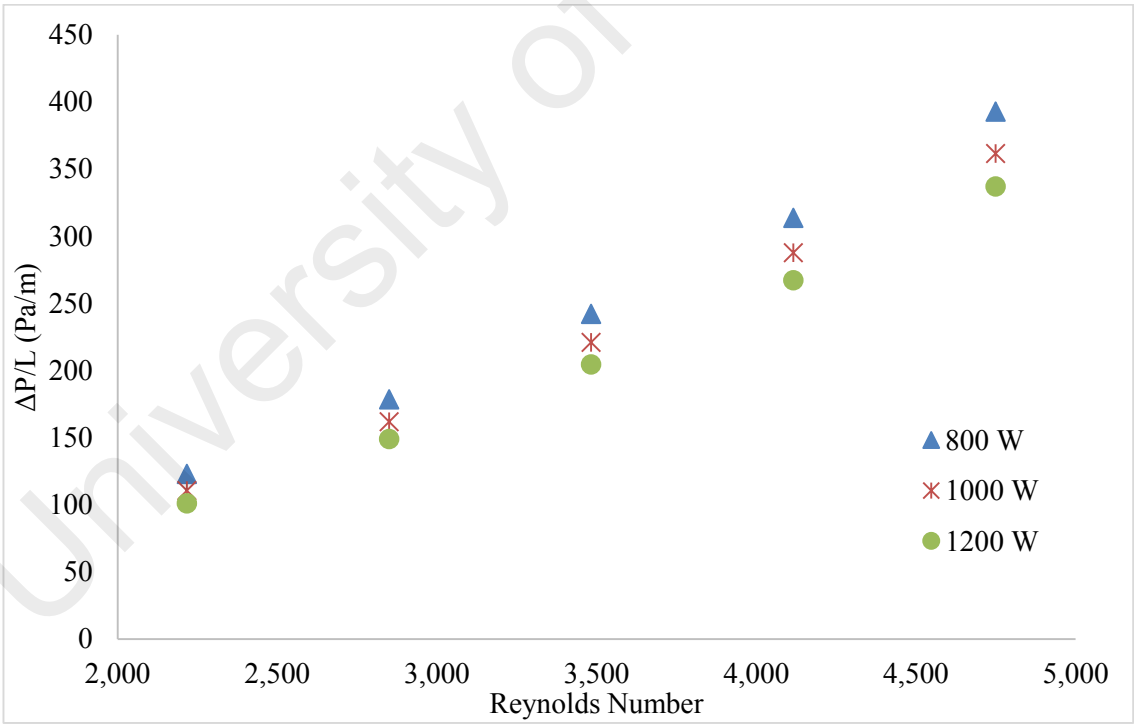

Figure 5.13: Test section pressure gradient versus Reynolds number for three different hear fluxes and at the concentration of 0.1%.

CHAPTER 7: THERMOPHYSICAL AND HEAT TRANSFER PERFORMANCE OF STABILIZED GRAPHENE NANOPLATELETS-ETHYLENE GLYCOL/WATER NANOFLUIDS THROUGH AN ANNULAR CHANNEL

The single-phase or two-phase approaches could be applied in simulating convective heat transfer by nanofluid. The single-phase method assumes that nanoparticles and base fluids move with the same velocity and they are in thermal equilibrium, so this method is easier and needs less computational time. But it is important and notable to find applicable equations which compute properties of single-phase nanofluids. However, the single-phase method has been employed in a number of numerical researches of convective heat transfer by nanofluids. (Akbarinia et al., 2007; Akbarinia et al., 2009; Barbés et al., 2014; Khanafer et al., 2003; Roy et al., 2004; Shahi et al., 2010; Sundar et al., 2010; Talebi et al., 2010). In general, the single-phase approach and the experimental results have not shown good agreement, due to lack of appropriate equations for predicting both nanoparticles and basefluid, which implies the low extent of validation in results and lack of realizing nanofluids properties. Also, some nanofluid parameters such as dispersibility, sedimentation, Brownian motion of nanoparticles in basefluids, Brownian forces, volume or weight concentration of solid particles in basefluids etc. may influence nanofluids flow regime and heat transfer rate. Therefore, the slip velocity between nanoparticles and basefluid must be considered for simulating nanofluid flows and/or heat transfer (Xuan et al., 2000). Due to Brownian movement of particles in basefluids, two-phase approach open a new gateway for introducing the main characteristics of nanofluids, indicating a good agreement with theorical and experimental results. Various multiphase approaches have been presented to predict and describe behaviour of complex flows. Numerous multiphase flow studies used the theory of interacting continua or the “Mixture Theory” (Crowe et al., 1996; Ishii, 1975; Manninen et al., 1996; Xu, 2004). This method works

based on the underlying theory that each phase can be mathematically defined as a continuum.

Lotfi and his colleagues (2010) employed single-phase, two-phase Eulerian and two-phase mixture approaches to simulate flow behaviour in the presence of nanofluids through a straight pipe. They concluded that two-phase mixture method has more accurate results than the other two approaches. Some investigators have used this approach to simulate the behaviour of nanofluids (Akbarinia et al., 2007; Akbarinia et al., 2009; Bianco et al., 2009; Mirmasoumi et al., 2008a, 2008b). Mirmasoumi and Behzadmehr (2008a) Akbarinia and Laur (2009) considered the influence of nanoparticles size on nanofluid flow in a horizontal pipe.

Abu-Nada et. al. (2008) investigated heat transfer rate of annular heat exchanger in the presence of Al_2O_3- based water nanofluid with single phase method. They considered different thermal conductivity and viscosity models to evaluate heat transfer improvement in the annular heat exchanger. Izadi et al. (2009) have also simulated laminar forced convection of Al_2O_3-based water nanofluid in a two dimensional annular heat exchanger with the single-phase method.

The present chapter introduces a promising, potential to industrially scalable, cost-effective functionalization approach for preparing ethylene glycol-treated Graphene Nanoplatelets (EGNP). Also, EGNP-based water-ethylene glycol nanofluids (EGNP-WEG) were prepared and the thermophysical properties of the synthesized samples were experimentally investigated for different weight fractions. Then, the numerical simulation of the convective heat transfer coefficient in an annular heat exchanger was evaluated. To realize this goal appropriately, two-phase mixture model wasemployed. The obtained

results by simulation with two-phase method was validated with the analytical results and the authenticity of the data was confirmed. Then, the nanofluids flow in a three dimensional annular pipe was investigated for different weight fractions and Reynolds numbers. As a result, Nusselt number profiles, friction factor and the performance index were measured for the synthesized nanofluids.

6.1 Preparation of EGNP-WEG Coolants

To prepare EGNP, the pristine GNP (0.5g) and $AlCl_3$ (9.27g) were first poured into a vessel of planetary ball mill and agitated at the speed of 500 rpm for 1 h. The black-mixture was again placed into another vessel filled with 80 ml of anhydrous EG and then sonicated for 15 min with a probe-sonicator to reach a homogeneous back suspension. The concentrated hydrochloric acid (1 ml) was used into the vessel over sonication time. After doing sonication, the suspension was transferred into a microwave (Milestone MicroSYNTH programmable microwave system) and heated for 15 min at 150°C. The resultant mixture was filtered and subsequently washed. Filtration cake was then dried for 48 h at 50°C and labelled as EGNP. While the raw GNP is not dispersed in most organic solvents, the EGNP is significantly dispersed in both water and EG. The easily-miscible functional group on the structure of EGNP could cause a significant increase in dispersibility of the functionalized GNP with EG in both the medias of water and EG. To synthesize EGNP-WEG at various weight concentrations, the known amount of EGNP was poured in to a vessel filled with a mixture of water and EG with a volumetric ratio of 40:60 and sonicated for 10 min with a probe-sonicator.

6.2 Thermophysical properties

The thermal conductivity of EGNP-WEG for the temperature range of 25-65°C and the weight concentrations of 0.01%, 0.05%, 0.1% and 0.2% are shown in Table 7.1. The

effect of concentration and temperature on the thermal conductivity of the nanofluids were systematically investigated. First, the thermal conductivity of EGNP-WEG is higher than that of water–EG mixture at different temperatures and concentrations. Similar to the conventional working fluids, the thermal conductivity of EGNP-WEG increases with increasing of the temperature. The main mechanism for increasing thermal conductivity with temperature is attributed to the Brownian motion of the EGNP suspended in the basefluid (Aravind et al., 2011). It can also be seen that there is a rising trend between the thermal conductivity of EGNP-WEG samples and the weight concentration of EGNP. For EGNP-WEG, the formation of surface nanolayers can be the main reason for heat transfer rate enhancement. Liquid molecules generate layers around the EGNP, thereby enhancing the local ordering of the liquid layer at the interface region. Thus, the liquid layer at the interface would exhibit a higher thermal conductivity compared to the basefluid (Aravind et al., 2011).

Table 6.1: Thermal conductivity of the water-EG mixture and EGNP-WEG as a function of temperature and weight concentration (W/mK).

Temperature (◦C)	Water-EG	0.01 wt%	0.05 wt%	0.1 wt%	0.2 wt%
25	0.28	0.3	0.37	0.42	0.46
35	0.31	0.32	0.39	0.43	0.47
45	0.33	0.35	0.4	0.44	0.49
55	0.33	0.36	0.41	0.45	0.51
65	0.34	0.38	0.43	0.46	0.53

Dynamic viscosities of water–EG mixture and EGNP-WEG were experimentally determined at high shear rate of 140 s^{-1} for different temperatures, which are illustrated in Table 7.2. It can be seen that the viscosity of EGNP-WEG increases with increasing the concentration of EGNP. Also, a decrease in the viscosity with increasing of temperature is another obvious trend in the figure, which is obtained from weakening of the intermolecular forces of the fluid itself (Ko et al., 2007).

Table 6.2: Dynamic viscosity (kg/ms) of the water-EG mixture and EGNP-WEG as a function of temperature and weight concentration at shear rate of 140 s-1.

TEMPERATURE (◦C)	WATER-EG	0.01 WT%	0.05 WT%	0.1 WT%	0.2 WT%
25	0.003964	0.003973	0.003998	0.004025	0.004041
35	0.002981	0.002992	0.003017	0.003039	0.003054
45	0.002207	0.002215	0.002241	0.002259	0.002271
55	0.001663	0.001671	0.00169	0.001701	0.001725
65	0.001317	0.001322	0.001347	0.00136	0.001381

Also, the densities of EGNP-WEG and water–EG mixture are illustrated for different temperatures and weight concentrations in Table 7-3. Obviously, as the temperature increases, the density of EGNP-WEG as well as the basefluid decreases. In addition, the density of EGNP-WEG increased with increasing the weight concentration of EGNP. It can be due to higher density of EGNP than the densities of both the water and the EG. Also, an insignificant decrease is obvious by increasing the temperature. The density of the EGNP-WEG at maximum concentration of 0.2wt% decreases by 2.8% as the temperature reached to 65 °C.

Table 6.3: Densities of the water-EG mixture and EGNP-WEG at different concentrations (gr⁄cm^3).

Temperature (◦C)	Water-EG	0.01 wt%	0.05 wt%	0.1 wt%	0.2 wt%
25	1.099823	1.099948	1.101984	1.102997	1.104208
35	1.093669	1.094165	1.096322	1.0985	1.100104
45	1.088013	1.089027	1.091543	1.093333	1.094942
55	1.080697	1.081706	1.083884	1.08525	1.087516
65	1.069211	1.070681	1.072951	1.074181	1.076158

The specific heat capacity of EGNP-WEG as a function of the temperature and weight concentration is illustrated in Table 7.4. The results suggest that an increase in the weight concentration of EGNP leads a drop in the specific heat capacity. Also, the specific heat capacity of all the samples increases gradually with the temperature, which is sharper in coolants including EGNP. It is noteworthy that the drop in the specific heat capacity of

samples in the presence of EGNP is due to the lower specific heat capacity of EGNP than that of the basefluid.

Table 6.4: Specific heat capacity of the water-EG mixture and EGNP-WEG at different concentrations (J/kgK).

Temperature (◦C)	Water-EG	0.01 wt%	0.05 wt%	0.1 wt%	0.2 wt%
25	3.21	3.19	3.15	3.101	3.051
35	3.221	3.195	3.155	3.105	3.06
45	3.232	3.2	3.16	3.111	3.065
55	3.245	3.205	3.165	3.115	3.07
65	3.256	3.21	3.17	3.119	3.075

6.3 Numerical study

Figure 7.1 (a-b) show the velocity and inner wall temperature distribution in the annular tube. Velocity vectors are in axial direction and the natural convection is negligible due to the turbulent regime. It is shown that the EGNP loading in the basefluid improves the thermal conductivity of fluid, which increases the wall temperature as compared to the conventional basefluid. The lower the temperature difference between bulk fluid and wall tube, the higher the convective heat transfer coefficient.

Variations of the convective heat transfer coefficient and Nusselt number of EGNP dispersed in a mixture of DI water–EG are studied and the results are presented in this section.

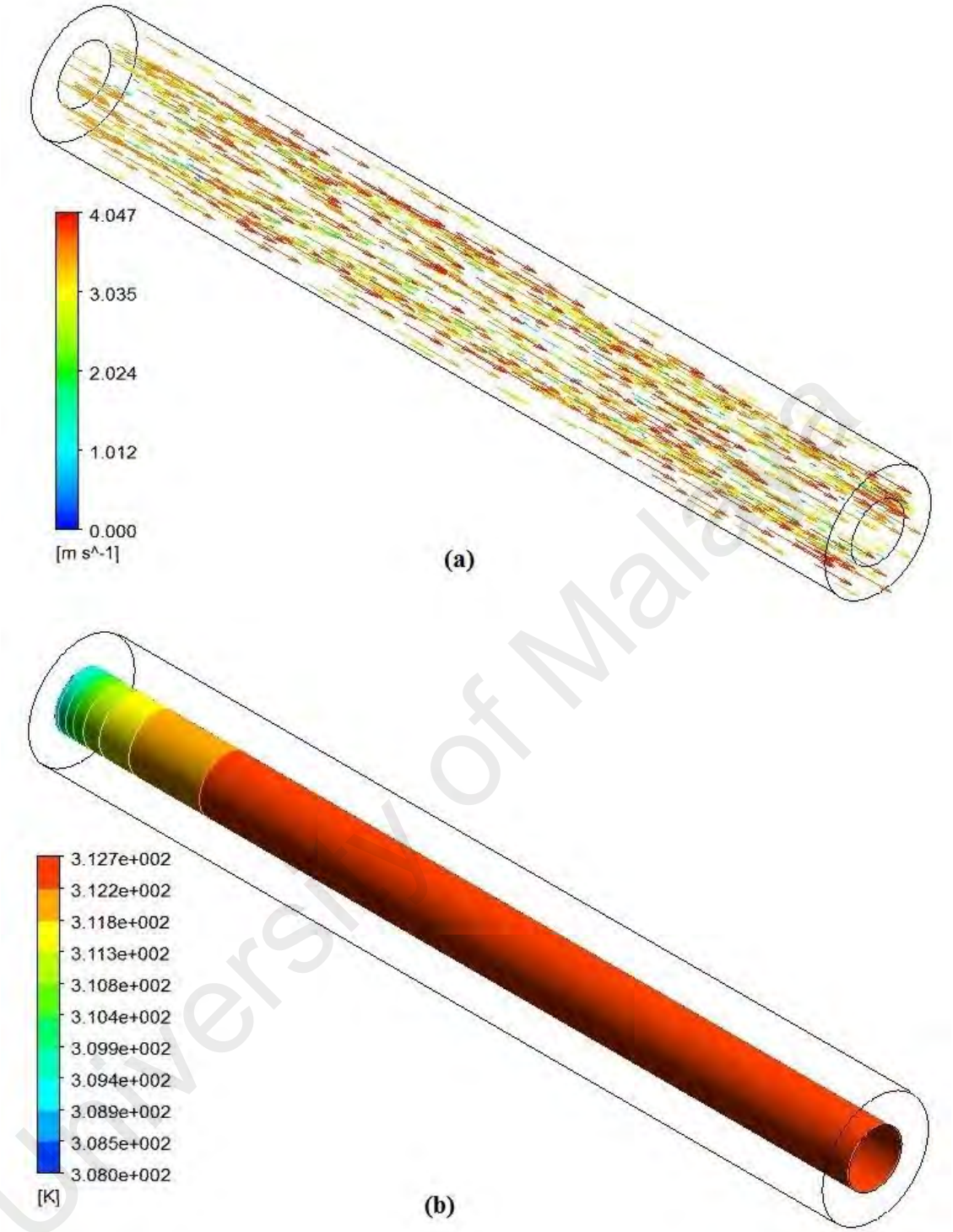

Figure 6.1: (a) Distributions of velocity and (b) inner wall temperature of EGNP-WEG fluid flow in an annular test section at Re=5000

Figure 7.2 shows the local Nusselt number at the inner wall at a constant heat flux (q″), different weight concentrations (ϕ), and various inlet velocities (u). The curves for all the simulations show the highest local Nu at the entry region due to entry length effect and

then there is an initial decrease in the local Nusselt number. After a certain distance the local Nu transform at the persistent minimum value, which (the local Nusselt number) remains constant in the axial direction due to the effect of fully developed turbulent flow regime. It is shown that the EGNP loading in the basefluid improves the thermal conductivity of the fluid, decrease the wall temperature as compared to the conventional basefluid. The lower temperature difference between bulk fluid and wall tube, the higher convective heat transfer coefficient is.

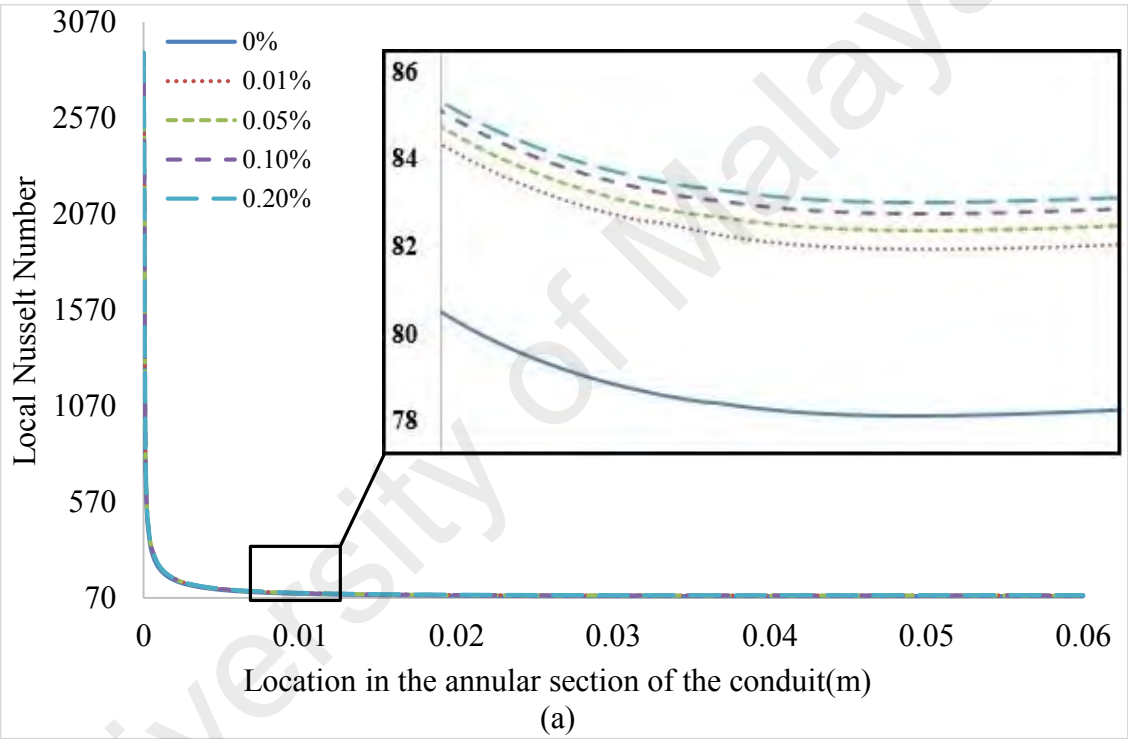

Figure 7.2 continued

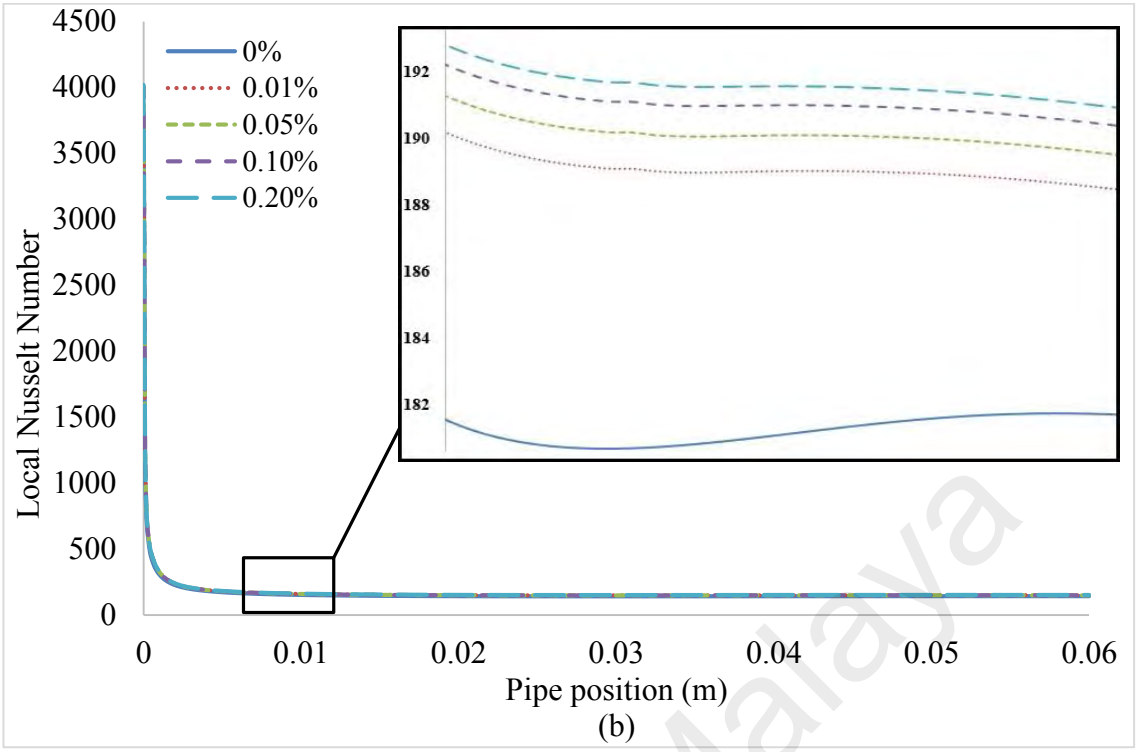

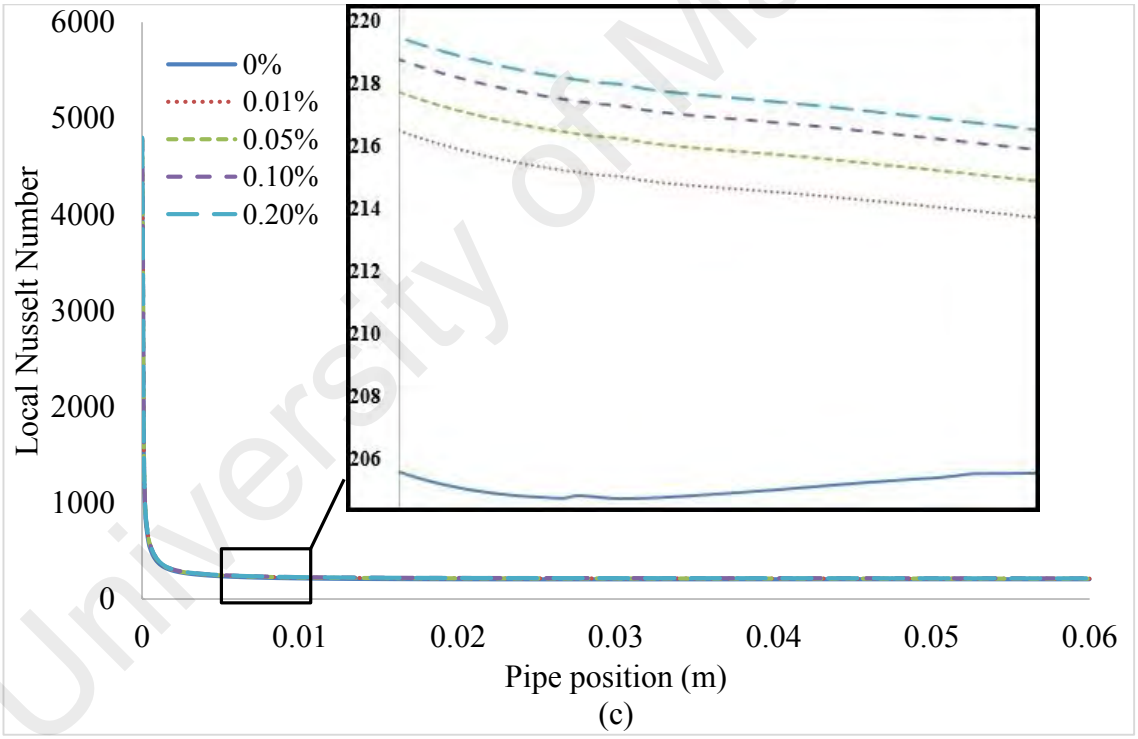

Figure 6.2: Variation of the local Nusselt number of EGNP-WEG fluid flow in the annular passage for different weight concentrations and Re=5000 (a), Re=10000 (b), Re=15000 (c).

Figure 7.3 shows the heat transfer coefficient plots of EGNP-WEG for five different Reynolds numbers and weight concentrations. It is realized that the enhancement of heat transfer coefficient of EGNP-WEG remarkably exceed those of the thermal conductivity

improvements for different weight concentrations. The maximum heat transfer coefficient at concentration of 0.2% and Reynolds number of 17,000 is 64%.

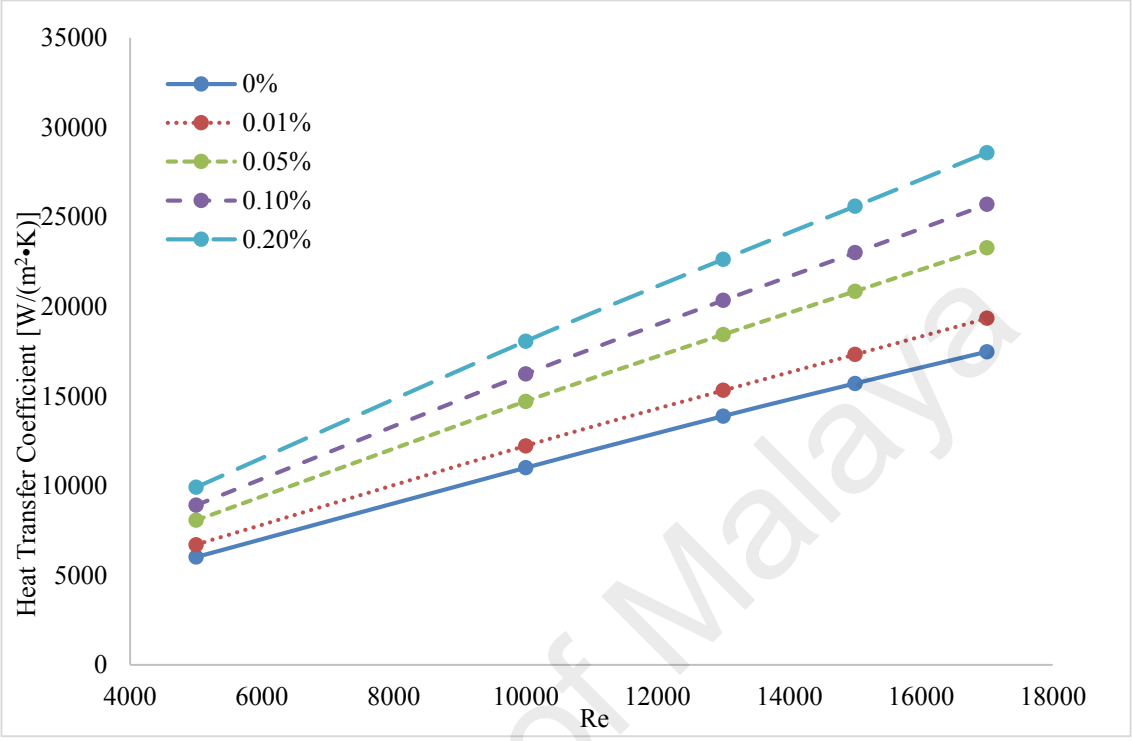

Figure 6.3: Average heat transfer coefficients for various Reynolds numbers and weight concentrations of EGNP-WEG coolants flow in annular test section.

Figure 7.4 shows the average Nusselt numbers of EGNP-WEG for various weight concentrations and Reynolds numbers. To evaluate the ratio of convective to conductive heat transfer of EGNP-WEG coolants, Nusselt number plots have been employed. The results suggest that the Nusselt number increases remarkably in the presence of treated samples in comparison to the applied basefluid. The EGNP loading in basefluid improves the thermal conductivity of basefluid, which leads to the lower temperature difference between the bulk fluid and wall of the tube, indicating higher Nusselt numbers and subsequently heat transfer rate.

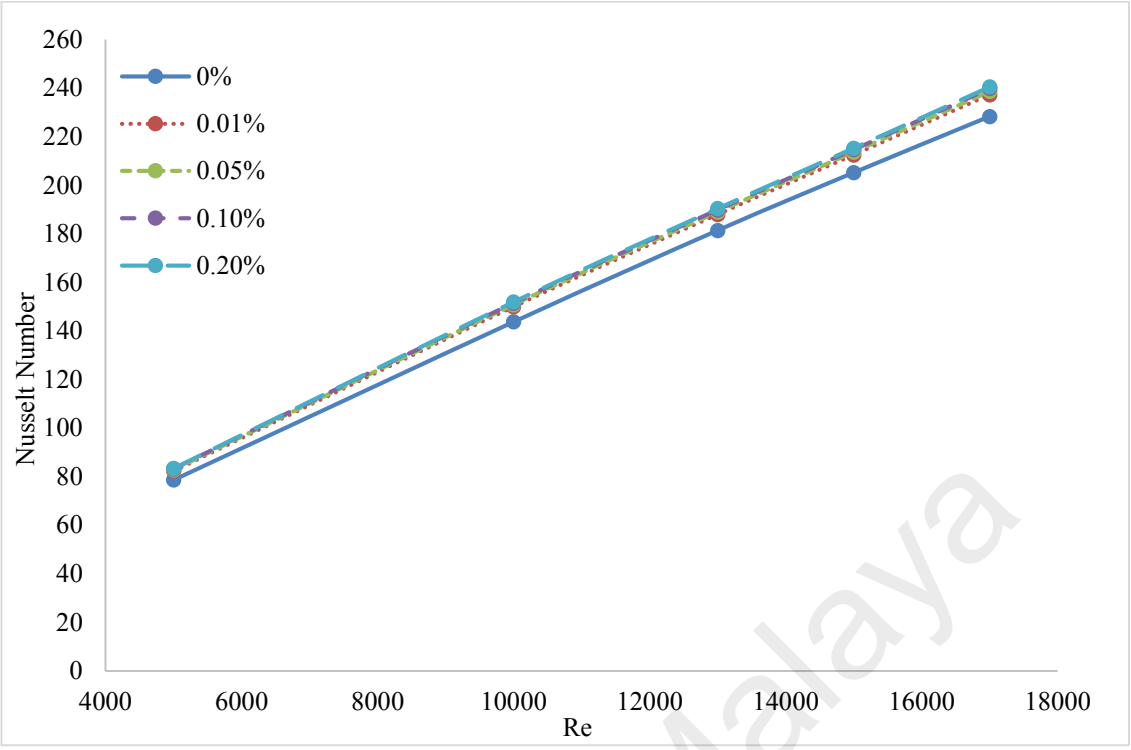

Figure 6.4: Average Nusselt numbers for various Reynolds numbers and weight concentrations of EGNP-WEG coolants flow in annular test section.

Figure 7.5 represents the friction factor for EGNP-WEG coolants in the annular tube at various weight concentrations and Reynolds numbers. Here the friction factor increases with the increase of concentration of EG-treated GNP. In addition, the friction factor decreases with increasing the flow velocity, which is a common phenomenon. The minimum value of the friction factor occurs for the basefluid.

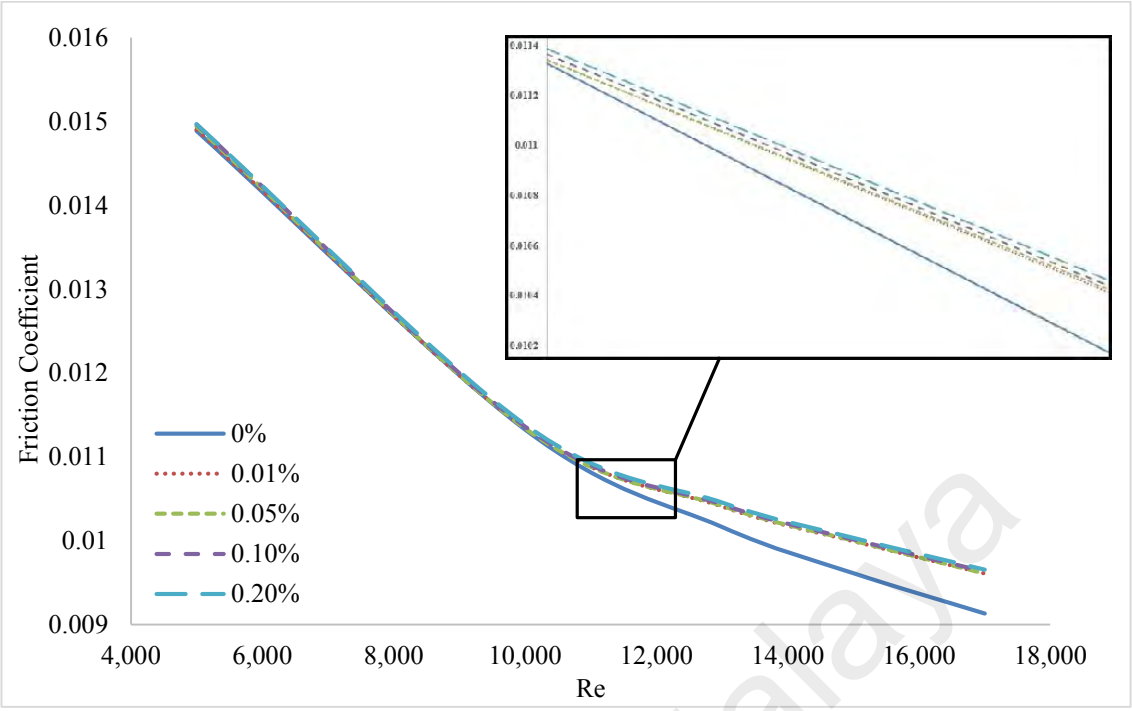

Figure 6.5: Friction factor at various Reynolds numbers.

The performance of the coolant is evaluated by considering both positive effects of increasing heat transfer coefficient and negative effects of increasing pressure drop in a cycle (Samira et al., 2015). Figure 7.6(a) shows the pressure distribution contour between inlet and outlet of the pipe. The pressure decreases dramatically with the increment of the Reynolds. Figure 7.6(b) present the performance index (ε) profile of EGNP-WEG nanofluid (equation 7.1) to clarify the effectiveness range of weight concentration and Reynolds number for employing this new type of coolant (Samira et al., 2015):

$$\varepsilon = \frac{h_{nf} / h_{bf}}{\Delta P_{nf} / \Delta P_{bf}} \tag{7.1}$$

Interestingly, the performance index of all the samples for all the Reynolds numbers is greater than 1, indicating the effectiveness of the prepared coolant in annular tube for different conditions. This figure also shows that the performance profile for different Reynolds numbers reach their peaks at the weight fraction of 0.05%, and that is followed

by a decrease in the performance index for further increase in the weight fraction of EGNP.

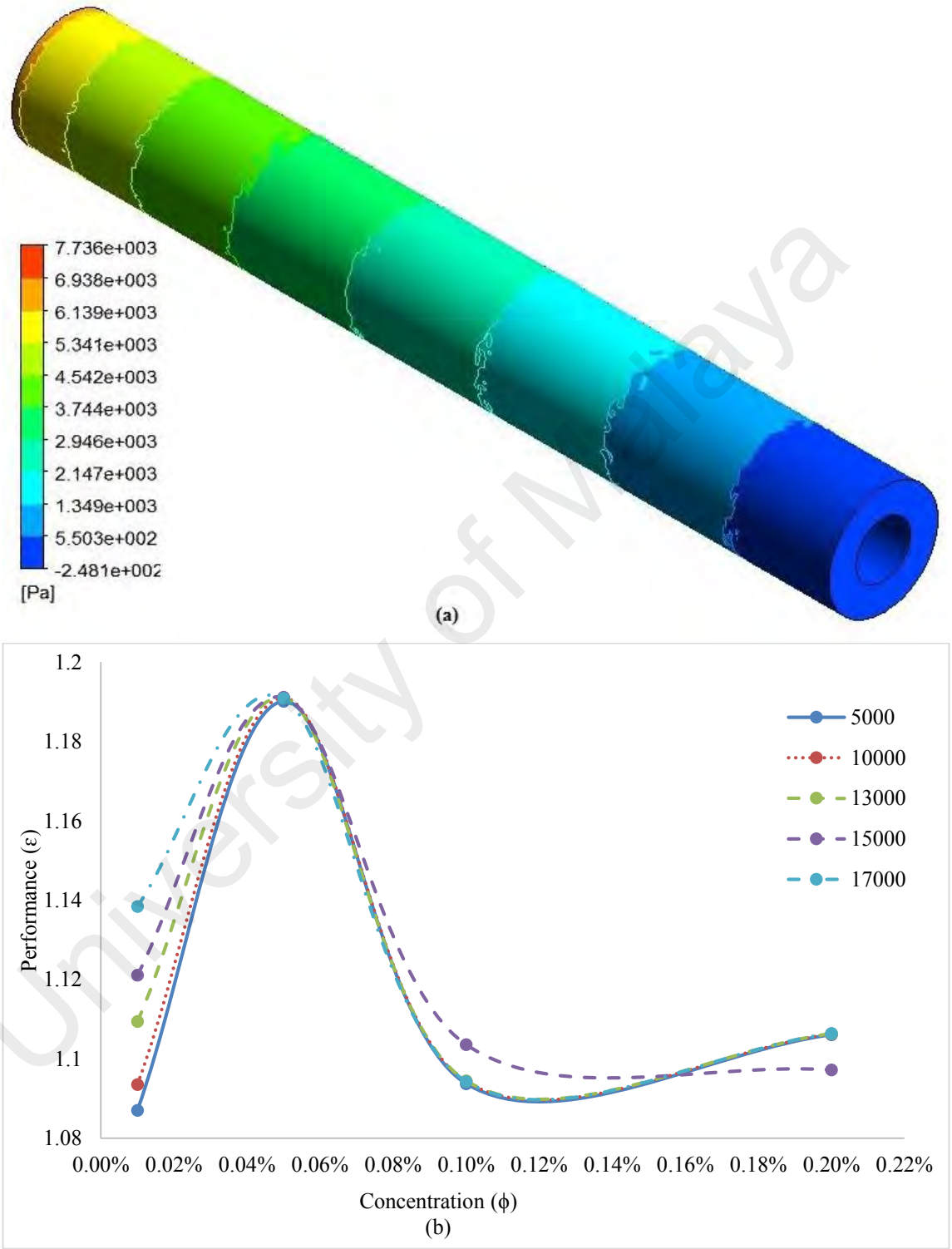

Figure 6.6: (a) Distribution of flow pressure and (b) the performance index of the synthesized coolant versus weight concentrations of EGGNP for various Reynolds numbers in annular flow.

CHAPTER 8: CONCLUSIONS AND FUTURE WORK

7.1 Conclusion

The new design of heat exchangers utilizing an annular distributor opens a new gateway for realizing higher energy transportation. To realize this goal, graphene nanoplatelet-Based Water Nanofluids with promising thermophysical properties were synthesized in the presence of covalent and non-covalent functionalization. Thermal conductivity, density, viscosity and specific heat capacity were investigated and employed as a raw data for ANSYS-Fluent for utilizing in two-phase approach. After validation of the obtained results by analytical equations, two special parameters the convective heat transfer coefficient and the pressure drop were investigated. The study followed by investigation of other heat transfer parameters in annular passage in the presence of graphene nanoplatelets-based water nanofluids at different weight concentrations, input powers and temperatures. As a result, Nusselt number profiles and friction factors are measured for both of the synthesized nanofluids.

In a novel direct amidation, the multi-walled carbon nanotubes (MWCNT) are covalently functionalized with Aspartic acid (Asp) to achieve a highly dispersible colloidal suspension including MWCNT. Stability of the colloidal suspensions were estimated with Uv-vis spectroscopy, where less than 20% sedimentation at the highest weight concentration of 0.1% could be obtained. The prepared coolants have the promising properties such as high thermal conductivity as compared with water. The prepared water-based coolants with different weight fractions of MWCNT-Asp were experimentally and numerically investigated in terms of heat transfer rate in a horizontal annular heat exchanger. Forced convection heat transfer coefficient and pressure drop were investigated in transition and turbulent regimes for three different heat fluxes and four

weight fractions. A significant increase in heat transfer rate in the annular heat exchanger has been obtained with the use of MWCNT-Asp nanofluid. Also poor change in the pressure drop in the presence of different weight concentrations ensures this novel alternative coolant as an alternative heat exchanging liquid. Also, the investigated insignificant increase in pumping power for the nanofluids show its suitability for industrial applications.

In order to improve the colloidal stability of Graphene Nanoplatelets (GNP) in aqueous media, they were first functionalized with tetrahydrofurfuryl polyethylene glycol in a quick electrophonic addition reaction method. To address this issue, surface functionalization of GNP was analyzed by Raman spectroscopy, and thermogravimetric analysis. In addition, the morphology of the treated samples were investigated by transmission electron microscopy (TEM). The thermophysical properties of the samples were experimentally investigated. In another investigation the convective heat transfer coefficient and pressure drop of water-based TFPEG-treated GNP nanofluids (TGNP/water) at various weight concentrations were numerically and experimentally investigated and compared with that of the base fluid in an annular heat exchanger. From the results it could be inferred that the addition of TGNP into the water improved the convective heat transfer coefficient dramatically. The pressure drop of the prepared samples generates an insignificant variation as compared with the base fluid. The steady-state forced convective heat transfer experiments and simulation have been confirmed the promising cooling capabilities of the TGNP/water.

Since graphene nanoplatelets (GNP) is a promising material due to desirable thermal properties. The thermo-physical and heat transfer performance of the covalently functionalized GNP-based water/ethylene glycol nanofluid in an annular channel has

been taken under consideration. After measuring thermophysical properties of the prepared samples, a computational fluid dynamics and experimental study has been carried out to study the heat transfer and pressure drop of well-dispersed and stabilized GNP nanofluids. The effect of concentration of GNP and Reynolds number at constant heat flux (Check) / wall temperature boundary condition under turbulent flow regime on convective heat transfer coefficient have been investigated. Based on the results, at different Reynolds numbers, the convective heat transfer coefficient of the prepared nanofluid is higher than that of the basefluid. Also, the enhancement of convective heat transfer coefficient and the thermal conductivity increase with increase of GNP concentration in basefluid. A significant enhancement on the heat transfer rate is associated with the loading and well-dispersion of the GNP in the basefluid.

7.2 Future work

Experimental and numerical works in this study have shown some potential improvements by using nanofluids for laminar convective heat transfer. The following questions, however, should be addressed in future work:

1. The aggregation stage of nanoparticles in suspension, calculated by DLVO theory or measured by DLS, was considered and thermal conductivity of nanofluid was able to be calculated (Prasher, Phelan, et al., 2006). However, he model did not include the effects from the flow field. Therefore, the aggregation kinetics and its related thermal conductivity models in flowing conditions are unknown and require further research.

2. From the data and analysis of nanofluid viscosity, this study showed that nanofluid could have an elongated aggregation chain in the flow field. Therefore, it is of interest to

understand how nanoparticles will align in the flow field and affect the convective heat transfer path.

3. Different base fluids and mixtures were studied. It was shown that different base fluids changed the Hamaker constant between nanoparticles and hence changed the adhesive potential between nanoparticles. The thermal conductivity results also indicated the nanoparticle aggregation stage could change the enhancement magnitude of nanofluid thermal conductivity. The change in adhesive potential between particles will also affect aggregation kinetics no matter if the nanofluid is stationary or under flow. Therefore, will different particle combinations affect convective heat transfer efficiency?

4. It is interesting to point out that since the size of nanoparticles is extremely small, the interaction phenomena between nanoparticles, fluid molecules and the tube wall remains unknown. Is there an optimal condition, such as flow loop geometry, nanoparticle size to flow loop diameter, etc., when utilizing specific nanofluids?

5. As for stability point of view, how will nanofluids perform over a long time period?

REFERENCES

Abu-Nada, E., Masoud, Z., & Hijazi, A. (2008). Natural convection heat transfer enhancement in horizontal concentric annuli using nanofluids. *International Communications in Heat and Mass Transfer, 35*(5), 657-665.

Abu-Nada, E., & Oztop, H. F. (2009). Effects of inclination angle on natural convection in enclosures filled with Cu–water nanofluid. *International Journal of Heat and Fluid Flow, 30*(4), 669-678.

Afshar, H., Shams, M., Nainian, S., & Ahmadi, G. (2009). Microchannel heat transfer and dispersion of nanoparticles in slip flow regime with constant heat flux. *International Communications in Heat and Mass Transfer, 36*(10), 1060-1066.

Akbari, M., Galanis, N., & Behzadmehr, A. (2011). A new model for nanofluid conductivity based on the effects of clustering due to Brownian motion. *Heat Transfer—Asian Research, 40*(4), 352-368.

Akbarinia, A., & Behzadmehr, A. (2007). Numerical study of laminar mixed convection of a nanofluid in horizontal curved tubes. *Applied Thermal Engineering, 27*(8), 1327-1337.

Akbarinia, A., & Laur, R. (2009). Investigating the diameter of solid particles effects on a laminar nanofluid flow in a curved tube using a two phase approach. *International Journal of Heat and Fluid Flow, 30*(4), 706-714.

Allen, C. L., Chhatwal, A. R., & Williams, J. M. (2012). Direct amide formation from unactivated carboxylic acids and amines. *Chemical Communications, 48*(5), 666-668.

Amiri, A., Ahmadi, G., Shanbedi, M., Savari, M., Kazi, S., & Chew, B. (2015). Microwave-assisted synthesis of highly-crumpled, few-layered graphene and nitrogen-doped graphene for use as high-performance electrodes in capacitive deionization. *Scientific reports, 5*.

Amiri, A., Maghrebi, M., Baniadam, M., & Heris, S. Z. (2011). One-pot, efficient functionalization of multi-walled carbon nanotubes with diamines by microwave method. *Applied Surface Science, 257*(23), 10261-10266.

Amiri, A., Maghrebi, M., Baniadam, M., & Zeinali Heris, S. (2011). One-pot, efficient functionalization of multi-walled carbon nanotubes with diamines by microwave method. *Applied Surface Science, 257*(23), 10261-10266. doi:http://dx.doi.org/10.1016/j.apsusc.2011.07.039

Amiri, A., Sadri, R., Ahmadi, G., Chew, B., Kazi, S., Shanbedi, M., & Alehashem, M. S. (2015). Synthesis of polyethylene glycol-functionalized multi-walled carbon nanotubes with a microwave-assisted approach for improved heat dissipation. *RSC Advances, 5*(45), 35425-35434.

Amiri, A., Sadri, R., Shanbedi, M., Ahmadi, G., Chew, B., Kazi, S., & Dahari, M. (2015). Performance dependence of thermosyphon on the functionalization approaches: An experimental study on thermo-physical properties of graphene nanoplatelet-based water nanofluids. *Energy Conversion and Management, 92*, 322-330.

Amiri, A., Sadri, R., Shanbedi, M., Ahmadi, G., Kazi, S., Chew, B., & Zubir, M. N. M. (2015). Synthesis of ethylene glycol-treated Graphene Nanoplatelets with one-pot, microwave-assisted functionalization for use as a high performance engine coolant. *Energy Conversion and Management, 101*, 767-777.

Amiri, A., Shanbedi, M., Eshghi, H., Heris, S. Z., & Baniadam, M. (2012). Highly dispersed multiwalled carbon nanotubes decorated with Ag nanoparticles in water and experimental investigation of the thermophysical properties. *The Journal of Physical Chemistry C, 116*(5), 3369-3375.

Anoop, K., Sundararajan, T., & Das, S. K. (2009). Effect of particle size on the convective heat transfer in nanofluid in the developing region. *International Journal of Heat and Mass Transfer, 52*(9), 2189-2195.

Aravind, S. J., & Ramaprabhu, S. (2013). Graphene–multiwalled carbon nanotube-based nanofluids for improved heat dissipation. *RSC Advances, 3*(13), 4199-4206.

Aravind, S. S. J., Baskar, P., Baby, T. T., Sabareesh, R. K., Das, S., & Ramaprabhu, S. (2011). Investigation of Structural Stability, Dispersion, Viscosity, and Conductive Heat Transfer Properties of Functionalized Carbon Nanotube Based Nanofluids. *The Journal of Physical Chemistry C, 115*(34), 16737-16744. doi:10.1021/jp201672p

Arzani, H. K., Amiri, A., Kazi, S., Chew, B., & Badarudin, A. (2015). Experimental and numerical investigation of thermophysical properties, heat transfer and pressure drop of covalent and noncovalent functionalized graphene nanoplatelet-based water nanofluids in an annular heat exchanger. *International Communications in Heat and Mass Transfer, 68*, 267-275.

Assael, M., Chen, C.-F., Metaxa, I., & Wakeham, W. (2004). Thermal conductivity of suspensions of carbon nanotubes in water. *International Journal of Thermophysics, 25*(4), 971-985.

Assael, M., Metaxa, I., Arvanitidis, J., Christofilos, D., & Lioutas, C. (2005). Thermal conductivity enhancement in aqueous suspensions of carbon multi-walled and double-walled nanotubes in the presence of two different dispersants. *International Journal of Thermophysics, 26*(3), 647-664.

Azizi, M., Hosseini, M., Zafarnak, S., Shanbedi, M., & Amiri, A. (2013). Experimental analysis of thermal performance in a two-phase closed thermosiphon using graphene/water nanofluid. *Industrial & Engineering Chemistry Research, 52*(29), 10015-10021.

Barbés, B., Páramo, R., Blanco, E., & Casanova, C. (2014). Thermal conductivity and specific heat capacity measurements of CuO nanofluids. *Journal of Thermal Analysis and Calorimetry, 115*(2), 1883-1891.

Behzadmehr, A., Saffar-Avval, M., & Galanis, N. (2007). Prediction of turbulent forced convection of a nanofluid in a tube with uniform heat flux using a two phase approach. *International Journal of Heat and Fluid Flow, 28*(2), 211-219.

Berber, S., Kwon, Y.-K., & Tománek, D. (2000). Unusually high thermal conductivity of carbon nanotubes. *Physical Review Letters, 84*(20), 4613.

Bianco, V., Chiacchio, F., Manca, O., & Nardini, S. (2009). Numerical investigation of nanofluids forced convection in circular tubes. *Applied Thermal Engineering, 29*(17), 3632-3642.

Brege, J. J., Gallaway, C., & Barron, A. R. (2007). Fluorescence quenching of single-walled carbon nanotubes in SDBS surfactant suspension by metal ions: Quenching efficiency as a function of metal and nanotube identity. *The Journal of Physical Chemistry C, 111*(48), 17812-17820.

Buschmann, M. H., & Franzke, U. (2014). Improvement of thermosyphon performance by employing nanofluid. *International Journal of Refrigeration, 40*, 416-428.

Calmidi, V., & Mahajan, R. (1999). The effective thermal conductivity of high porosity fibrous metal foams. *Journal of Heat transfer, 121*(2), 466-471.

Carslaw, H. S., & Jaeger, J. C. (1959). Conduction of heat in solids. *Oxford: Clarendon Press, 1959, 2nd ed.*

Cheng, S., & Vachon, R. (1969). The prediction of the thermal conductivity of two and three phase solid heterogeneous mixtures. *International Journal of Heat and Mass Transfer, 12*(3), 249-264.

Choi, S., Zhang, Z., Yu, W., Lockwood, F., & Grulke, E. (2001). Anomalous thermal conductivity enhancement in nanotube suspensions. *Applied physics letters, 79*(14), 2252-2254.

Crowe, L. M., Reid, D. S., & Crowe, J. H. (1996). Is trehalose special for preserving dry biomaterials? *Biophysical journal, 71*(4), 2087.

Das, S. K., Choi, S. U., Yu, W., & Pradeep, T. (2007). *Nanofluids: science and technology*: John Wiley & Sons.

Das, S. K., Putra, N., Thiesen, P., & Roetzel, W. (2003). Temperature dependence of thermal conductivity enhancement for nanofluids. *Journal of Heat transfer, 125*(4), 567-574.

Ding, Y., Alias, H., Wen, D., & Williams, R. A. (2006). Heat transfer of aqueous suspensions of carbon nanotubes (CNT nanofluids). *International Journal of Heat and Mass Transfer, 49*(1), 240-250.

Duka, B., Ferrario, C., Passerini, A., & Piva, S. (2007). Non-linear approximations for natural convection in a horizontal annulus. *International Journal of Non-Linear Mechanics, 42*(9), 1055-1061.

Eastman, J., Choi, U., Li, S., Thompson, L., & Lee, S. (1996). *Enhanced thermal conductivity through the development of nanofluids.* Paper presented at the MRS proceedings.

Eastman, J. A., Choi, S., Li, S., Yu, W., & Thompson, L. (2001). Anomalously increased effective thermal conductivities of ethylene glycol-based nanofluids containing copper nanoparticles. *Applied physics letters, 78*(6), 718-720.

Eastman, J. A., Phillpot, S., Choi, S., & Keblinski, P. (2004). Thermal transport in nanofluids 1. *Annu. Rev. Mater. Res., 34*, 219-246.

Evans, W., Fish, J., & Keblinski, P. (2006). Role of Brownian motion hydrodynamics on nanofluid thermal conductivity. *Applied physics letters, 88*(9), 093116.

Evans, W., Prasher, R., Fish, J., Meakin, P., Phelan, P., & Keblinski, P. (2008). Effect of aggregation and interfacial thermal resistance on thermal conductivity of nanocomposites and colloidal nanofluids. *International Journal of Heat and Mass Transfer, 51*(5), 1431-1438.

Fernandez-Seara, J., Uhía, F. J., Sieres, J., & Campo, A. (2007). A general review of the Wilson plot method and its modifications to determine convection coefficients in heat exchange devices. *Applied Thermal Engineering, 27*(17), 2745-2757.

Fotukian, S., & Esfahany, M. N. (2010a). Experimental investigation of turbulent convective heat transfer of dilute γ-Al 2 O 3/water nanofluid inside a circular tube. *International Journal of Heat and Fluid Flow, 31*(4), 606-612.

Fotukian, S., & Esfahany, M. N. (2010b). Experimental study of turbulent convective heat transfer and pressure drop of dilute CuO/water nanofluid inside a circular tube. *International Communications in Heat and Mass Transfer, 37*(2), 214-219.

Garg, P., Alvarado, J. L., Marsh, C., Carlson, T. A., Kessler, D. A., & Annamalai, K. (2009). An experimental study on the effect of ultrasonication on viscosity and heat transfer performance of multi-wall carbon nanotube-based aqueous nanofluids. *International Journal of Heat and Mass Transfer, 52*(21), 5090-5101.

GHOBADIAN, R., & MOHAMMADI, K. (2011). Simulation of subcritical flow pattern in 180 uniform and convergent open-channel bends using SSIIM 3-D model. *水科学与水工程 4*(3).

Hamilton, R., & Crosser, O. (1962). Thermal conductivity of heterogeneous two-component systems. *Industrial & Engineering chemistry fundamentals, 1*(3), 187-191.

Heris, S. Z., Etemad, S. G., & Esfahany, M. N. (2006). Experimental investigation of oxide nanofluids laminar flow convective heat transfer. *International Communications in Heat and Mass Transfer, 33*(4), 529-535.

Hone, J., Whitney, M., Piskoti, C., & Zettl, A. (1999). Thermal conductivity of single-walled carbon nanotubes. *Physical Review B, 59*(4), R2514.

Hong, K., Hong, T.-K., & Yang, H.-S. (2006). Thermal conductivity of Fe nanofluids depending on the cluster size of nanoparticles. *Applied physics letters, 88*(3), 031901.

Hong, T.-K., Yang, H.-S., & Choi, C. (2005). Study of the enhanced thermal conductivity of Fe nanofluids. *Journal of Applied Physics, 97*(6), 064311.

Hosseini, S. M., Moghadassi, A., & Henneke, D. (2011). Modelling of the effective thermal conductivity of carbon nanotube nanofluids based on dimensionless groups. *The Canadian Journal of Chemical Engineering, 89*(1), 183-186.

Hwang, Y., Lee, J., Lee, C., Jung, Y., Cheong, S., Lee, C., . . . Jang, S. (2007). Stability and thermal conductivity characteristics of nanofluids. *Thermochimica Acta, 455*(1), 70-74.

Iijima, S. (1991). Helical microtubules of graphitic carbon. *nature, 354*(6348), 56-58.

Ishii, M. (1975). Thermo-fluid dynamic theory of two-phase flow. *NASA STI/Recon Technical Report A, 75*, 29657.

Islam, M., Rojas, E., Bergey, D., Johnson, A., & Yodh, A. (2003). High weight fraction surfactant solubilization of single-wall carbon nanotubes in water. *Nano letters, 3*(2), 269-273.

Izadi, M., Behzadmehr, A., & Jalali-Vahida, D. (2009). Numerical study of developing laminar forced convection of a nanofluid in an annulus. *International Journal of Thermal Sciences, 48*(11), 2119-2129.

Jang, S. P., & Choi, S. U. (2004). Role of Brownian motion in the enhanced thermal conductivity of nanofluids. *Applied physics letters, 84*(21), 4316-4318.

Jeffrey, D. J. (1973). *Conduction through a random suspension of spheres.* Paper presented at the Proceedings of the Royal Society of London A: Mathematical, Physical and Engineering Sciences.

Jha, N., & Ramaprabhu, S. (2008). Synthesis and Thermal Conductivity of Copper Nanoparticle Decorated Multiwalled Carbon Nanotubes Based Nanofluids. *The Journal of Physical Chemistry C, 112*(25), 9315-9319. doi:10.1021/jp8017309

Jiang, W., Ding, G., & Peng, H. (2009). Measurement and model on thermal conductivities of carbon nanotube nanorefrigerants. *International Journal of Thermal Sciences, 48*(6), 1108-1115.

Kashani, A., Jalali-vahid, D., & Hossainpour, S. (2013). Numerical study of laminar forced convection of water/Al2O3 nanofluid in an annulus with constant wall temperature. *IIUM Engineering Journal, 14*(1).

Keblinski, P., Phillpot, S., Choi, S., & Eastman, J. (2002). Mechanisms of heat flow in suspensions of nano-sized particles (nanofluids). *International Journal of Heat and Mass Transfer, 45*(4), 855-863.

Khanafer, K., Vafai, K., & Lightstone, M. (2003). Buoyancy-driven heat transfer enhancement in a two-dimensional enclosure utilizing nanofluids. *International Journal of Heat and Mass Transfer, 46*(19), 3639-3653.

Ko, G. H., Heo, K., Lee, K., Kim, D. S., Kim, C., Sohn, Y., & Choi, M. (2007). An experimental study on the pressure drop of nanofluids containing carbon nanotubes in a horizontal tube. *International Journal of Heat and Mass Transfer, 50*(23), 4749-4753.

Koo, J., & Kleinstreuer, C. (2005). Impact analysis of nanoparticle motion mechanisms on the thermal conductivity of nanofluids. *International Communications in Heat and Mass Transfer, 32*(9), 1111-1118.

Kumar, D. H., Patel, H. E., Kumar, V. R., Sundararajan, T., Pradeep, T., & Das, S. K. (2004). Model for heat conduction in nanofluids. *Physical Review Letters, 93*(14), 144301.

Kwak, K., & Kim, C. (2005). Viscosity and thermal conductivity of copper oxide nanofluid dispersed in ethylene glycol. *Korea-Australia Rheology Journal, 17*(2), 35-40.

Launder, B. E., & Spalding, D. (1974). The numerical computation of turbulent flows. *Computer methods in applied mechanics and engineering, 3*(2), 269-289.

Lee, D.-L., & Irvine, T. F. (1997). Shear rate dependent thermal conductivity measurements of non-Newtonian fluids. *Experimental Thermal and Fluid Science, 15*(1), 16-24.

Lee, D. (2007). Thermophysical properties of interfacial layer in nanofluids. *Langmuir, 23*(11), 6011-6018.

Lee, D., Kim, J.-W., & Kim, B. G. (2006). A new parameter to control heat transport in nanofluids: surface charge state of the particle in suspension. *The Journal of Physical Chemistry B, 110*(9), 4323-4328.

Lee, S., Choi, S.-S., Li, S., and, & Eastman, J. (1999). Measuring thermal conductivity of fluids containing oxide nanoparticles. *Journal of Heat transfer, 121*(2), 280-289.

Li, C. H., Williams, W., Buongiorno, J., Hu, L.-W., & Peterson, G. (2008). Transient and Steady-State Experimental Comparison Study of Effective Thermal Conductivity of Al2O3⁄Water Nanofluids. *Journal of Heat transfer, 130*(4), 042407.

Li, Y., Tung, S., Schneider, E., & Xi, S. (2009). A review on development of nanofluid preparation and characterization. *Powder Technology, 196*(2), 89-101.

Liu, M.-S., Lin, M. C.-C., Huang, I.-T., & Wang, C.-C. (2005). Enhancement of thermal conductivity with carbon nanotube for nanofluids. *International Communications in Heat and Mass Transfer, 32*(9), 1202-1210.

Liu, M.-S., Lin, M. C.-C., Tsai, C., & Wang, C.-C. (2006). Enhancement of thermal conductivity with Cu for nanofluids using chemical reduction method. *International Journal of Heat and Mass Transfer, 49*(17), 3028-3033.

Liu, Z.-H., & Liao, L. (2010). Forced convective flow and heat transfer characteristics of aqueous drag-reducing fluid with carbon nanotubes added. *International Journal of Thermal Sciences, 49*(12), 2331-2338.

Liu, Z.-h., Yang, X.-f., & Guo, G.-l. (2010). Influence of carbon nanotube suspension on the thermal performance of a miniature thermosyphon. *International Journal of Heat and Mass Transfer, 53*(9), 1914-1920.

Lotfi, R., Saboohi, Y., & Rashidi, A. (2010). Numerical study of forced convective heat transfer of nanofluids: comparison of different approaches. *International Communications in Heat and Mass Transfer, 37*(1), 74-78.

Mahian, O., Kianifar, A., Kleinstreuer, C., Moh'd A, A.-N., Pop, I., Sahin, A. Z., & Wongwises, S. (2013). A review of entropy generation in nanofluid flow. *International Journal of Heat and Mass Transfer, 65*, 514-532.

Manninen, M., Taivassalo, V., & Kallio, S. (1996). On the mixture model for multiphase flow: Technical Research Centre of Finland Finland.

Maxwell, J. C. (1904). A Treatise on Electricity and Magnetism, vol. II. Clarendon: Oxford.

Mehta, B., & Khandekar, S. (2007). *Two-phase closed thermosyphon with nanofluids.* Paper presented at the 14th International Heat Pipe Conference, April 22-27, 2007, Florianopolis, Brazil.

Meibodi, M. E., Vafaie-Sefti, M., Rashidi, A. M., Amrollahi, A., Tabasi, M., & Kalal, H. S. (2010). The role of different parameters on the stability and thermal conductivity of carbon nanotube/water nanofluids. *International Communications in Heat and Mass Transfer, 37*(3), 319-323.

Mirmasoumi, S., & Behzadmehr, A. (2008a). Effect of nanoparticles mean diameter on mixed convection heat transfer of a nanofluid in a horizontal tube. *International Journal of Heat and Fluid Flow, 29*(2), 557-566.

Mirmasoumi, S., & Behzadmehr, A. (2008b). Numerical study of laminar mixed convection of a nanofluid in a horizontal tube using two-phase mixture model. *Applied Thermal Engineering, 28*(7), 717-727.

Mohammed, H. A. (2008). Laminar mixed convection heat transfer in a vertical circular tube under buoyancy-assisted and opposed flows. *Energy Conversion and Management, 49*(8), 2006-2015.

Murshed, S., Leong, K., & Yang, C. (2005). Enhanced thermal conductivity of TiO 2—water based nanofluids. *International Journal of Thermal Sciences, 44*(4), 367-373.

Nagasaka, Y., & Nagashima, A. (1981). Absolute measurement of the thermal conductivity of electrically conducting liquids by the transient hot-wire method. *Journal of Physics E: Scientific Instruments, 14*(12), 1435.

Nan, C.-W., Birringer, R., Clarke, D. R., & Gleiter, H. (1997). Effective thermal conductivity of particulate composites with interfacial thermal resistance. *Journal of Applied Physics, 81*(10), 6692-6699.

Nanda, J., Maranville, C., Bollin, S. C., Sawall, D., Ohtani, H., Remillard, J. T., & Ginder, J. (2008). Thermal conductivity of single-wall carbon nanotube dispersions: role of interfacial effects. *The Journal of Physical Chemistry C, 112*(3), 654-658.

Özerinç, S., Kakaç, S., & Yazıcıoğlu, A. G. (2010). Enhanced thermal conductivity of nanofluids: a state-of-the-art review. *Microfluidics and Nanofluidics, 8*(2), 145-170.

Pang, C., Jung, J.-Y., Lee, J. W., & Kang, Y. T. (2012). Thermal conductivity measurement of methanol-based nanofluids with Al 2 O 3 and SiO 2 nanoparticles. *International Journal of Heat and Mass Transfer, 55*(21), 5597-5602.

Passerini, A., Ferrario, C., & Thäter, G. (2008). Natural convection in horizontal annuli: a lower bound for the energy. *Journal of Engineering Mathematics, 62*(3), 247-259.

Patel, H., Anoop, K., Sundararajan, T., & Das, S. K. (2008). Model for thermal conductivity of CNT-nanofluids. *Bulletin of Materials Science, 31*(3), 387-390.

Patel, H. E., Anoop, K., Sundararajan, T., & Das, S. K. (2006). *A micro-convection model for thermal conductivity of nanofluids.* Paper presented at the International Heat Transfer Conference 13.

Patel, H. E., Das, S. K., Sundararajan, T., Nair, A. S., George, B., & Pradeep, T. (2003). Thermal conductivities of naked and monolayer protected metal nanoparticle based nanofluids: Manifestation of anomalous enhancement and chemical effects. *Applied physics letters, 83*(14), 2931-2933.

Patel, H. E., Sundararajan, T., & Das, S. K. (2008). A cell model approach for thermal conductivity of nanofluids. *Journal of Nanoparticle Research, 10*(1), 87-97.

Patel, H. E., Sundararajan, T., & Das, S. K. (2010). An experimental investigation into the thermal conductivity enhancement in oxide and metallic nanofluids. *Journal of Nanoparticle Research, 12*(3), 1015-1031.

Prasher, R., Evans, W., Meakin, P., Fish, J., Phelan, P., & Keblinski, P. (2006). Effect of aggregation on thermal conduction in colloidal nanofluids. *Applied physics letters, 89*(14), 143119.

Prasher, R., Phelan, P. E., & Bhattacharya, P. (2006). Effect of aggregation kinetics on the thermal conductivity of nanoscale colloidal solutions (nanofluid). *Nano letters, 6*(7), 1529-1534.

Putnam, S. A., Cahill, D. G., Braun, P. V., Ge, Z., & Shimmin, R. G. (2006). Thermal conductivity of nanoparticle suspensions. *Journal of Applied Physics, 99*(8), 084308.

Roy, G., Nguyen, C. T., & Lajoie, P.-R. (2004). Numerical investigation of laminar flow and heat transfer in a radial flow cooling system with the use of nanofluids. *Superlattices and Microstructures, 35*(3), 497-511.

Ryglowski, B. K. (2009). *Characterization of Carbon Nanotube-Enhanced water as a phase change material for thermal energy storage systems.* Monterey, California. Naval Postgraduate School.

Sakiadis, B. (1961). Boundary-layer behavior on continuous solid surfaces: I. Boundary-layer equations for two-dimensional and axisymmetric flow. *AIChE Journal, 7*(1), 26-28.

Samira, P., Saeed, Z. H., Motahare, S., & Mostafa, K. (2015). Pressure drop and thermal performance of CuO/ethylene glycol (60%)-water (40%) nanofluid in car radiator. *Korean Journal of Chemical Engineering, 32*(4), 609-616.

Sarsam, W. S., Amiri, A., Zubir, M. N. M., Yarmand, H., Kazi, S. N., & Badarudin, A. (2016). Stability and thermophysical properties of water-based nanofluids containing triethanolamine-treated graphene nanoplatelets with different specific surface areas. *Colloids and Surfaces A: Physicochemical and Engineering Aspects, 500*, 17-31. doi:http://dx.doi.org/10.1016/j.colsurfa.2016.04.016

Sastry, N. V., Bhunia, A., Sundararajan, T., & Das, S. K. (2008). Predicting the effective thermal conductivity of carbon nanotube based nanofluids. *Nanotechnology, 19*(5), 055704.

Schwartz, L. M., Garboczi, E. J., & Bentz, D. P. (1995). Interfacial transport in porous media: Application to dc electrical conductivity of mortars. *Journal of Applied Physics, 78*(10), 5898-5908.

Shahi, M., Mahmoudi, A. H., & Talebi, F. (2010). Numerical study of mixed convective cooling in a square cavity ventilated and partially heated from the below utilizing nanofluid. *International Communications in Heat and Mass Transfer, 37*(2), 201-213.

Shaikh, S., Lafdi, K., & Ponnappan, R. (2007). Thermal conductivity improvement in carbon nanoparticle doped PAO oil: An experimental study. *Journal of Applied Physics, 101*(6), 064302.

Shanbedi, M., Zeinali Heris, S., Baniadam, M., & Amiri, A. (2013). The effect of multi-walled carbon nanotube/water nanofluid on thermal performance of a two-phase closed thermosyphon. *Experimental Heat Transfer, 26*(1), 26-40.

Shih, T. M. (1984). *Numerical heat transfer*: CRC Press.

Shin, S., & Lee, S.-H. (2000). Thermal conductivity of suspensions in shear flow fields. *International Journal of Heat and Mass Transfer, 43*(23), 4275-4284.

Shukla, R. K., & Dhir, V. K. (2005). *Numerical study of the effective thermal conductivity of nanofluids.* Paper presented at the ASME 2005 Summer Heat Transfer

Conference collocated with the ASME 2005 Pacific Rim Technical Conference and Exhibition on Integration and Packaging of MEMS, NEMS, and Electronic Systems.

Silvera-Batista, C. A., Scott, D. C., McLeod, S. M., & Ziegler, K. J. (2011). A mechanistic study of the selective retention of SDS-suspended single-wall carbon nanotubes on agarose gels. *The Journal of Physical Chemistry C, 115*(19), 9361-9369.

Sun, Z., Kohama, S.-i., Zhang, Z., Lomeda, J. R., & Tour, J. M. (2010). Soluble graphene through edge-selective functionalization. *Nano Research, 3*(2), 117-125.

Sundar, L. S., & Sharma, K. (2010). Turbulent heat transfer and friction factor of Al 2 O 3 nanofluid in circular tube with twisted tape inserts. *International Journal of Heat and Mass Transfer, 53*(7), 1409-1416.

Suttipong, M., Tummala, N. R., Kitiyanan, B., & Striolo, A. (2011). Role of surfactant molecular structure on self-assembly: aqueous SDBS on carbon nanotubes. *The Journal of Physical Chemistry C, 115*(35), 17286-17296.

Talebi, F., Mahmoudi, A. H., & Shahi, M. (2010). Numerical study of mixed convection flows in a square lid-driven cavity utilizing nanofluid. *International Communications in Heat and Mass Transfer, 37*(1), 79-90.

Tian, R., Wang, X., Li, M., Hu, H., Chen, R., Liu, F., . . . Wan, L. (2008). An efficient route to functionalize singe-walled carbon nanotubes using alcohols. *Applied Surface Science, 255*(5), 3294-3299.

Tillman, P., & Hill, J. M. (2007). Determination of nanolayer thickness for a nanofluid. *International Communications in Heat and Mass Transfer, 34*(4), 399-407.

Venerus, D. C., Kabadi, M. S., Lee, S., & Perez-Luna, V. (2006). Study of thermal transport in nanoparticle suspensions using forced Rayleigh scattering. *Journal of Applied Physics, 100*(9), 094310.

Vishwanadula, H. (2008). *Experimental investigations on the flow of nanofluids through circular pipes*: Southern Illinois University at Carbondale.

Wakeham, W. A., Nagashima, A., & Sengers, J. (1991). *Measurement of the transport properties of fluids* (Vol. 3): Blackwell Science Inc.

Wang, X.-Q., & Mujumdar, A. S. (2008). A review on nanofluids-part I: theoretical and numerical investigations. *Brazilian Journal of Chemical Engineering, 25*(4), 613-630.

Wang, X., Xu, X., & S. Choi, S. U. (1999). Thermal conductivity of nanoparticle-fluid mixture. *Journal of thermophysics and heat transfer, 13*(4), 474-480.

Wen, D., & Ding, Y. (2004). Effective thermal conductivity of aqueous suspensions of carbon nanotubes (carbon nanotube nanofluids). *Journal of thermophysics and heat transfer, 18*(4), 481-485.

Williams, W., Buongiorno, J., & Hu, L.-W. (2008). Experimental investigation of turbulent convective heat transfer and pressure loss of alumina/water and zirconia/water nanoparticle colloids (nanofluids) in horizontal tubes. *Journal of Heat transfer, 130*(4), 042412.

Wong, K. V., & Castillo, M. J. (2010). Heat transfer mechanisms and clustering in nanofluids. *Advances in Mechanical Engineering, 2*, 795478.

Xie, H.-q., Wang, J.-c., Xi, T.-g., & Liu, Y. (2002). Thermal conductivity of suspensions containing nanosized SiC particles. *International Journal of Thermophysics, 23*(2), 571-580.

Xie, H., Lee, H., Youn, W., & Choi, M. (2003). Nanofluids containing multiwalled carbon nanotubes and their enhanced thermal conductivities. *Journal of Applied Physics, 94*(8), 4967-4971.

Xie, H., Wang, J., Xi, T., Liu, Y., Ai, F., & Wu, Q. (2002). Thermal conductivity enhancement of suspensions containing nanosized alumina particles. *Journal of Applied Physics, 91*(7), 4568-4572.

Xie, H., Yu, W., Li, Y., & Chen, L. (2011). Discussion on the thermal conductivity enhancement of nanofluids. *Nanoscale research letters, 6*(1), 124.

Xu, H.-K. (2004). Viscosity approximation methods for nonexpansive mappings. *Journal of Mathematical Analysis and Applications, 298*(1), 279-291.

Xuan, Y., & Li, Q. (2000). Heat transfer enhancement of nanofluids. *International Journal of Heat and Fluid Flow, 21*(1), 58-64.

Xue, H., Fan, J., Hu, Y., Hong, R., & Cen, K. (2006). The interface effect of carbon nanotube suspension on the thermal performance of a two-phase closed thermosyphon. *Journal of Applied Physics, 100*(10), 104909.

Xue, L., Keblinski, P., Phillpot, S., Choi, S.-S., & Eastman, J. (2004). Effect of liquid layering at the liquid–solid interface on thermal transport. *International Journal of Heat and Mass Transfer, 47*(19), 4277-4284.

Xue, Q.-Z. (2003). Model for effective thermal conductivity of nanofluids. *Physics letters A, 307*(5), 313-317.

Xue, Q. (2006). Model for the effective thermal conductivity of carbon nanotube composites. *Nanotechnology, 17*(6), 1655.

Xue, Q., & Xu, W.-M. (2005). A model of thermal conductivity of nanofluids with interfacial shells. *Materials Chemistry and Physics, 90*(2), 298-301.

Yoo, D.-H., Hong, K., & Yang, H.-S. (2007). Study of thermal conductivity of nanofluids for the application of heat transfer fluids. *Thermochimica Acta, 455*(1), 66-69.

You, S., Kim, J., & Kim, K. (2003). Effect of nanoparticles on critical heat flux of water in pool boiling heat transfer. *Applied physics letters, 83*(16), 3374-3376.

Yu, C.-J., Richter, A., Datta, A., Durbin, M., & Dutta, P. (1999). Observation of molecular layering in thin liquid films using X-ray reflectivity. *Physical Review Letters, 82*(11), 2326.

Yu, W., & Choi, S. (2003). The role of interfacial layers in the enhanced thermal conductivity of nanofluids: a renovated Maxwell model. *Journal of Nanoparticle Research, 5*(1-2), 167-171.

Yu, W., France, D. M., Routbort, J. L., & Choi, S. U. (2008). Review and comparison of nanofluid thermal conductivity and heat transfer enhancements. *Heat Transfer Engineering, 29*(5), 432-460.

Yu, W., & Xie, H. (2012). A review on nanofluids: preparation, stability mechanisms, and applications. *Journal of Nanomaterials, 2012*, 1.

Yu, W., Xie, H., & Bao, D. (2009). Enhanced thermal conductivities of nanofluids containing graphene oxide nanosheets. *Nanotechnology, 21*(5), 055705.

Zhang, Z., & Lockwood, F. E. (2004). Preparation of stable nanotube dispersions in liquids: Google Patents.

Zhu, H., Zhang, C., Liu, S., Tang, Y., & Yin, Y. (2006). Effects of nanoparticle clustering and alignment on thermal conductivities of Fe3O4 aqueous nanofluids. *Applied physics letters, 89*(2), 23123-23123.

LIST OF PUBLICATIONS AND PAPER PRESENTED

ISI publications

1- Experimental and numerical investigation of thermophysical properties, heat transfer and pressure drop of covalent and noncovalent functionalized graphene nanoplatelet-based water nanofluids in an annular heat exchanger, *HK Arzani, A Amiri, SN Kazi, BT Chew, A Badarudin, International Communications in Heat and Mass Transfer 68, 267-275 (2015)*

2- Experimental investigation of thermophysical properties and heat transfer rate of covalently functionalized MWCNT in an annular heat exchanger, *HK Arzani, A Amiri, SN Kazi, BT Chew, A Badarudin, International Communications in Heat and Mass Transfer 75, 67-77 (2016)*

3- Toward improved heat transfer performance of annular heat exchangers with water/ethylene glycol-based nanofluids containing graphene nanoplatelets, *HK Arzani, A Amiri, S Rozali , SN Kazi, A Badarudin, Journal of Thermal Analysis and Calorimetry (2016)*

4- Heat transfer performance of water-based tetrahydrofurfuryl polyethylene glycol-treated graphene nanoplatelet nanofluids*, HK Arzani, A Amiri, SN Kazi, A Badarudin, BT Chew, RSC Advances 6 (70), 65654-65669 (2016)*

5- Backward-facing step heat transfer of the turbulent regime for functionalized graphene nanoplatelets based water–ethylene glycol nanofluids, *A Amiri, HK Arzani, SN Kazi, BT Chew, A Badarudin, International Journal of Heat and Mass Transfer 97, 538-546 (2016)*

Conference Papers

1- Numerical Study of Developing Laminar Forced Convection Flow of Water/CuO Nanofluid in a Circular Tube with a 180 Degrees Curve*, HK Arzani, HK Arzani, SN Kazi, A Badarudin, International Conference on Nanomaterials Science and Engineering (2016)*

2- Thermophysical and Heat Transfer Performance of Covalent and Noncovalent Functionalized Graphene Nanoplatelet-Based Water Nanofluids in an Annular Heat Exchanger, *HK Arzani, A Amiri, HK Arzani, SN Kazi, A Badarudin, International Conference on Nanomaterials Science and Engineering (2016)*